Arnstein Norheim

Experimental investigation of Solid Oxide Fuel Cells using biomass gasification producer gases

Department of Energy and Process Engineering
Norwegian University of Science and Technology
N-7491 Trondheim, Norway

Experimental investigation of Solid Oxide Fuel Cells using biomass gasification producer gases
Arnstein Norheim
arnstein.norheim@ntnu.no
Norwegian University of Science and Technology (NTNU)
http://www.ntnu.no/
N-7491 Trondheim, Norway
Dr.ing.-thesis 2005:188
ISBN 82-471-7269-0 (printed)
ISBN 82-471-7269-2 (electronic)
ISSN: 1503-8181
Department of Energy and Process Engineering (EPT), NTNU
http://www.ept.ntnu.no
Kolbjørn Hejes vei 1B, N-7491 Trondheim, Norway
EPT Report 2005:188
ISSN 1503-8181

The Norwegian University of Science and Technology
Norges Teknisk-Naturvitenskapelige Universitet

ADDRESS:
NTNU
DEPARTMENT OF ENERGY AND PROCESS Engineering
Kolbjørn Hejes vei 1A
N-7491 Trondheim - NTNU

TELEPHONE
Switchboard NTNU: 73 59 40 00
Department office: 73 59 27 00
Hydropower section: 73 59 38 57

TELEFAX
Department office: 73 59 83 90
Hydropower section: 73 59 38 54

Report no:
2005:188

Classification:
Open

Title of report Experimental investigation of Solid Oxide Fuel Cells using biomass gasification producer gases	Date September 2005
	No. Of pages/appendixes 140/36
Author Arnstein Norheim	Project manager Johan E. Hustad
Division Faculty of Engineering Science and Technology Department of Energy and Process Engineering	Project no.
ISBN no. 82-471-7269-0	Price group

Client/sponsor of Project The Nordic Graduate School of Biofuel Science and Technology	Client's ref.

Abstract
The main objective of this thesis is theoretical and experimental investigations related to utilisation of biomass gasification producer gases as fuel for Solid Oxide Fuel Cells (SOFC). Initial fundamental steps towards a future system of combined heat and power production based on biomass gasification and SOFC are performed and include:

- Theoretical modeling of the composition of biomass gasification producer gases.
- Experimental investigation of SOFC performance using biomass gasification producer gas as fuel.
- Experimental investigation of SOFC performance using biomass gasification producer gas containing high sulphur concentration.

The modeling of the composition of gasifier producer gas was performed using the program FactSage. The main objective was to investigate the amount and speciation of trace species in the producer gases as several parameters were varied. Thus, the composition at thermodynamic equilibrium of sulphur, chlorine, potassium, sodium and compounds of these were established. This was done for varying content of the trace species in the biomass material at different temperatures and fuel utilisation i.e. varying oxygen content in the producer gas. The temperature interval investigated was in the range of normal SOFC operation. It was found that sulphur is expected to be found as H_2S irrespective of temperature and amount of sulphur. Only at very high fuel utilisation some SO_2 is formed. Important potassium containing compounds in the gas are gaseous KOH and K. When chlorine is present, the amount of KOH and K will decrease due to the formation of KCl. The level of sodium investigated here was low, but some Na, NaOH and NaCl is expected to be formed. Below a certain temperature, condensation of alkali rich carbonates may occur. The temperature at which condensation begins is mainly depending on the amount of potassium present; the condensation temperature increases with increasing potassium content.

In the first experimental work performed here, the SOFC performance at varying inlet fuel gas composition was studied. In particular, variations in the fractions of hydrogen and carbon monoxide were studied. Switching from a hydrogen rich to a carbon monoxide rich fuel gas causes a significant reduction in the cell performance. However, even at 90% CO, the SOFC is able to produce power thus showing high fuel flexibility. It was further found that the SOFC performance was essentially the same when switching from a fuel gas composition similar to reformed natural gas to a gas composition similar to biomass gasification producer gases. These fuel gases were, however, mixed from gas bottles and therefore contained none of the trace species that may be present in gasifier producer gases.

The second experimental series aimed at investigating the SOFC performance degradation as sulphur (H_2S) was added to the fuel gas. At an operating temperature of 800°C the sulphur concentrations added were in the range from 5 to 240 ppm. During the first 400 hours of operation, the reference cell performance increased, i.e. the cell resistance at 0 ppm H_2S decreased steadily making it difficult to quantify the effect of sulphur exactly. However, during the period when the cell was exposed to the highest sulphur concentrations the reference cell performance was constant and clearer conclusions could be drawn. It was found that the performance reduction was equal when the sulphur concentration in the fuel gas was 80, 120 and 240 ppm H_2S. The results leads to the conclusion that the anode structure is saturated with sulphur at a relatively low sulphur concentration, probably in the vicinity of
10-20 ppm H_2S. Further increasing the sulphur concentration in the fuel gas thus only causes marginal additional performance degradation. Post-experimental analysis of the cell structure gave no evidence of sulphur reacting chemically with the anode material. By repeating two of the experiments at 850°C no clear temperature dependency of the poisoning effect of H_2S was found.

	Indexing Terms: English	Norwegian
Group 1	Solid Oxide Fuel Cell	Fastoksid brenselcelle
Group 2	Biomass gasification	Gassifisering av biomasse
Selected by author	Producer gas composition	Sammensetning av syngas
	Performance characteristics	Karakterisering av ytelse
	Sulphur rich fuel gass	Svovelrik brenselgass

PREFACE

This thesis is submitted in partial fulfilment of the requirements for the degree Doktor Ingeniør at the Norwegian University of Science and Technology (NTNU).

The work was carried out at the Department of Energy and Process Engineering at the Faculty of Engineering Science and Technology. Professor Johan E. Hustad has supervised the work.

The research was funded by the Nordic Graduate School of Biofuel Science and Technology.

ACKNOWLEDGEMENTS

First of all I wish to thank my academic advisor, Professor Johan E. Hustad for his guidance and support throughout the work leading to this thesis. His visions and scientific skills have been essential and his enthusiasm and encouragement have been important for my motivation.

Bjørn Thorud, my good friend and SOFC colleague has been of great help through many discussions and tricky questions. His contribution of making relevant comments to the first draft of this thesis is further greatly acknowledged. Øyvind Skreiberg (NTNU) and Arild Vik (Prototech) also receive sincere gratitude for their help on the way from the draft to the final version of the thesis. Arild Vik is also acknowledged for his constant willingness to discuss SOFC problems and for always saying yes to my requests for laboratory time at Prototech. I also wish to thank Jan Byrknes at Prototech for many interesting and fruitful discussions and a good friendship. The other members of the SOFC group at Prototech, Matteo Cé, Paal Bratland, Bahareh Ganji and Ivar Wærnhus are also thanked for their assistance during my stays in Bergen. Sincere gratitude also goes to Helge Folgerø-Holm and Alf Berland for their design and production of the single cell setup at Prototech.

Rainer Backman and Daniel Lindberg at Åbo Akademi, Finland, receive many thanks for making my stay there possible and for guiding me through the modeling work performed there. Anders Nordin and Markus Broström at Umeå University, Sweden, are also thanked for their assistance and cooperation on the ongoing work there.

The staff members at the Thermal Energy group, Anita Yttersian, Gunhild Valsø Engdal and Per Bjørnaas, are further greatly acknowledged for their assistance on all practical matters. My other present and past colleagues at the department are also thanked for their encouragement and all social activities.

The Nordic Graduate School of Biofuel Science and Technology is acknowledged for funding this work.

My dear Margit also deserves my deepest gratitude for always being there and giving me support through troubled times. Without her, this work would have stranded years ago. My family is finally thanked for showing interest to my work and especially my parents receive many thanks for their support.

ABSTRACT

The main objective of this thesis is theoretical and experimental investigations related to utilisation of biomass gasification producer gases as fuel for Solid Oxide Fuel Cells (SOFC). Initial fundamental steps towards a future system of combined heat and power production based on biomass gasification and SOFC are performed and include:

- Theoretical modeling of the composition of biomass gasification producer gases.
- Experimental investigation of SOFC performance using biomass gasification producer gas as fuel.
- Experimental investigation of SOFC performance using biomass gasification producer gas containing high sulphur concentration.

The modeling of the composition of gasifier producer gas was performed using the program FactSage. The main objective was to investigate the amount and speciation of trace species in the producer gases as several parameters were varied. Thus, the composition at thermodynamic equilibrium of sulphur, chlorine, potassium, sodium and compounds of these were established. This was done for varying content of the trace species in the biomass material at different temperatures and fuel utilisation i.e. varying oxygen content in the producer gas. The temperature interval investigated was in the range of normal SOFC operation. It was found that sulphur is expected to be found as H_2S irrespective of temperature and amount of sulphur. Only at very high fuel utilisation some SO_2 is formed. Important potassium containing compounds in the gas are gaseous KOH and K. When chlorine is present, the amount of KOH and K will decrease due to the formation of KCl. The level of sodium investigated here was low, but some Na, NaOH and NaCl is expected to be formed. Below a certain temperature, condensation of alkali rich carbonates may occur. The temperature at which condensation begins is mainly depending on the amount of potassium present; the condensation temperature increases with increasing potassium content.

In the first experimental work performed here, the SOFC performance at varying inlet fuel gas composition was studied. In particular, variations in the fractions of hydrogen and carbon monoxide were studied. Switching from a hydrogen rich to a carbon monoxide rich fuel gas causes a significant reduction in the cell performance. However, even at 90% CO, the SOFC is able to produce power thus showing high fuel flexibility. It was further found that the SOFC performance was essentially the same when switching from a fuel gas composition similar to reformed natural gas to a gas composition similar to biomass gasification producer gases. These fuel gases were, however, mixed from gas bottles and therefore contained none of the trace species that may be present in gasifier producer gases.

The second experimental series aimed at investigating the SOFC performance degradation as sulphur (H_2S) was added to the fuel gas. At an operating temperature of 800^{o}C the sulphur concentrations added were in the range from 5 to 240 ppm. During the first 400 hours of operation, the reference cell performance increased, i.e. the cell

resistance at 0 ppm H_2S decreased steadily making it difficult to quantify the effect of sulphur exactly. However, during the period when the cell was exposed to the highest sulphur concentrations the reference cell performance was constant and clearer conclusions could be drawn. It was found that the performance reduction was equal when the sulphur concentration in the fuel gas was 80, 120 and 240 ppm H_2S. The results leads to the conclusion that the anode structure is saturated with sulphur at a relatively low sulphur concentration, probably in the vicinity of 10-20 ppm H_2S. Further increasing the sulphur concentration in the fuel gas thus only causes marginal additional performance degradation. Post-experimental analysis of the cell structure gave no evidence of sulphur reacting chemically with the anode material. By repeating two of the experiments at 850^oC no clear temperature dependency of the poisoning effect of H_2S was found.

CONTENTS

1. INTRODUCTION

Small scale combined heat and power production based on biomass combustion and gasification is one of several key technologies for today's energy production. Biomass is dispersed over the earth's surface and is thus available nearly world wide. If utilised at the same rate as new biomass material grows, energy production based on biomass does not give any net contribution to the atmospheric CO_2 emission level. Additionally, by utilising the biomass material locally, the cost and emissions connected to transport is minimised.

Biomass gasification, by means of atmospheric fluidised bed technology, may be the best option for production of a syngas that can be utilised in a subsequent power production unit. As schematically shown in Figure (1.1), the technology is well developed compared to other gasification technologies.

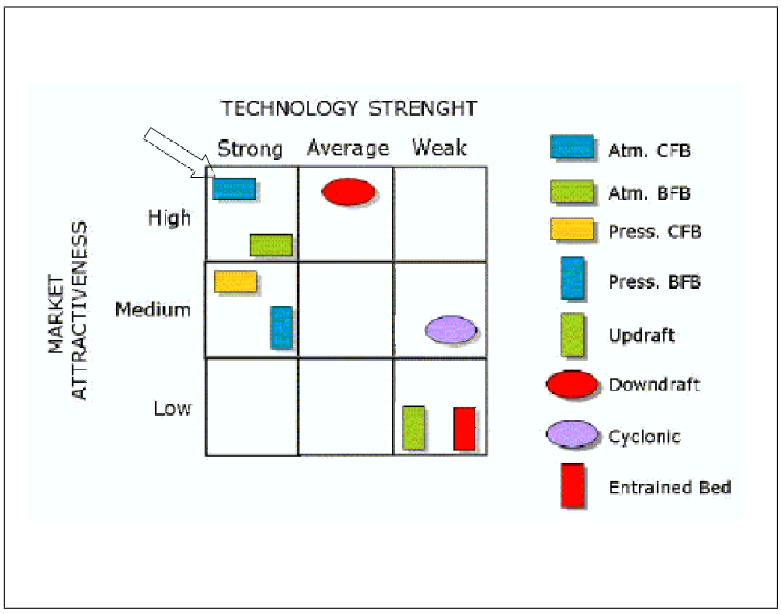

Fig. 1.1: Status of different gasification technologies (from Maniatis [1]).

Several biomass materials can be gasified. However, due to operation related problems and availability, woody biomass materials, refuse derived fuels and short rotation coppice have the highest market potential as shown in Figure (1.2)

Fuel cells may, due to the potentially high efficiency in power production, be an option for power production based on syngas from biomass gasification. Energy production from biomass is believed to be most suitable in the small to medium scale range ($<$ 1 MW) and fuel cells may thus be the best technology for power production as indicated in Figure (1.3).

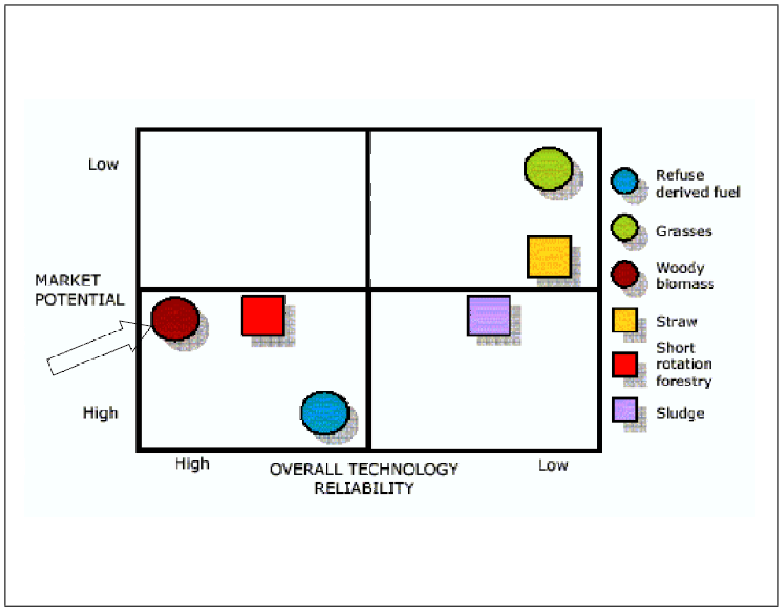

Fig. 1.2: Technology reliability versus market potential (from Maniatis [1]).

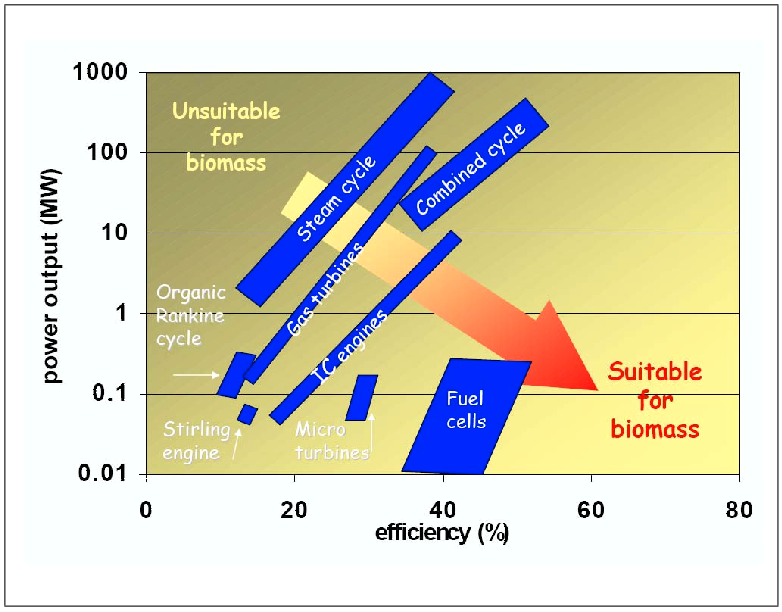

Fig. 1.3: Different power production technologies, efficiency and scale versus suitability towards utilisation of biomass as energy source.

1.1 Motivation

One of the most successful biomass gasification plants worldwide today is the FICFB-plant (Fast Internally Circulating Fluidised Bed) in Güssing, Austria [2]. As shown in Figure (1.4), the gasification plant consists of two chambers; one combustion chamber and one gasification chamber. Heat is supplied to the endothermic steam gasification process from the combustion reactor by means of a circulating bed material. The flue gas from the combustion chamber is kept separated from the gasifier producer gas. The gasification gas is therefore of relatively high quality and is at present utilised in an internal combustion engine. Nitrogen is kept very low in the producer gas since steam,

and not air, is used as gasification medium.

The producer gas from the Güssing plant is suitable as fuel for high temperature fuel cells. It leaves the gasifier at around 900°C, and could be directly utilised in a fuel cell operating at or around this temperature. Furthermore, as the producer gas contains mainly H_2, CO, H_2O, CO_2 and CH_4, the fuel cells requiring pure hydrogen are ruled out due to the poisoning effect of especially CO. There are two types of high temperature fuel cells, namely the Molten Carbonate Fuel Cell (MCFC) and the Solid Oxide Fuel Cell (SOFC). Both may be fuelled by a variety of gas mixtures and are not poisoned by CO.

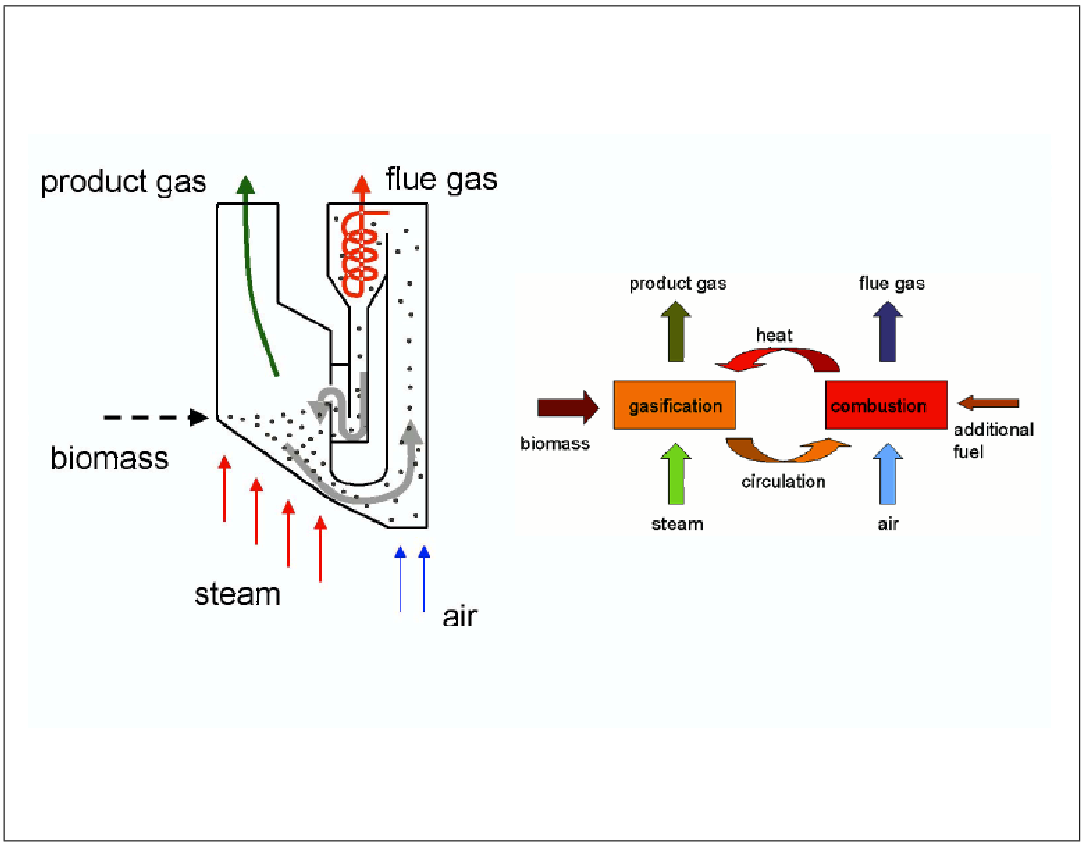

Fig. 1.4: Schematic of the operating principle of the FICFB-gasification plant in Güssing.

Important drawbacks regarding biomass gasifier producer gases are the potential fuel cell polluting or performance degrading fractions; particles, tars and trace species containing sulphur, chlorine and alkali metals. Thus, there is a need for filtration of the producer gas even in a system that uses high temperature fuel cells. The filtration should be carried out at an as high temperature as possible to be able to maximise the overall efficiency of the system.

The panel bed filter investigated by Risnes [3] can be utilised for high temperature gas filtration. As shown in Figure (1.5) the filter has two modes of operation; filtration mode and cleaning mode. During normal operation the gas to be filtered passes through the filter material held in place by louvres. Particles are deposited in the filter material causing a so-called filter cake build up. As the filter cake grows, the pressure drop over the filter increases. When the pressure drop over the filter reaches a pre-defined level, a short (ms) puff-back pulse is applied to remove the filter cake and normal operation is immediately restored. The panel bed filter may so far be operated at temperatures of

up to 550°C and is still undergoing substantial development. At present particles and some alkali metal compounds are removed in the filter.

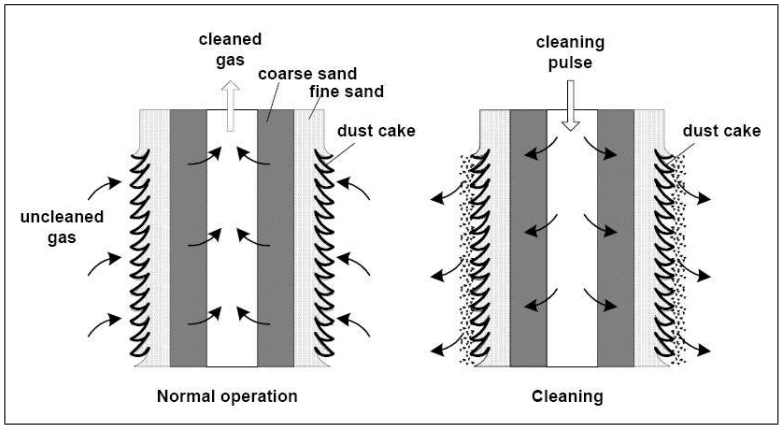

Fig. 1.5: Schematic of the working principle of the panel bed filter (from Risnes [3]).

The Solid Oxide Fuel Cell (SOFC) is a high temperature fuel cell operated at 700-1000°C. It has a high flexibility towards fuel gas composition and quality. In addition to power produced at a potentially high efficiency, high temperature heat is produced in the SOFC. Due to the all-solid construction, there is no concerns regarding electrolyte management as is the case for the Molten Carbonate Fuel Cell (MCFC). Thus, the relatively simple construction of the SOFC is a great advantage.

1.2 System description

As briefly described above, a system for combined heat and power production based on biomass gasification and Solid Oxide Fuel Cells is the working hypothesis in the present work. Taking into account the potential need for gas filtration, the system is schematically described as shown in Figure (1.6).

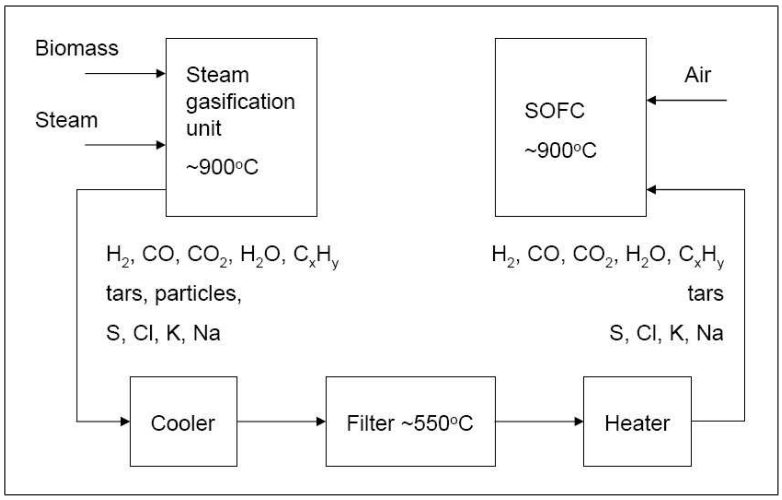

Fig. 1.6: Schematic of system of biomass gasification and Solid Oxide Fuel Cell.

In biomass gasification, air, steam, carbon dioxide or oxygen can be used as gasification medium. The latter is normally not an option due to the high cost of producing

oxygen. Air and steam gasification produce gases containing H_2, CO, H_2O, CO_2, CH_4 and N_2. The main difference between the two producer gases is the nitrogen and hydrogen content. Air gasification produces gases rich in nitrogen (up to 50 vol-%), whereas steam gasifier producer gases normally have a low nitrogen content (1-5 vol-%; from the nitrogen present in the biomass material), but have a significantly higher hydrogen content. Gases from steam gasification therefore have a higher energy content and may consequently be more suitable as fuel for the SOFC.

Solid Oxide Fuel Cells operate at temperatures between 700 to 1000°C. The high operating temperature enables electrochemical oxidation of both hydrogen and carbon monoxide. Light hydrocarbons may furthermore be internally reformed to H_2 and CO and may thus contribute at least indirectly to the power production in the fuel cell. Most of the work on SOFCs so far has been concerned with the use of natural gas or hydrogen as fuel. Utilisation of biomass gasifier producer gases in SOFCs has therefore not yet been paid much attention. SOFC performance and long-term stability when using gasifier producer gases are therefore not known.

Sulphur, particularly H_2S is known to reduce the SOFC performance even at concentrations down to a few ppm. Most of the work on the detrimental effect of sulphur on SOFC performance has, however, been performed at sulphur levels relevant for operation on natural gas. In biomass gasifier producer gases the sulphur level may, however, be significantly higher. The influence these high sulphur concentrations have on the SOFC performance has not yet been fully investigated.

Besides sulphur, gasifier producer gases may contain significant amounts of other trace species. Of importance are compounds of chlorine and alkali metals, particularly potassium and sodium. The amount of these species in the producer gas depends on the amount present in the raw biomass materials. Furthermore, the speciation varies with operational conditions such as temperature and level of fuel conversion i.e. the level of oxygen present in the gas. When alkali metals are present, there is also a risk of condensation resulting in liquid or solid phases in the gas. The temperature at which condensation occurs depends on the amount of alkali metals present in the gas. The influence gaseous and condensed trace components may have on the SOFC performance is not yet known.

1.3 Thesis overview

Chapter 2 in this thesis gives a short overview of biomass materials and their construction, with main emphasis on woody biomass materials. In chapter 3, thermal conversion techniques are presented focusing mainly on biomass gasification. In chapter 4 the operating principles of fuel cells in general are presented. Additionally, an overview of the different fuel cell types is given. In chapter 5, a more detailed presentation on SOFC fundamentals and reported operation is given. In chapter 6 and 7 results from modelling on the composition of trace species present in biomass gasifier producer gases are presented. Chapter 6 includes modelling on parameters influencing the temperature at which condensation of particularly alkali carbonates occur. In chapter 7 (Paper I), a parametric study on the conversion of the trace species is performed. The amount of the species, temperature and fuel conversion is varied and the results are presented.

In chapter 8, a summary of the experimental work on SOFC performance leading up to Paper II and Paper III is given. In addition, the experimental setup used for the experiments is described in detail. Chapter 9 (Paper II) presents results from exper-

imental work on SOFC performance at varying fuel gas composition. Furthermore, a comparison is made of the SOFC performance when utilising gas mixtures simulating reformed natural gas and gasifier producer gases. In chapter 10 (Paper III) performance data of a SOFC running on a fuel gas containing sulphur at levels up to 240 ppm is presented. Finally, in chapter 11 overall conclusions are drawn and recommendations for future work are presented.

2. BIOMASS MATERIALS

2.1 Introduction

Department of Energy and Process Engineering at NTNU has been and still is focusing on many aspects of biomass materials and thermal conversion techniques. Grønli [4] performed a detailed study on the degradation processes of thermal conversion of several biomass materials. Skreiberg [5] studied wood log combustion focusing mainly on emissions from incomplete combustion and NO_x emission mechanisms. Sørum [6] focused on thermal degradation of municipal waste (MSW) and also studied mechanisms causing NO_x emissions from MSW combustion.

Biomass gasification was studied in detail by Barrio [7]. Risnes [3] next investigated high temperature filtration of biomass gasification gases. Finally, Fossum [8] investigated biomass gasification and the subsequent combustion of the producer gas.

The present work is thus a natural continuation of the previous work at the department. Thermal conversion of biomass materials is not studied here as such, but rather the end use of gasifier producer gases in a Solid Oxide Fuel Cell system. Therefore, only a brief presentation of biomass materials and their properties is given.

2.1.1 Definition

Biomass is defined as all materials that are derived, directly or indirectly, from contemporary photosynthesis reactions [4],[9]. This includes all vegetal matter and their derivatives; wood fuel, wood-derived fuels, fuel crops, agricultural and agro-industrial by-products and animal by-products. Biomass is considered a renewable energy source as long as it is based on sustainable utilisation. If consumed at the same rate as new biomass is grown, there is no net atmospheric CO_2 emission connected to the consumption of biomass materials.

Compared to fossil fuels, biomass is more evenly dispersed over the earth's surface and is thus suitable for distributed local energy production. Energy production from biomass is also in general regarded cleaner than fossil fuels in terms of environmental pollution [4], [7].

However, as studied in detail by Skreiberg [5] and Sørum [6], biomass combustion may produce significant emissions of components caused by incomplete combustion (CO, UHC (unburned hydrocarbons), particles/tars, dioxins) and NO_x components. In addition, some biomass materials, typically waste materials and non-woody biomass materials, may contain significant amounts of heavy metals, sulphur and chlorine. During combustion or gasification these species may follow the gas stream or end up in the ash fraction. Thus, if the biomass conversion technology is not carefully designed, the energy production may cause significant emissions of pollutants and toxic species.

A detailed knowledge of the composition of the raw biomass material is therefore needed. In addition, it is important to know where the different species end up during the thermal processing, i.e. in which stream fraction (e.g. gas stream, bottom ash, fly

ash, deposition). Furthermore, the speciation may be important for end-use applications, e.g. fuel cells.

2.2 Biomass material characteristics

Biomass materials are very young compared to fossil fuels, and therefore have a significantly different composition. As the biomass materials are converted under high pressure and temperature to fossil fuels, a process taking millions of years, most species diffuse away from the original biomass materials. The resulting fossil fuel eventually consist of mainly carbon, some hydrogen and oxygen and an ash fraction. Thus, going from typical biomass materials, via peat and lignite, the typical coals have significantly lower oxygen-to-carbon (O:C) and hydrogen-to-carbon (H:C) ratios. The van Krevlen diagram shown in Figure (2.1) indicates the O:C and H:C ratios and heating value gradient for the different fuels. In thermal conversion of any fuel, the energy content of the fuel is of great interest. The biomass materials are in Figure (2.1) seen to contain significantly less energy per unit mass than the fossil fuels.

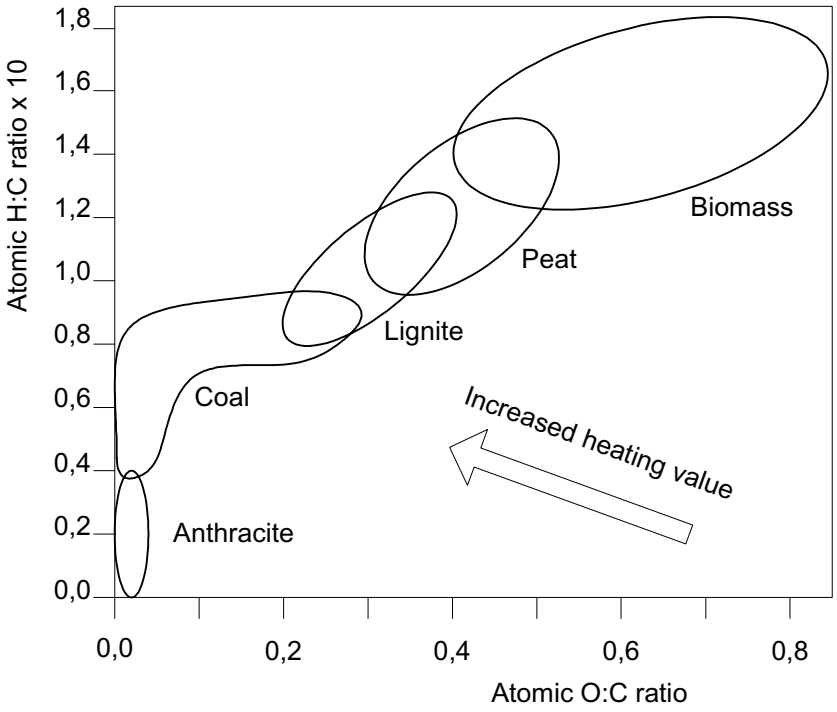

Fig. 2.1: Van Krevlen diagram for various solid fuels.

2.2.1 Classification

Raw biomass materials can be divided into different groups based on their origin or place and type of growth as referred to by Grønli [4]:

- Woody plants i.e. perennial lignocellulosic crops. This group can be further divided into long term (15-50 year rotation) and short term (6-15 year rotation) single stem forestry and short term (3-5 year rotation) multiple stem coppicing of perennial crops

- Herbaceous plants/grasses i.e. annual crops
- High sugar/starch crops i.e. suitable for ethanol production
- Oil-containing crops which may be suitable for production of vegetable oils
- Aquatic plants

In addition several biomass wastes may be utilised for energy production:

- Forestry residues, e.g. branches and tops from felling, storm damaged trees and thinnings
- Agricultural residues e.g. straw form cereal production
- Residues from manufacturing of wood based products e.g. bark and sawdust from sawmills and bark and black liquor from pulp and paper industry
- Municipal and industrial solid wastes
- Manures

2.2.2 Construction

Even though there are differences between the different biomass materials, there are basic similarities between wood and most other land plants regarding the plant structure and basic cell construction [4]. In the following the focus is on the woody biomass materials.

The building materials of wood cells are cellulose, hemicellulose and lignin appearing in varying fractions depending on the type of material. In addition, there may be small amounts of other light organic compounds, or extractives, present [4], [10]. Cellulose, hemicellulose and lignin contribute by 95 to 98% of the total mass of the wood [4]. Simplified, cellulose forms a skeleton that is surrounded by hemicellulose and lignin working as matrix and encrusting materials, respectively [4].

Cellulose

Cellulose being the main part of the wood cell, is a linear polysaccharide. This long chained glucose polymer may consist of above 10000 units of glucose in unaltered wood [4]. The elemental formula of cellulose is $(C_6H_{10}O_5)_n$.

Hemicellulose

Comprising all non-cellulosic polysaccharides and related substances, hemicellulose is a heterogeneous branched polysaccharide consisting of primarily five- and six-carbon sugars [4], [10]. Hemicellulose generally consists of 50 to 200 units and is more branched than the linear cellulose structure [4]. The hemicelluloses are also more soluble than cellulose and are more easily chemically degraded [4].

Lignin

Lignin both binds the wood cells together and is responsible for the rigidity of the cell walls [4]. Lignin is a complex three dimensional polymer [4] and is believed to be made of a three carbon chain attached to rings of six carbon atoms called phenyl-propanes [10]. The solubility of lignin is very poor in most solvents [4]. It is hard to isolate lignin in wood without altering the chemical structure i.e. many bonds are broken in order to separate the substance [4]. The resulting lignin is therefore often named after the process name e.g. Kraft lignin, Klason lignin etc.

Extractives

The extractives in wood include aliphatic, aromatic and alicyclic compounds in addition to hydrocarbons, alcohols, ketones and acids, esters, phenolic compounds, resins and terpenes amongst others [4]. Extractives are soluble in organic solvents or water.

Ash

The ash fraction of wood consists of inorganic compounds of alkali metals, heavy metals, sulphur, chlorine and silicates. Normally, the ash content of wood does not exceed 0.5 to 1.0% by weight [4].

General aspects

Hardwoods contain in general a larger portion of cellulose and hemicellulose than softwoods. Consequently, the lignin content is higher in softwoods compared to hardwoods [4].

The woody biomass materials have a higher proportion of lignin than the herbaceous plants. As lignin binds the cellulosic fibres together, this is indicated by the slower growth and the more tightly bound fibres of the woody plants [10]. The usually perennial herbaceous plants are growing more rapidly and have more loosely bound fibres [10]. Cellulose contributes to around 40-50% of the biomass material by weight and the hemicellulose adds 20-40% [10].

2.2.3 Proximate analysis

Proximate analysis of a fuel is performed to establish key properties such as:

- Moisture content
- Calorific value
- Amount of fixed carbon
- Amount of volatiles
- Ash/residue content

In Table (2.1), proximate analysis of several fuels are shown. Standard test methods (ASTM E870-82) are established for the analysis.

	Proximate analysis (wt%)					
Material	Moisture	Volatile matter	Fixed carbon	Ash	LHV (MJ/kg)	Ref.
Barley straw	30	46	18	6	16.1	[10]
Birch	-	90.4	9.4	0.2	19.13 (HHV)	[4]
Bituminous coal	11	35	45	9	34	[10]
Lignite	34	29	31	6	26.8	[10]
Pine	-	87.6	12.3	0.1	19.03 (HHV)	[4]
Sawdust (pine)	8	82.29	17.16	0.55	20.54 (HHV)	[13]
Spruce	-	86.7	13.2	0.1	19.30 (HHV)	[4]
Wheat straw	16	59	21	4	17.3	[10]
Wood	20	82	17	1	18.6	[10]

Tab. 2.1: Proximate analysis of different biomass materials.

Moisture content

The moisture content (M) of the biomass material is the mass fraction of moisture, on oven-dry basis, contained in the material. Oven-dry basis is defined as the constant mass obtained after the wood is dried in air in an oven maintained at 102±3°C for 24 hours:

$$M = \frac{m_s - m_{sd}}{m_{sd}} = M_b + M_l \tag{2.1}$$

where

m_s = green or moist mass

m_{sd} = oven-dry mass

M_b = bound water

M_l = free water

The moisture content in biomass materials may be divided into intrinsic and extrinsic moisture [10]. The intrinsic moisture takes into account the moisture of the biomass itself, whereas the extrinsic moisture also takes into account the influence of the weather conditions during harvesting [10].

The intrinsic moisture in wood can exist in three forms [4], [11], [12]:

- Water vapour in the pores.
- Capillary or free (liquid) water in the pores. This water is found in the voids of the wood and the amount is limited by the porosity of the wood. The free water is only held back by week capillary forces.
- Hygroscopic bound water in the solid structure. The bound water is believed to be hydrogen bonded mainly to the hydroxyl groups of cellulose and hemicellulose. When the biomass material contains bound water only, an equilibrium state is obtained between the moisture in the biomass and the humidity in the surrounding air.

Calorific value

The calorific value (CV) of a material is the measured heat released when burnt in air. The CV is normally stated in terms of the energy content per unit mass or volume.

There are two different expressions for the CV; HHV: higher heating value and LHV: lower heating value.

The HHV, also called the gross calorific value (GCV), is the total energy released from the fuel sample including the latent heat in the produced water vapour. This value thus represents the maximum energy available in the fuel sample. The HHV values of biomass materials are normally in the range between 18 and 21 MJ/kg; the lower values for herbaceous materials and the higher values are for fresh wood fuels [9]. The HHV can be accurately determined in a bomb calorimeter. However, a reasonable estimate can be calculated from the following empirical equation [9]:

$$\begin{aligned} HHV &= 0.3491 \cdot X_C + 1.1783 \cdot X_H + 0.1005 \cdot X_S - 0.0151 \cdot X_N \\ &\quad -0.1034 \cdot X_O - 0.0211 \cdot X_{ash} \; [MJ/kg, d.b.] \end{aligned} \tag{2.2}$$

where

X_i = weight fraction (wt% d.b.) of element i in the sample

X_{ash} = weight fraction (wt% d.b.) of ash in the sample

Normally, the latent heat of the water vapour cannot be utilised. Therefore the LHV is introduced being the HHV minus the heat of evaporation of the water in the fuel. This normally represents the energy available for use in a subsequent process. The lower heating value, also called the net calorific value (NCV) can be calculated from the HHV by the following equation [9]:

$$\begin{aligned} LHV &= HHV \cdot \left(1 - \frac{w}{100}\right) - 2.447 \cdot \frac{w}{100} \\ &\quad -2.447 \cdot \frac{h}{100} \cdot 8.99 \cdot \left(1 - \frac{w}{100}\right) \; [MJ/kg, w.b.] \end{aligned} \tag{2.3}$$

where

w = weight fraction of moisture in the fuel (wt% w.b.)

h = weight fraction of hydrogen in the fuel (wt% d.b.)

Volatile matter

The volatile matter (VM) is the portion of the biomass material that is driven off as gas by heating the fuel sample in a covered crucible to 950^{o}C and keeping this temperature for 7 minutes. Since no air is added, the fuel sample is not burnt and both the char and ash fractions remain in the crucible. The sample is thus carbonised.

The fraction of volatile matter in the sample is:

$$X_{VM} = \frac{m_{VM}}{m_{bio}} \tag{2.4}$$

Ash

Determination of the ash content in the fuel sample is done by burning the sample in an open crucible at 600^{o}C for 4 to 6 hours. The ash fraction is thus:

$$X_{ash} = \frac{m_{ash}}{m_{bio}} \tag{2.5}$$

Fixed carbon

Finally, the fixed carbon (FC) content of the fuel sample can be calculated as:

$$X_{FC} = 100 - (X_{VM} + X_{ash}) \tag{2.6}$$

The VM and FC contents of the fuel give a measure of the material's suitability towards ignition and thus gasification and oxidation [10].

2.2.4 Ultimate analysis

On an atomic scale, biomass materials are made of mainly carbon, hydrogen, oxygen and nitrogen. Additionally, sulphur, chlorine, alkali metals and also heavy metals are present in varying quantities.

Ultimate analysis of the biomass materials provides the weight percentages of the elements present. Table (2.2) shows data from ultimate analysis of several dry ash free (daf) biomass materials and some coal types for comparison. Furthermore, data from ultimate analysis of some refined biomass materials and several waste materials are shown in Table (2.3).

All woody biomass materials contain around 6% hydrogen and 38-44% oxygen. On an average basis hardwoods contain 47-50% carbon and softwoods contain 50-53% carbon. This is contributed to varying lignin and extractives content [14]. Sulphur is below 0.5% for most woody biomass materials and the nitrogen content is in the range of 0.1-1%.

Coals on the other hand, may contain as much as 80% carbon, the rest being more or less evenly divided between hydrogen, oxygen and ash. Most biomass materials contain a relatively small amount of ash forming materials, and the ash fraction is therefore smaller for these materials compared to coals. The straw materials however, have generally a higher ash fraction, mainly due to the higher chlorine content.

	Ultimate analysis, daf (wt%)									
Material	C	H	O	N	S	Cl	K	Na	Ash (d.b. wt%)	Ref.
Ash	49.9	6.9	43.2	-	-	-	-	-	0.3	[10]
Barley	47.8	6.0	43.8	0.54	0.13	0.42	1.15	0.21	-	[15]
Barley straw	50.2	6.7	42.1	0.44	0.44	0.11	-	-	6.0	[10]
Beech	52.0	6.3	41.7	-	-	-	-	-	-	[10]
Cacao shell	51.3	5.7	36.4	3.28	0.21	0.02	2.99	0.003	10.5	[16]
Cedar	52.7	6.1	40.2	0.52	0.39	-	-	-	0.79	[17]
Cypress	55.2	6.5	38.3	-	-	-	-	-	0.4	[10]
Cypress	52.0	6.2	40.7	0.66	0.46	-	-	-	0.7	[17]
Hemlock	52.0	6.2	40.8	0.60	0.38	-	-	-	0.4	[17]
Lucerne	49.3	6.2	37.6	3.27	0.26	0.63	2.64	0.10	-	[15]
Miscanthus	49.9	5.6	43.8	0.52	<0.1	-	-	-	2.8	[10]
Peat	58.1	6.0	34.1	1.49	0.26	0.10	0.02	0.01	-	[15]
Peat average	58.9	6.1	32.6	2.0	0.26	0.09	0.03	0.01	-	[15]
Poplar	49.1	6.0	44.3	0.50	0.01	0.10	-	-	1.3	[18]
Rape	49.7	6.1	41.7	0.82	0.18	0.24	1.08	0.15	-	[15]
Rice husk	42.9	6.4	49.7	0.33	0.64	-	-	-	14.8	[19]
Rice straw	47.5	5.7	45.8	0.80	0.12	-	-	-	-	[10]
Salix	48.7	5.9	44.5	0.53	0.06	0.01	0.31	0.01	-	[15]
Timothy	48.2	6.5	41.5	1.25	0.17	0.03	2.28	0.06	-	[15]
Verge grass	48.7	6.4	42.5	1.90	0.14	0.39	-	-	8.4	[18]
Verge grass	48.5	5.5	39.8	2.40	0.18	0.84	2.55	0.18	17.6	[16]
Wheat	48.6	6.1	43.4	0.62	0.08	0.16	0.99	0.04	-	[15]
Willow	48.5	5.9	44.4	0.88	0.05	0.02	0.26	0.02	2.13	[16]
Wood	51.9	6.0	41.8	0.12	0.01	0.02	0.04	0.02	-	[15]
Bituminous coal	80.9	6.1	9.6	1.55	1.88	-	-	-	9.0	[10]
Lignite	70.0	5.2	22.8	1.99	-	-	-	-	5.0	[10]

Tab. 2.2: Ultimate analysis of different biomass materials.

	Ultimate analysis, daf (wt%)									
Material	C	H	O	N	S	Cl	K	Na	Ash (d.b. wt%)	Ref.
Bark	53.5	5.8	40.0	0.41	0.03	0.02	0.17	0.04	-	[15]
Chip board	50.2	5.9	42.2	1.44	0.08	0.09	0.09	0.12	2.9	[16]
Demolition wood	48.9	5.2	45.6	0.15	0.03	0.08	-	-	0.9	[18]
Demolition wood	50.9	5.5	42.8	0.46	0.04	0.07	0.07	0.05	2.08	[16]
MSW	48.7	7.0	40.3	2.52	0.28	0.84	0.20	0.24	-	[15]
ODW	51.7	6.7	38.6	2.19	0.50	0.3	-	-	18.9	[18]
Park wood	50.9	5.6	40.8	1.15	0.25	0.03	0.74	0.44	18.3	[16]
PPGW	51.1	5.9	42.4	0.26	0.05	0.06	0.23	0.05	3.23	[16]
PRS	43.1	5.5	48.5	1.36	0.64	0.05	0.69	0.07	47.3	[16]
Railroad ties	54.4	5.8	39.4	0.27	0.10	0.02	0.03	0.02	2.60	[16]
Sawdust	48.2	6.1	45.6	0.15	0.05	-	-	-	0.32	[20]
Sawdust (pine)	50.8	7.1	41.3	0.15	0.57	-	-	-	0.55	[13]
Sawdust (SPF)	50.8	6.3	41.9	0.62	0.34	-	-	-	0.70	[17]
Sewage sludge	52.6	7.2	30.3	7.01	2.70	0.19	-	-	37.5	[18]
Sewage sludge	51.9	7.2	30.5	7.02	2.59	0.15	0.34	0.26	36.0	[16]
WEF/ODW	49.5	5.6	40.7	1.52	0.25	0.07	1.74	0.68	42.8	[16]
Wood chips	51.8	6.3	41.6	0.22	<0.05	-	-	-	0.60	[2]
Wood pellets	50.5	6.9	42.3	0.30	-	-	-	-	0.39	[7]

MSW = Municipal Solid Waste
ODW = Organic Domestic Wood
PPGW = Park and Public Garden Wood
PRS = Paper Residue Sludge
SPF = Spruce, Pine and Fir mixed
WEF/ODW = Woody Excess Fraction of ODW

Tab. 2.3: Ultimate analysis of different secondary biomass materials.

3. BIOMASS GASIFICATION

3.1 Introduction

Energy is stored in biomass materials as chemical energy. To be able to utilise this energy, a conversion technique must be applied. By direct combustion, the chemical energy is converted to heat. This heat can be used for heating purposes or for power production in e.g. a steam turbine. It is also possible to convert biomass materials to gases, liquids or carbon rich solids which can be used for heat and power production in a subsequent process such as combustion engines, gas turbines or fuel cells. Thus, there are several possibilities for production of heat, electrical power or a combination of the two from biomass materials. There are, as referred by Grønli [4], three different types of conversion techniques:

- Biochemical conversion
- Physical/chemical conversion
- Thermochemical conversion

The biochemical conversion method comprises digestion to produce biogas and fermentation to produce ethanol. Physical conversion include mechanical extraction which is normally connected to the production of bio-diesel. These methods are not in the scope of this work and will therefore not be further presented here. The focus here is on the thermochemical conversion techniques. In the following these are briefly presented.

3.2 Thermochemical conversion techniques

Thermochemical conversion, or degradation, of biomass materials may be divided into four distinguishable processes:

- Combustion
- Pyrolysis
- Liquefaction
- Gasification

The primary products will be a mixture of gases, liquids/tars, char and heat depending on the conversion technology. By secondary processing higher value products may be produced. Most petroleum derived products may be produced from biomass.

The choice of conversion technology in a specific case has to be determined by the type and quantity of feedstock, required type of energy i.e. heat, electrical power or chemical components, economic and environmental requirements and factors specific to the actual project [21]. Thus, it is often the wanted form of energy that determines the choice of process technology, followed by the available biomass feedstock i.e. type and quantity.

3.2.1 Combustion

Combustion is the term used for complete oxidation of the fuel material. The combustion process produces hot gases at temperatures around 800-1000^{o}C. Thus, the chemical energy stored in the biomass may be converted into heat or mechanical energy in various process equipment e.g. stoves, furnaces, boilers, Stirling engines and steam turbines. Prior to combustion, drying and pyrolysis are essential initial process steps.

Combustion plants ranges in size from small domestic stoves to large-scale industrial plants in the range of 100-3000 MW [21].

3.2.2 Pyrolysis

Pyrolysis is a thermal conversion technique, also called devolatilisation, in which no oxidising agent is introduced. The fuel is heated to temperatures of 200-500^{o}C and the main products are a highly reactive char fraction, gases and liquid tars [4]. The proportions of the different products will depend on temperature, pressure, heating rate and reaction time [4] but a final char yield of nearly 40% on a mass basis is achievable [22]. The gaseous products are all light molecular weight products, mainly CO, CO_2, CH_4 and H_2 whereas the tars is a mixture of several high molecular weight products. These are volatile at the pyrolysis temperature, but condense at lower temperatures. The pyrolysis liquids will also include water either from the moisture in the fuel or from chemical reactions producing water. Thus, the pyrolysis process may serve several purposes by adjusting the process conditions.

The char from pyrolysis may be refined to activated carbon or used in the metallurgical industry. In addition it may be used as domestic cooking fuel or for barbecuing [4]. A very recently proposed application is the use of the char in the bio-carbon fuel cell. The use of a direct carbon fuel cell has been studied e.g. by Zecevic [23].

The pyrolysis gases may be combusted to produce heat or synthesised to produce methanol or ammonia [4]. It is also possible to use the gases as fuel for a high temperature fuel cell like the SOFC or MCFC. The liquids may be upgraded to high grade liquid fuels for combustion engines or be combusted directly for heat production [4].

3.2.3 Liquefaction

Liquefaction is a thermal conversion process in the liquid phase at low temperatures (250-350^{o}C), high H_2 partial pressure and high total pressures (100-200 bar). Normally a catalyst is used to enhance the reaction rates and to control the product composition. The process aims at maximising the liquid yield. The heating value of the liquid products have higher heating values than the liquids from pyrolysis; 35-40 MJ/kg compared to 20-25 MJ/kg [4]. Additionally, the low oxygen content of the liquid makes the fuel more stable and less effort is required to upgrade it to a hydrocarbon fuel [4].

3.3 Gasification

Gasification is also called pyrolysis by partial oxidation indicating that the fuel is not completely oxidised as in combustion. This process is normally carried out at 800-1100^{o}C and its aim is to maximise the gas yield. However, significant amounts of tars, particles and ashes may be produced depending on the operating conditions, gasification technology and fuel.

The main gaseous components from biomass gasification are H_2, CO, CH_4, H_2O and CO_2 in addition to small amounts of other light hydrocarbons. If air is used as oxidising agent, the producer gas will contain significant (up to 50%-vol) amounts of N_2 due to the nitrogen content of air [7], [24]. The nitrogen content in the producer gas may therefore be significantly reduced by using steam or oxygen as oxidising agent. The steam gasification plant in Güssing, Austria, for example, produces a gas containing 3-5 vol% nitrogen only [25].

Due to the high nitrogen content in the producer gas, air gasification produces a low heating value gas of 4-6 MJ/Nm^3 (HHV) [24]. Oxygen and steam gasification on the other hand may produce a medium heating value gas of 10-18 MJ/Nm^3 (HHV) [2], [25]. According to Barrio [7], the advantages and disadvantages of using the different gasification media can be summarised as shown in Table (3.1).

Gasification agent	Advantages	Disadvantages	Heating value of product gas [MJ/Nm^3]
Air	Inexpensive	Low heating value	4-7
Oxygen	N_2-free product gas Medium heating value	Expensive	10-18
Steam	N_2-free product gas Medium heating value Enhanced H_2 content	Very endothermic process	10-18

Tab. 3.1: Comparison of gasification agents (from Barrio [7]).

Gasifier producer gases may be used as fuel in gas turbines, internal combustion engines or high temperature fuel cells. The heat from these processes may be utilised in a bottoming cycle e.g. a steam turbine. For all three applications fuel gas cleaning is essential in long term operation.

In addition, the gasification gas may be used to produce heat directly in a boiler or the gas may be upgraded to methanol, methane and synthetic natural gas by e.g. the Fischer-Tropsch process.

3.3.1 Advantages of biomass gasification

According to Fossum [8] there are several advantages of biomass gasification compared to direct combustion:

- Numerous options for power production including gas engines, gas turbines and fuel cells. Direct combustion on the other hand is limited to mainly steam processes in addition to Stirling engines and indirectly fired gas turbines.
- Easier combustion control due to combustion of gaseous fuel, compared to the inherently more complex control necessary for combustion of solid fuels.
- Relatively lower emission due to the fact that some components can be removed in the gasifier itself, in addition to in the gas cleaning system.
- Integration or co-firing in existing natural gas or coal fired power plants thus reducing the net CO_2 emissions.

- Hydrogen production or production of a high-yield hydrogen gas mixture.
- Basis for further chemical synthesis potentially able to produce a wide range of chemicals.

3.3.2 Gasification process

Gasification is the thermo-chemical conversion of a solid fuel into a gaseous fuel by partial oxidation. Essentially, gasification involves heating the solid material in the presence of a gasification medium, or oxidising agent, such as air, oxygen or steam.

By only partially oxidising the fuel in the gasification process, the conversion of the chemical energy stored in the biomass material can be carried out in a two step process. Thus, the gas produced can be used to power gas engines [25], [26],[27], gas turbines [28], [29], [30] or fuel cells [31], [32].

The gasification process occurs in the following sequential steps:

1. Drying - moisture is evaporated.
2. Pyrolysis - to produce gas, vaporised tars and a solid char residue.
3. Gasification - of the pyrolysis tars and the solid char residue.

Thus, as the biomass material enters the gasification reactor, it is first heated and dried. Next, as the temperature increases, the volatile matter is released i.e. pyrolysis or devolatilisation occurs. The gaseous pyrolysis products are partially burnt if oxygen is present i.e. if air or oxygen is used as gasifying medium. This process, called flaming pyrolysis [33] supplies heat to the drying and pyrolysis processes and the final char gasification. The gases from the flaming pyrolysis, mainly CO_2 and H_2O, finally react with the char in absence of oxygen to produce hydrogen and carbon monoxide by the Boudouard reaction Eq. (3.1) and the water-gas reaction Eq. (3.2):

$$C + CO_2 \leftrightarrow 2CO \qquad \Delta H = 161 kJ/mol \tag{3.1}$$

$$C + H_2O \leftrightarrow H_2 + CO \qquad \Delta H = 118 kJ/mol \tag{3.2}$$

Both reactions are endothermic and very slow at temperatures below 800^{o}C. Details regarding these two reactions can be found in the work of Barrio [7].

The heat needed for char gasification may be provided by combustion of volatile matter Eq.(3.3) and char combustion Eq.(3.4):

$$[C_xH_y + CO + H_2 + CH_4] + O_2 \rightarrow CO_2 + H_2O + \text{heat} \tag{3.3}$$

$$C + O_2 \rightarrow CO_2 + \text{heat} \tag{3.4}$$

Methane may be formed through the following exothermic reaction providing heat to the system also:

$$CO + 3H_2 \rightarrow CH_4 + H_2O \tag{3.5}$$

This reaction is rather slow, but increasing pressure shifts the reaction towards methane formation.

The water-gas shift reaction Eq. (3.6) finally governs the interactions between the gaseous components and thus has an influence on the distribution of the species.

$$CO_2 + H_2 \leftrightarrow CO + H_2O \tag{3.6}$$

The three sequential gasification processes described above may, as reported by Barrio et al. [26], be observed to occur in distinguishable zones in a stratified downdraft gasifier. In a fluidised bed gasifier, however, the fuel material is continuously stirred and mixed. The different processes will therefore take place simultaneously all over the bed and not in separate zones.

3.3.3 Gasification technology

There are two main types of biomass gasification technologies; fixed bed and fluidised bed gasifiers. Within both categories there are several subtypes. The fixed bed gasifier has a relatively simple design and is recognised by a static bed consisting of fuel material at different levels of conversion at different, distinguishable locations.

Fluidised bed technology on the other hand has a bed consisting mainly of inert fine-grained sand, dolomite or alumina and only a few percent fuel material. The fluidisation of the bed ensures good mixing of the hot bed material, products and the biomass feed. The uniform temperature distribution in the gasification zone is regarded as the main advantage over fixed bed gasifiers [24].

The fixed bed gasification is considered a robust and simple technology, whereas the fluidised bed technology is regarded more sophisticated [21].

Fixed bed gasification

Fixed bed gasifiers are in general suitable for small-scale applications. They are simple in construction but have limited potential for scale-up. The scale-up problems are connected with the problems of establishing the required high temperature tar cracking zone as the reactor diameter increases. Normal capacities are therefore below 1 MW.

The char bed in fixed bed reactors may act as a particle filter itself and the producer gases from these reactors may therefore be very low on particulates [26].

There are several sub-categories of the fixed bed gasification technology. Depending on the direction of the gas flow, one can distinguish between updraft, downdraft and crossdraft fixed bed gasifiers.

Updraft gasification: In an updraft or counter-current gasifier, the fuel is fed from the top of the gasifier and the oxidising medium is introduced in the lower part of the reactor through a grate as shown in Figure (3.1). Both the oxidising medium and the gases produced flow upwards, whereas the fuel gradually moves in the downward direction.

As the fuel enters the gasifier at the top of the reactor, it is first dried, cooling the passing product gases to around 200-300^{o}C [24]. Further down in the gasifier, in the pyrolysis or devolatilisation zone, the volatile compounds are released together with significant amounts of tar components. The tars either condense on the biomass material in the drying zone or leave the gasifier with the product gases. On the grate solid char is combusted at temperatures around 1000^{o}C [24].

Since the tars do not pass any high temperature zone in which they may be cracked, the producer gases from updraft gasifiers normally contain high tar concentrations [34]. On the other hand, the low temperature of the gases leaving the gasifier gives a high thermal efficiency of the process [24], and biomass materials containing up to 50% moisture can be gasified without pre-drying [34].

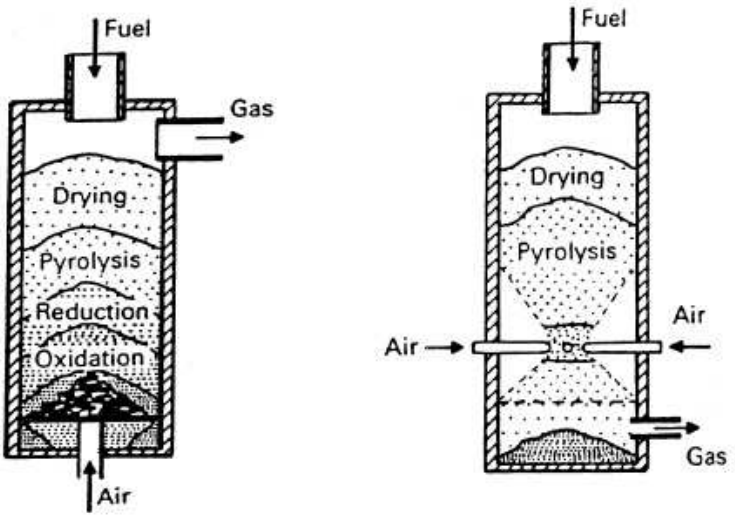

Fig. 3.1: Schematic of fixed bed gasifiers; updraft (left) and downdraft (right).

The particulate content may be kept low due to the filtration of the gases when passing the fuel material on the way out of the reactor [24].

Downdraft gasification: In a downdraft or co-current gasifier, the gases and biomass material flow downwards as shown in Figure (3.1). Above the intake of the oxidising agent, the fuel is dried and pyrolysed. At, or near, the inlet the solid pyrolysis char and tar is partially combusted at temperatures around 1000^oC . Below this zone, the solid char is gasified.

Since the tars, and gases, must pass the high temperature combustion zone before leaving the reactor, parts of the tars may be cracked. The downdraft gasifiers therefore in general produce gases with a lower tar content compared to the updraft reactors. However, the tars leaving the gasifier may be more stable, potentially causing problems in tar removal [34] or other downstream processes. The high temperature of the product gases results in low overall energy efficiency of the downdraft gasifier [24]. Moreover, the particle content of the product gases may be high. The downdraft gasifier demands relatively small sized particles with a low moisture content ($<$20 wt% d.b.) [34].

Crossdraft gasification: In a crossdraft or crossflow gasifier, oxidising agent inlet and product gas outlet are placed at the same height in the gasifier. Fuel material is introduced from the top and is combusted close to the oxidising agent inlet. Above or in front of this high temperature zone, the fuel is dried and pyrolysed. The product gas has a high tar concentration and leaves the gasifier at temperatures around 800-900^oC, giving a low overall energy efficiency [24].

Fluidised bed gasification

Fluidised bed gasification has been widely used for coal gasification, and are normally divided into two categories; bubbling fluidised bed (BFB) and circulating fluidised bed (CFB). The two types are schematically shown in Figure (3.2). The main difference between the two is the velocity of the fluidising gas; in the BFB reactor the bed is more

defined in the lower part of the reactor whereas in the CFB reactor the bed is completely fluidised occupying the whole reactor interior.

Fluidised bed gasifiers are by many regarded the best design option for biomass gasification. Among the advantages is high fuel flexibility including the use of low-density materials. They have higher throughput capability than the fixed bed reactors and require limited pre-processing of the fuel materials. The producer gases leave at high temperature (800-1000^{o}C) giving a risk of high alkali content due to limited condensation of alkali rich phases. In addition, the producer gases generally contain high particle concentrations.

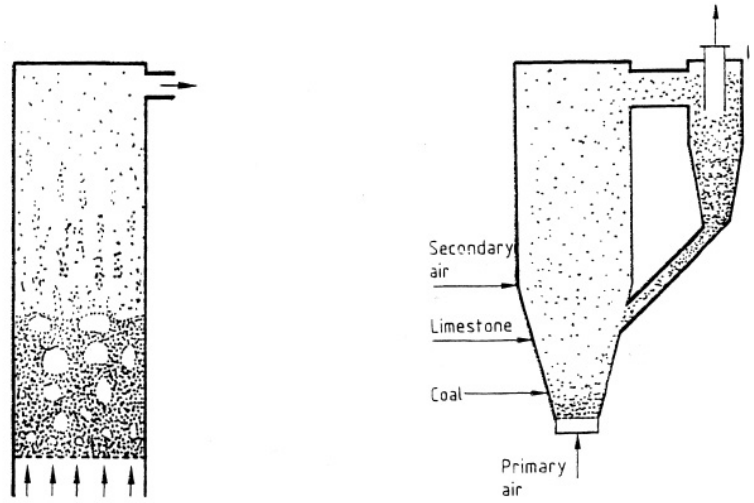

Fig. 3.2: Schematic of fluidised bed gasifiers; bubbling bed (left) and circulating bed (right).

Bubbling fluidised bed: In the BFB gasifier the oxidising agent is introduced at moderate velocities through a grate at the bottom of the reactor. The bed material is only occupying the lower part of the gasifier. The biomass material is first pyrolysed in contact with the hot, inert bed material, normally kept at 700-900^{o}C. The char is further gasified and the pyrolysis tars are cracked in the hot bed. The product gases thus normally contain low tar concentrations.

Circulating fluidised bed: In the CFB the velocity of the fluidisation gases is kept high, causing the bed to occupy the whole interior of the gasifier. The bed material is thus circulated between the gasification reactor and a cyclone separating the ash from the bed material and char. The char and bed material can then be returned to the gasification chamber.

4. FUEL CELLS

4.1 Introduction

A fuel cell is a device that directly converts the chemical energy of a fuel to electricity and surplus heat. Due to the direct conversion from chemical to electrical energy, fuel cells have the potential for high efficiencies; the theoretical maximum efficiency of fuel cells are higher than that of piston or turbine based engines.

The different fuel cell types operate on equal principles, but there are variations in material, charge carrier, fuel gas quality limitations, operating temperature and application feasibility as briefly discussed in Section (4.2).

Emissions of particularly NO_x species may be kept low in fuel cell operation since there is no combustion in these devices. This is valid even for the high temperature fuel cells operating at temperatures of up to 1000^oC.

The advantages of fuel cells are, in addition to potentially high efficiency and low emissions, silent operation due to no moving parts, fuel flexibility (mostly for the high temperature fuel cells) and application flexibility. Important disadvantages are high production cost and limited operational lifetime. In some cases fuel cells are still immature due to the limitations and that better options exist.

A single fuel cell consists of three parts; two electrodes and a membrane or electrolyte separating the two. At the fuel electrode, the anode, fuel gas (H_2, CO, CH_4) is introduced. The fuel gas then diffuses towards the boundary between the anode and the electrolyte. In the zone were anode, electrolyte and fuel gas coexist (three phase boundary - TPB), the fuel components are oxidised thus liberating electrons (e^-). The electrolyte is not electron conducting, and the electrons therefore must travel through an external circuit to the air or oxygen electrode, the cathode. By putting a load in the external circuit, power is produced. At the cathode, the electrons are accepted by oxygen atoms. Depending on the type of fuel cell, one charge carrier or another must travel through the electrolyte and combine with either the fuel gas components at the anode or the reduced air atoms at the cathode. In the PEMFC (Proton Exchange Membrane Fuel Cell) as an example, hydrogen is oxidised at the anode producing electrons and protons (H^+). The protons are allowed through the PEMFC membrane and combines with oxygen ionised by electrons entering from the external circuit to produce water at the cathode. This process is schematically shown in Figure (4.1).

4.2 Fuel cell types

In this section a short overview of the different fuel cell types is given. Operating conditions are presented indicating main limitations and applications. Table (4.1) gives an overview of the operating temperatures and charge carriers for the different fuel cell types.

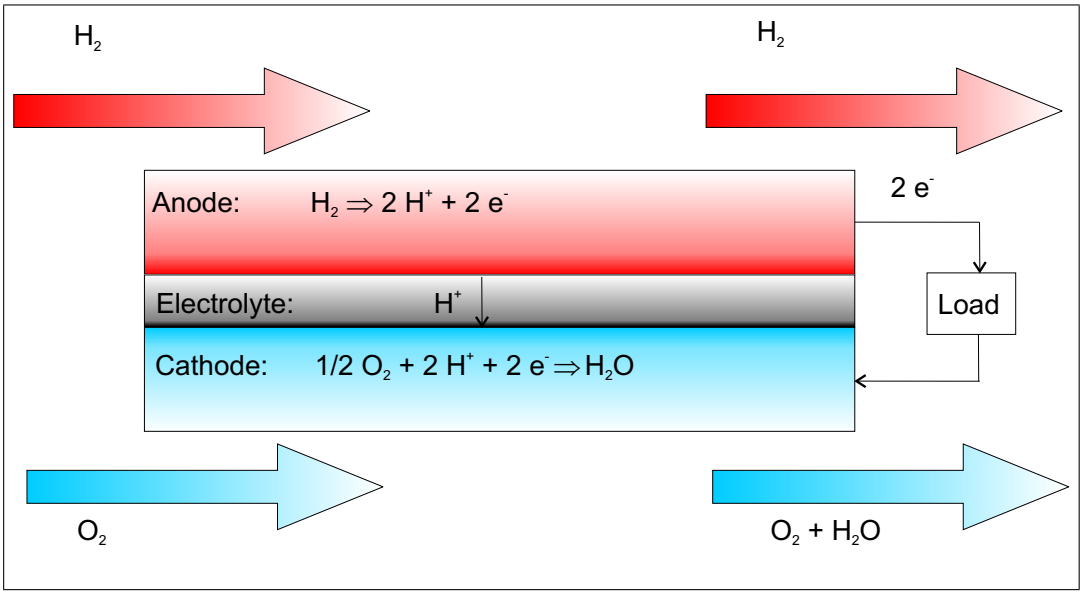

Fig. 4.1: General construction and working principle of a PEM fuel cell.

Fuel cell type	Charge carrier	Operating temperature [^{o}C]
PEMFC	H^+	50-200
AFC	OH^-	50-200
PAFC	H^+	$\sim$ 220
MCFC	CO_3^{2-}	$\sim$ 650
SOFC	O^{2-}	600-1000

Tab. 4.1: Fuel cell types and operational data (from Larminie & Dicks [35]).

4.2.1 Polymer electrolyte membrane fuel cell - PEMFC

The PEM fuel cell is a low temperature fuel cell operated at 50-200^{o}C. It has a humidified solid polymer electrolyte, thus the acronym polymer electrolyte membrane fuel cell. Protons (H^+) are the mobile charge carriers in the PEMFC electrolyte.

Due to the low operating temperatures of this fuel cell, the reaction rates are slow. This is compensated for by incorporating platinum in the anode material thus catalysing the reactions.

The PEMFC runs on hydrogen only and is very intolerant to impurities in the fuel gas. CO even in as low concentrations as 10 ppm lead to a significant performance loss due to CO adsorption on the anode Pt catalyst. This Pt-CO bond is stronger than the Pt-H bond thus effectively blocking the cell reactions. CO_2 in the fuel gas is also a problem since it may be converted to CO via the water-gas shift reaction.

PEMFC is considered to be suitable for small- and medium-scaled power plants and in vehicle applications [36], [37].

4.2.2 Alkaline fuel cell - AFC

The AFC is best known for its space applications. It was also the first fuel cell technology producing electricity from hydrogen in a feasible way. Nowadays the PEMFC has by far overrun the AFC in terms of research effort [38].

AFCs are, like the PEMFCs, operated at low temperatures in the range of 50-200^{o}C and must be fuelled by hydrogen. The electrolyte is a liquid alkaline solution (KOH or NaOH) where OH^- are the mobile charge carriers. As for the PEM fuel cell the AFC also needs means to overcome the problem of slow reaction rates. In the AFC this is done by using highly porous electrodes and platinum catalysts. The AFC can additionally be operated at elevated pressures to boost the performance [35].

It has been reported that the AFC has no tolerance towards CO_2 in the cathode feed stream [35], [38]. CO_2 is believed to reduce the ionic conductivity of the electrolyte and/or to have a blocking effect on the pores in the electrodes [38]. However, in a recent work by Gülzow and Schulze [39] it is concluded that there is no evidence for any effect on the cell performance of introducing 5% CO_2 to the cathode feed. On the anode side, CO and CO_2 are reported to have a negative effect on the cell performance. This effect is, however, reported to be reversible in most cases [38].

The AFC is considered as an option for transportation [40] and residential applications [36].

4.2.3 Phosphoric acid fuel cell - PAFC

The PAFC is a medium temperature fuel cell operated at approximately 220^{o}C. It has porous electrodes and platinum catalysts to speed up the reaction kinetics. As for the PEMFC and AFC pure hydrogen must be used as fuel. The electrolyte is made of liquid phosphoric acid contained in a silicon carbide matrix. Protons are the charge carriers in the PAFC electrolyte [35].

The PAFC experiences performance losses if CO is introduced to the anode gas flow. Even at CO levels below 1 vol% the performance loss is significant. It has also been reported that the losses due to CO poisoning increase with increasing operating temperatures [41].

The PAFC has been demonstrated to be suitable for stationary applications in the 50-500 kW range [42]. Larger PAFC systems (1 to 10 MW) for on-site power production e.g. for large buildings or industry are also being developed [36], [37].

4.2.4 Molten carbonate fuel cell - MCFC

Operated at around 650^{o}C, the MCFC is a high temperature fuel cell. As the name indicates, the electrolyte in the MCFC is a molten mixture of alkali metal carbonates, usually a binary mixture of lithium and potassium carbonates or lithium and sodium carbonates [35]. The MCFC requires CO_2 at the cathode as the net cathode reaction is:

$$O_2 + 2CO_2 + 4e^- \rightarrow 2CO_3^{2-} \tag{4.1}$$

The carbonate ions (CO_3^{2-}) facilitates charge transport through the electrolyte. At the anode the following net reaction occurs:

$$2H_2 + CO_3^{2-} \rightarrow 2H_2O + 2CO_2 + 4e^- \tag{4.2}$$

At the high operating temperature of the MCFC the catalytic properties of nickel are sufficient to give high reaction rates at the anode. Noble metal catalysts are therefore not needed thus reducing the production cost.

Unlike the other lower temperature fuel cells, CO may be electrochemically oxidised in the MCFC, in addition to hydrogen. The high operating temperature also makes internal reforming of light hydrocarbons in the fuel cell itself possible.

There are, however, several drawbacks connected to the MCFC technology. The most important ones are:

- Dissolution of the NiO cathode [35], [43].
- Electrolyte losses due to reactions between electrolyte and other fuel cell stack components [43], [44].
- Corrosion caused by the molten carbonate electrolyte [35], [43], [45].
- Low tolerance to impurities, especially sulphur [35], [43].

Furthermore, the required continuous supply of CO_2 to the cathode is considered to be a disadvantage [45].

In addition to electrical power, high temperature heat is produced in the MCFC. Medium to large scale MCFC plants combined with bottoming cycles such as a steam turbine or other heat demanding processes are therefore considered as application options [37], [45].

4.2.5 Solid oxide fuel cell - SOFC

The SOFC is a high temperature fuel cell which operates at temperatures between 600 and 1000^{o}C. The advantages gained at these high temperatures are similar to those for the MCFC:

- No expensive nobel metal catalyst is needed, nickel is sufficient.
- Fast reaction kinetics.
- Light hydrocarbons may be internally reformed in the fuel cell.
- Electrochemical oxidation of CO is possible.
- High temperature heat suitable for bottoming cycles is produced.

On the other hand, the high operating temperature of the SOFC limits the choice of cell materials. Only a few materials have been found to be suitable, and even these experience degradation during operation thus limiting the life time of the cells. The SOFC is furthermore reported to have low tolerance towards sulphur impurities.

The SOFC is an all-solid-state device making the fuel cell simpler in concept than the other fuel cell types as only gas and solid are involved in the operation [35]. The SOFC is considered as an option mainly for stationary power production [37].

A more detailed presentation of the SOFC is given in Chapter 5.

4.3 Choice of fuel cell type

Fuel gas quality and thus the required fuel pre-processing is becoming increasingly important as the fuel cell operating temperature decreases. The two high temperature fuel cells, the MCFC and SOFC, therefore have the lowest fuel quality demands as indicated in Table (4.2). Most importantly, in contrast to the other fuel cell types, CO is not a

poison to the MCFC and the SOFC, and may even be directly electrochemically oxidised in these fuel cells. The high operating temperature of the MCFC and SOFC furthermore enables internal reforming of light hydrocarbons to hydrogen and carbon monoxide. A wide range of fuels are therefore suitable for these two fuel cell types. At present the required fuel pre-processing for the MCFC and SOFC is limited to desulphurisation of the fuel gas.

Gas specie	PEMFC	AFC	PAFC	MCFC	SOFC
H_2	Fuel	Fuel	Fuel	Fuel	Fuel
CO	Poison	Poison	Poison	Fuel	Fuel
CH_4	Diluent	Diluent	Diluent	Fuel[1]	Fuel[1]
CO_2/H_2O	Diluent	Poison	Diluent	Diluent	Diluent
S	Unknown	Unknown	Poison	Poison	Poison

[1]By reforming to H_2 and CO

Tab. 4.2: Fuel cell types and fuel requirements (from Larminie & Dicks [35]).

In a system of combined heat and power production, the high temperature fuel cells are also the most suitable ones since a significant amount of surplus high temperature heat is produced, in addition to electrical power.

Comparing the MCFC and SOFC, one major advantage of the latter is the relatively simple all-solid construction. The problems associated with the molten electrolyte of the MCFC are thus eliminated and more stable long-term operation may be expected for the SOFC. In addition, the required CO_2 supply to the cathode is a disadvantage of the MCFC adding significantly to system complexity.

Biomass gasification is normally carried out at temperatures around 900°C, i.e. in the SOFC operating temperature interval. Thermal integration of biomass gasifiers and SOFCs may therefore, in principle, be simple. However, there is a need for filtration of biomass gasifier producer gases prior to the SOFC inlet and the gas must therefore most probably be cooled down to the filter's operating temperature, and then heated again before entering the SOFC unit.

Biomass gasifier producer gases may contain significant amounts of sulphur components. At present, sulphur is known to reduce the SOFC performance and desulphurisation of the producer gas may therefore be required. In addition, particles present in the producer gas should most probably be removed to avoid blocking of the porous SOFC anode structure. Tars present may be cracked or reformed to light hydrocarbons and may therefore contribute to the power production in the fuel cell. However, the tars may also cause carbon build up on the anode structure thus reducing the cell performance. No work has so far been published confirming either of these possibilities. Furthermore, gasifier producer gases may contain significant amounts of alkali metals and chlorine. Their effect on SOFC performance and material stability is not yet known.

Summing up, the SOFC may be the most promising fuel cell technology for utilisation of biomass gasifier producer gases. There are, however, many unknown factors that need to be investigated to be able to draw any clear conclusions. In the following chapters, some steps towards these conclusions are carried out. First, a more detailed study on SOFC fundamentals is presented. Results from modeling on the composition of gasifier producer gases are then presented. Focus is put on the trace species, sulphur, potassium, sodium and chlorine and their conversion as amount of the different species, temperature and fuel conversion are varied. Next, the SOFC performance under varying inlet fuel

composition is experimentally investigated. A comparison of the SOFC performance when switching fuel from reformed natural gas to gasifier producer gas is also done. Finally, SOFC performance degradation at high levels of sulphur is investigated.

5. SOLID OXIDE FUEL CELLS

In this chapter a more detailed description of the Solid Oxide Fuel Cell (SOFC) is given. Focus is put on the most common SOFC, namely the zirconia based type. Essentials on SOFC materials and structure, operation and limitations are presented. Furthermore, some of the literature on reported fuel flexibility of the SOFC is cited.

5.1 Introduction

The SOFC is an all-solid fuel cell operated at high temperatures (500-1000^{o}C). The state-of-the-art SOFC still uses zirconia (ZrO_2) as electrolyte material, over a century after Nernst first found zirconia to be an oxygen ion conductor. Due to the temperature dependency of the conductivity of zirconia, these SOFCs are normally operated at temperatures above 700^{o}C. In addition to power produced at potentially high efficency, high temperature heat is produced. Thus, several cell and system configurations have been proposed and investigated, and the SOFC may be well suited for combined heat and power production. The surplus heat may also be used in a bottoming cycle.

The SOFC may utilise a variety of fuels since both hydrogen and carbon monoxide may be electrochemically oxidised in these fuel cells. This flexibility is further increased by the possibility of internal reforming of hydrocarbon fuels thus producing a mixture of H_2 and CO. Emissions of especially NO_x species is believed to be kept low since there is no combustion occurring in fuel cells. The direct conversion from chemical to electrical energy also implies that the energy conversion is not governed by the Carnot efficiency limit[1]. There are, however, other factors limiting the SOFC conversion efficiency as described later.

5.2 History

Nernst described stabilised (doped) zirconia as an oxygen ion conductor at temperatures between 600 and 1000^{o}C in the late 19th century. In the 1930s Baur and Preis demonstrated a zirconia based lab scale fuel cell. Then, in the 1950s experiments were performed using flat plate zirconia cells in a more robust setup similar to the ones still in use today. The problems of structural integrity in scale-up and gas leakages became evident in this period, and the tubular design was suggested and investigated. Westinghouse (now Siemens Westinghouse) has continued their research on the tubular design until today, and has also demonstrated rather successfully combined SOFC gas turbine (SOFC/GT) plants. This demonstrates that the problems related to gas leakages can be overcome as the SOFC/GT plants utilise pressurised tubular SOFC stacks. During the 1990s, the flat plate design has regained interest, and a large research effort has been put down at universities and companies worldwide.

[1] The Carnot limit is defined as η=(T_1-T_2/T_1), where T_1 is the maximum temperature of the heat engine and T_2 is the temperature at which the heated fluid is released

The Norwegian SOFC effort started by a research project called NorCell. It was initiated by the late Professor Per Kofstad at the University of Oslo in the 1980s and was a co-operation between Norwegian companies (Statoil and Statkraft among others) and SINTEF and the Research Council of Norway. The project ended in 1991, followed by NorCell II. Statoil left this project and Elkem joined through its US subsidiary, Ceramatec. In NorCell II a 1.4 kW planar SOFC stack was demonstrated, but the project was ended one year before planned due to impatient commercial partners.

Statoil, however, continued its SOFC research through the Mjøllner project. Several researchers from the terminated NorCell II project joined in and NTNU and SINTEF were included in the project in addition to the the CMR offspring, Prototech in Bergen. The Mjøllner was concluded by the demonstration of a 10 kW planar SOFC stack operating on natural gas. After the project ended, Statoil withdrew from SOFC related research. Prototech is still today the only Norwegian company concerned with SOFC component and system development.

5.3 Operation

A single SOFC is made of three parts; anode, electrolyte and cathode. The electrolyte is made dense and gas tight thus separating the fuel and air streams to the anode and cathode, respectively as schematically shown in Figure (5.1). The cathode and anode are made porous to facilitate diffusion of the gaseous reactants and reaction products through the electrodes.

Apart from separating the gas streams, the purpose of the electrolyte is to conduct oxygen ions from the cathode to the anode. At the three-phase boundary (TPB), where cathode material, electrolyte material and gaseous oxygen meet, oxygen molecules are reduced to oxygen ions by accepting electrons from the cathode material (Eq. 5.1). The oxygen ions are transported through the electrolyte to the three-phase boundary on the anode side. Here, in the region where anode material, electrolyte material and fuel meet, the oxygen ions react with H_2 and CO to produce H_2O (Eq. 5.2) and CO_2 (Eq. 5.3), respectively. The electrons thus liberated are conducted through the external circuit to the cathode thus closing the complete circuit as shown in Figure (5.1). By including a load in the external circuit, electrical power is produced.

$$1/2O_2 + 2e^- \rightarrow O^{2-} \quad \text{Cathode reaction} \tag{5.1}$$

$$H_2 + O^{2-} \rightarrow H_2O + 2e^- \quad \text{Anode reaction} \tag{5.2}$$

$$CO + O^{2-} \rightarrow CO_2 + 2e^- \quad \text{Anode reaction} \tag{5.3}$$

When utilising hydrocarbon fuels, these need to be reformed to CO and H_2 as shown for methane in Eq. (5.4). This is done to avoid carbon build-up on the anode surface.

$$CH_4 + H_2O \leftrightarrow 3H_2 + CO \quad \text{Reforming reaction} \tag{5.4}$$

$$H_2 + CO_2 \leftrightarrow H_2O + CO \quad \text{Water-gas shift reaction} \tag{5.5}$$

In addition, the water-gas shift reaction (Eq. 5.5) will, if equilibrated at the operating temperature, alter the gas composition in the anode chamber. The Ni-based SOFC anode is believed to facilitate this equilibration. The variation in the equilibrium gas

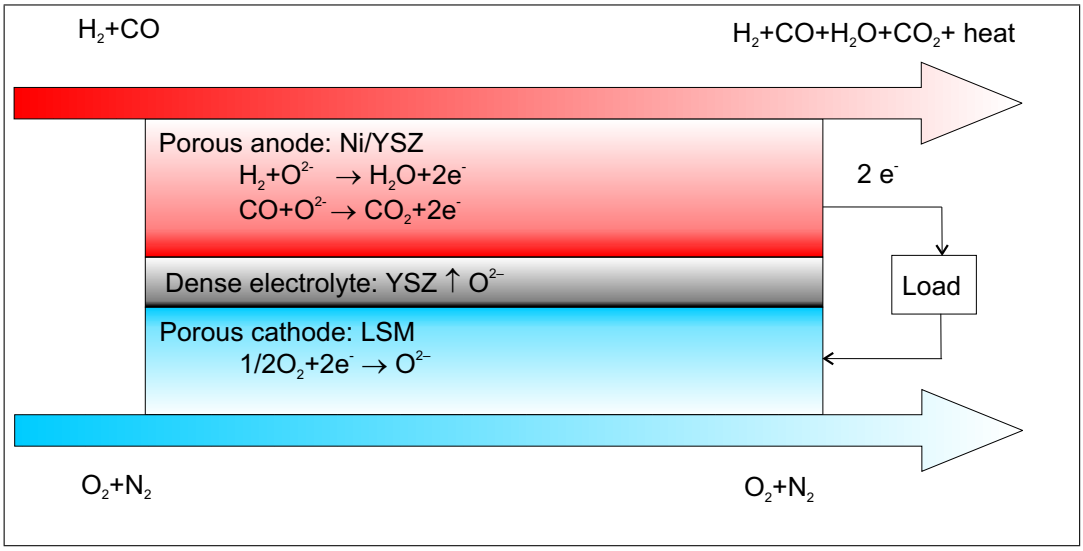

Fig. 5.1: Schematic of construction (not to scale) and main reactions of the Solid Oxide Fuel Cell.

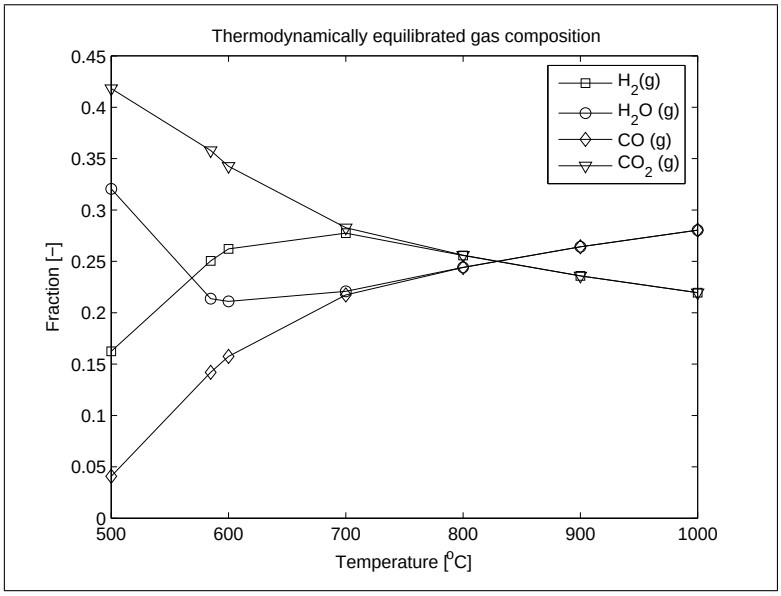

Fig. 5.2: Calculated equilibrium gas composition versus temperature for a mixture of 50:50 (vol-%) H_2:CO_2.

composition versus temperature for a gas mixture of 50:50 (vol-%) H_2:CO_2 is shown in Figure (5.2). The calculation was performed by the program FactSage [46].

The cell voltage of a single cell is governed by the Nernst equation for H_2 fuel (Eq. 5.6) and CO fuel (Eq. 5.7) given all the partial pressures are expressed in bar.

$$E_{emf} = \frac{-\Delta G^0_{H_2}}{2F} + \frac{RT}{2F} \ln \left(\frac{p_{H_2} \cdot p_{O_2}^{1/2}}{p_{H_2O}} \right) \tag{5.6}$$

$$E_{emf} = \frac{-\Delta G^0_{CO}}{2F} + \frac{RT}{2F} \ln \left(\frac{p_{CO} \cdot p_{O_2}^{1/2}}{p_{CO_2}} \right) \tag{5.7}$$

$$\tag{5.8}$$

The maximum cell voltage is obtained at no load conditions and is thus called OCV, open circuit voltage. The theoretical maximum voltage can be calculated by the Nernst equation, and may be measured in an experimental setup at least as long as the gas leakages are insignificant. As current passes through the cell, however, the voltage drops from the OCV due to three main voltage loss mechanisms; activation losses, ohmic losses and concentration losses. These loss mechanisms are discussed in more detail in Section (5.10). As shown in Figure (5.3), the different loss mechanisms dominates at different levels of current density.

The theoretical maximum voltage of a SOFC is around 1 V, depending on fuel gas mixture and operating temperature. However, under load a single cell is normally operated between 0.6 and 0.7 V. Several single cells are therefore stacked in order to produce the required stack voltage. The cell area dictates the maximum current that can pass through the stack. Between each single cell in a stack, interconnect plates are used to separate the electrodes in two adjoining cells and to distribute air and fuel to the cells.

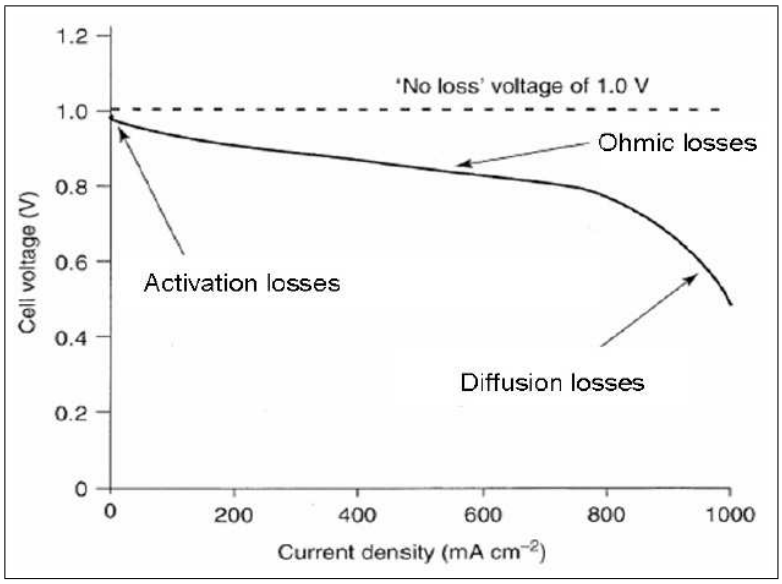

Fig. 5.3: Different voltage loss mechanisms and their importance versus current density (from Larminie & Dicks [35]).

When current is passing through the cell, the reactants (H_2 and CO) are consumed producing H_2O and CO_2. If all reactants are consumed, it can be seen from the Nernst equations that the cell voltage drops to zero. It is therefore normal practice to keep the fuel utilisation below 85% and to run the cells at high air excess ratios.

5.4 Stack design

There are at present three major SOFC cell and stack designs; planar, tubular and monolithic. The monolithic design experiences severe problems of sealing and thermally induced stresses which may cause delamination and cracking of the cells. Despite the fact that this design may show the highest power density, most cells and stack produced today are based on the planar and tubular design.

The tubular so-called seal-less design has been developed mainly by Siemens Westinghouse. The inner cathode tube is the mechanical support for the electrolyte and the anode. Interconnects are placed as a strip along the tube which is closed in one end. Air

is supplied through an inner tube introducing the air in the closed end of the cell. Fuel is flowing co-currently along the outside of the tube as shown in Figure (5.4).

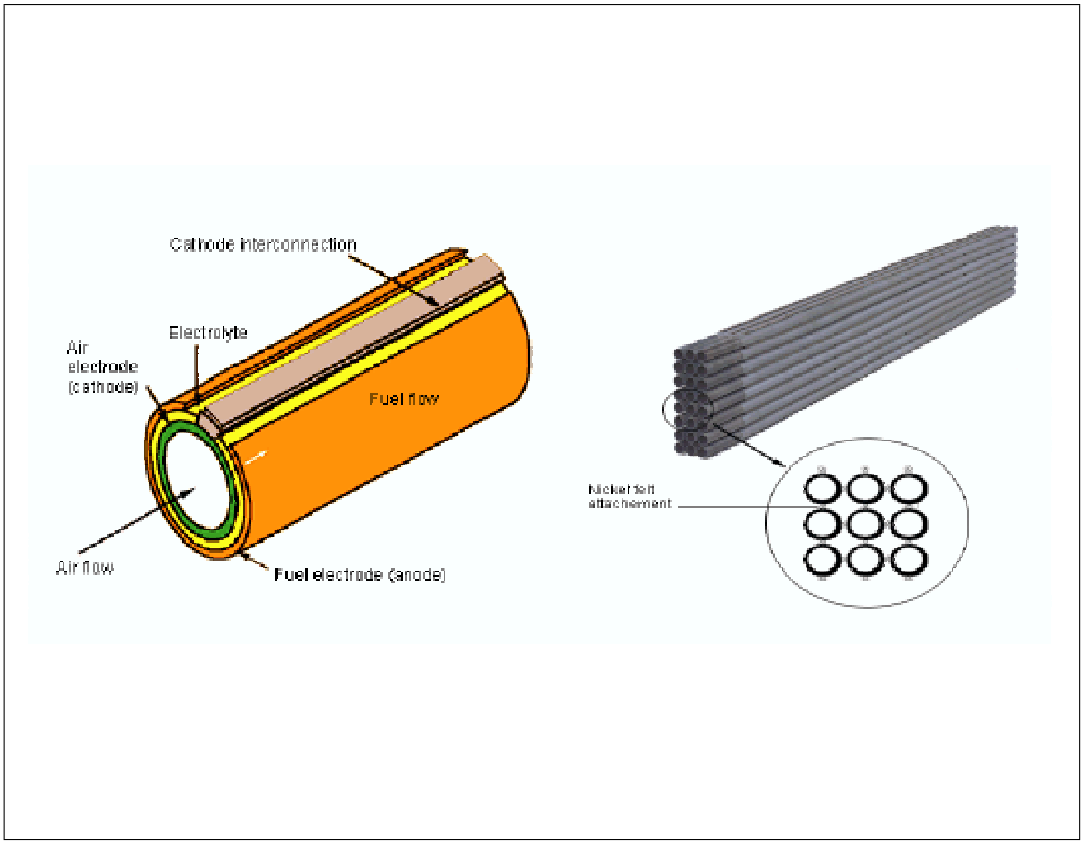

Fig. 5.4: Tubular cell and stack design (courtesy Siemens Westinghouse).

The planar SOFC cell and stack design has been paid an increasing level of attention through the latest decades. The design is schematically shown in Figure (5.5). It is currently being developed by many companies such as Sulzer Hexis and HTCeramix in Switzerland, Forschungzentrum Jülich in Germany and Haldor Topsoe and Prototech in Denmark and Norway, respectively. Geometrically the cells may be produced as circular, quadratic or rectangular flat plates and are normally anode supported. Active cell areas around 100 cm^2 are normal and the power density is generally higher in these cells than for the tubular cell design. The planar cells are rather easily produced by relatively cheap processes such as screen printing and can be stacked together with narrow flow channels. The cells in a stack are connected in electrical series which is a disadvantage in case one of the cells fail. A further challenge is that of sealing the stack to prevent fuel and air cross-over. The sealant should also not interact with other cell components.

5.5 SOFC materials

The properties of the materials in the SOFC and their structure are of great importance in achieving high performance and long term durability. The thermal compatibility of the adjoining cell layers (cathode, electrolyte, anode, interconnect) is governed by the choice of materials. Furthermore, the microstructure of the electrodes dictates the performance through its direct influence on the voltage loss mechanisms. The microstructure and the composition of the cell components also have an influence on the long term stability

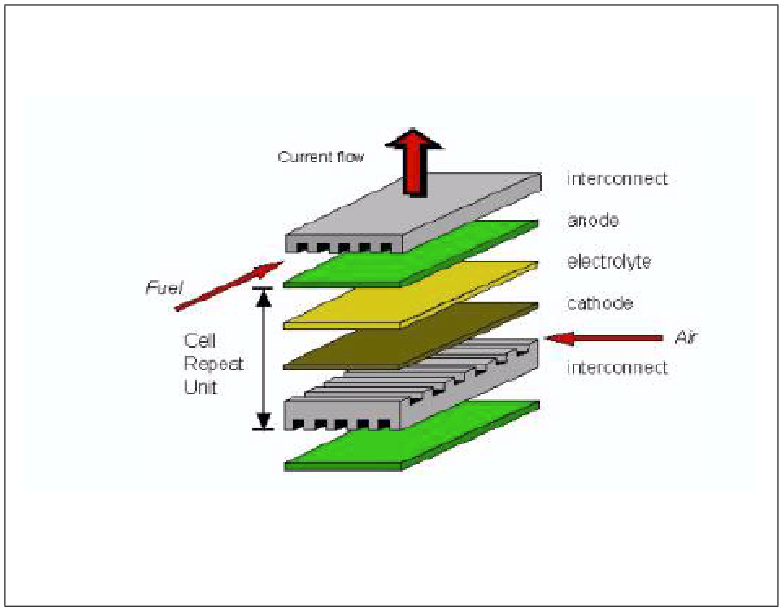

Fig. 5.5: Planar cell and stack design (courtesy Craig Fisher).

of the SOFC and thus limits or enhances the life time of the cell. Apart from cost reduction, the lifetime of the SOFC is by many regarded the major obstacle towards full commercialisation of the SOFC technology.

In addition to the electrodes and electrolyte, the interconnect separating the cell plates or tubes in a stack, is of great importance. The different materials must be chemically and physically stable at the operating temperature. In addition their thermal expansion coefficients must be compatible to prevent cracking and delamination. Morphological stability and stability towards phase transformation is important in order to maintain gas transport through the electrodes and ionic and electronic conduction through electrolyte and electrodes, respectively. Chemical interaction between the cell components may increase interfacial resistances between the different layers and should therefore be avoided.

The anode material must be stable in reducing atmospheres and have high electronic conductivity and high catalytic activity for the electrochemical oxidation of the fuel components. The cathode need, correspondingly, a high catalytic activity for the oxidant reduction and high electronic conductivity. It must also be stable in oxidising atmospheres. Both electrodes need high porosity to allow gas diffusion to and from the reaction sites at the electrolyte boundaries.

Since the electrolyte is situated between the two electrodes the material must be stable in both reducing and oxidising atmospheres. High ionic conductivity and low electronic conductivity is required in addition to complete gas impermeability. The interconnect material must also be stable in reducing and oxidising atmospheres, and must have high electronic conductivity in both. Additionally, gas impermeability is important to keep oxidant and fuel gas separated.

Usually, one of the electrodes or the electrolyte give the cell its mechanical strength. Thus, depending on the choice of supporting component, this material is additionally required to have a high strength. Due to the relatively low ionic conductivity of the state-of-the art electrolyte, it is now common to make the electrolyte as thin as possible. The tubular SOFCs of Siemens Westinghouse is supported by a thick cathode whereas

the planar SOFCs now normally are anode supported. The advantages of planar cells are shorter current path length compared to the tubular cells giving a higher performance and the possibility of cheap wet process fabrication methods such as tape casting. The tubular design has a great advantage in easier gas control reducing gas leakages.

The state-of-the-art SOFC electrolyte is zirconia (ZrO_2) stabilised by yttria (Y_2O_3) leading to the acronym YSZ (yttria stabilised zirconia). A composite of Ni and YSZ (Ni-YSZ) is used as anode material and the cathode is normally made of Sr-doped lanthanum manganite (LSM). In the following a more detailed presentation on aspects of the SOFC materials is given. Emphasis is given on the anode and electrolyte materials in the state-of-the-art SOFC. Other electrolyte and electrode materials have been investigated throughout the years. The underlying rationale is often to solve problems connected to the state-of-the-art SOFCs. However, in many cases new problems arise e.g. poor performance or a very narrow range of potential applications. This effort can nevertheless turn out to be a significant contribution in the work towards overcoming the problems of the most common SOFC technology.

5.6 Anode

The most important properties of the anode material are its catalytic activity and electrical conductivity. The anode must further provide reaction sites for the electrochemical oxidation reactions of the fuel gas and facilitate transport of electrons from the electrolyte/anode reaction boundary to the interconnect. Transport of gaseous reactants and reaction products must also be taken care of. The anode material must withstand the operating environment, i.e. high temperature and reducing atmosphere, for a preferential long period of time. This also includes chemical compatibility with the neighbouring components i.e. no reaction with the electrolyte, interconnect or sealant materials.

Fuel flexibility is important and the anode should therefore withstand impurities such as sulphur without degradation. Direct dry electrochemical oxidation of hydrocarbons without carburisation should be possible. Additionally, thermal compatibility is of great importance in the sense that the thermal expansion of the anode should be close to that of the electrolyte and interconnect. Finally, easy and cheap production is of paramount importance for market competitiveness and introduction into the market of heat and power generation.

Thus, there are several physical and chemical requirements for the optimum SOFC anode. The electronic and electrochemical nature of the fuel cell requires the anode to conduct electrons from the electrolyte interface to the interconnect, suggesting a metallic anode. At the same time it must be as porous as possible to allow unrestricted gas transport to and from the reaction sites at the boundary between anode and electrolyte. This interface must facilitate intimate contact on a microstructural level between anode and electrolyte. The three-phase boundary (TPB) between fuel, anode and electrolyte should not be confined to a two-dimensional plane but rather extend into the anode structure to ensure that a large reaction zone with many reaction sites is available[2].

The state-of-the art SOFC anode is the porous Ni-YSZ ceramic-metal composite (cermet) anode. This anode has gone through and is still under extensive research and development. The material has several advantages such as low cost, its thermal expansion is close to that of the electrolyte, it is chemically stable in reducing atmospheres and the intrinsic charge transfer resistance at the Ni/YSZ interface is low. Nickel is furthermore

[2] It is, however, most common to measure the TPB in one-dimensional length (m).

catalysing reforming reactions and is also a good electrocatalyst for the electrochemical oxidation reactions. The YSZ supports the Ni particles thus inhibiting agglomeration or coarsening of the nickel powder during operation. The YSZ, having predominantly ionic conductivity, additionally facilitates a broadening of the three-phase boundary. The metallic nickel finally provides the necessary electronic conductivity for the anode. Apart from its mechanical support functions and ion conduction, the YSZ in the anode may also take a more active part in the electrochemical reactions at the TPB. Mogensen and Lindegaard [47] has suggested that the YSZ surface participates by not only supplying oxygen ions, but also by hosting reaction intermediates.

5.6.1 Microstructure

For the electrochemical reactions to take place, the oxygen ions from the electrolyte must be able to discharge electrons to the anode. This is possible in the area where the gaseous fuel comes in simultaneous contact with the electrolyte phase (YSZ) and the metal phase (Ni), i.e. in the three-phase boundary (TPB). Due to the incorporation of YSZ in the anode composite, the TPB area is extended into the anode and not only confined to the two-dimensional interface between the anode and electrolyte. This increase in the TPB length, or TPB zone, directly improves the SOFC performance by reducing the operating voltage loss [48]. Thus there is a clear correlation between the length of the TPB and the SOFC performance [49].

In addition to the TPB length, the electrical conductivity and porosity of the anode, i.e. its microstructure, governs the performance of the anode and thus to some extent that of the SOFC. An optimisation of the anode microstructure and anode/electrolyte interface is therefore important to maximise the SOFC performance. In addition, durability of the microstructure is essential for long term operation.

When fabricated, the anode consists of YSZ and NiO particles which, during initial operation, are reduced to Ni in situ when exposed to hydrogen. During the reduction from NiO to Ni the porosity of the cermet anode increases. The pore volume may account for about 50% of the anode volume [50]. The porous structure makes diffusion of gaseous reactants and products to and from the reaction sites, respectively, possible. The porosity also provides a large internal surface in the electrode. Thus, the internal current density and losses are kept low even if the external current density is high [50].

5.6.2 Particle size

The YSZ particles in the anode cermet should be small to ensure a large TPB for the electrochemical reactions [51] and to reduce the risk of mechanical failure caused by macrocracks. Large YSZ particles are more prone to shrinkage during firing and the subsequent in situ reduction of NiO to Ni. However, a large size ratio between YSZ and Ni, i.e d_{YSZ}/d_{NiO} increases the electrical conductivity of the anode cermet due to better nickel-to-nickel contact [52], [53], [54]. Additionally, large YSZ particles increases the porosity of the anode and thus enhances gas transport. Another disadvantage of small YSZ particles, as pointed out by Mogensen and Skaarup [50] is the resulting large tortuosity and connectivity factors in addition to a large amount of grain boundaries.

Koide et al. [55] suggested only fine grains of YSZ (0.1μm) and Ni particles of 1μm but proposed a two-layered anode structure in terms of the Ni/YSZ volume ratio. A 40μm thick interfacial layer, with a Ni/YSZ volume ratio of 61:39 was first applied in order to minimise the contact resistance between the anode and the electrolyte. On top

of the interfacial layer a 160μm thick bulk layer (Ni/YSZ 40:60 volume ratio) was applied in order to reduce activation polarisation. By this structure, it is claimed, that even the outer bulk layer contributes as a triple phase zone i.e. it is electrochemically active.

Another suggestion made by Mogensen and Skaarup [50] is to make a binary Ni-YSZ cermet consisting of a network of small YSZ particles ($< 1\mu$m) combined with a significant volume of larger (10-20μm) YSZ particles. The small YSZ particles will then provide a large TPB to the Ni particles with small diffusion lengths for the reacting species. The large YSZ grains, on the other hand, will carry oxide ions far into the anode cermet thus broadening the electrochemically active region of the anode.

However, the high resistivity of YSZ towards oxide ion transport may limit the active electrode thickness [56], [57]. Primdahl and Mogensen [58] and Brown et al. [57] found that the electrochemical active thickness of the anode was 20μm or less and 10μm, respectively, in their experiments at 1000^{o}C. Virkar et al. [51] seems to confirm this by calculations of the effective charge transfer resistance (R_{ct}^{eff} see Section 5.10) as a function of electrode thickness. If the ionic conductivity of the MIEC (mixed ionic-electronic conducting) electrode is sufficiently high (above $\sim$0.001S cm^{-1}), the charge transfer resistance decreases with increasing composite electrode thickness up to somewhere between 10 and 100μm. A plausible explanation seems to be that the electrochemical active thickness is, in this case, more than 10μm but less than 100μm. Furthermore, by reducing the operating temperature, the active anode thickness may be even thinner as the oxide ion conduction in YSZ is strongly dependent on temperature.

Apart from the electrochemically active region of the anode, the anode cermet thus acts as a current collector and gas distribution system between the active functional layer and interconnect [48] and may also, when applicable, act as a catalyst for the reforming reactions of hydrocarbon fuels [54].

The Ni particle size has bee found to probably be of less importance (1-5 μm) than that of the YSZ grains [50]. However, Dees et al. [59] found the interfacial resistance between the Ni-YSZ anode and YSZ electrolyte to decrease by reducing the nickel particle separation. This was accomplished rather by reducing the nickel particle size than by increasing the nickel content of the anode. van Berkel et al. [48] also agreed on preferentially keeping the Ni particles small, but, in contradiction to many authors, concluded that the d_{YSZ}/d_{NiO} ratio of the anode should be kept large to increase the TPB length. As pointed out by Primdahl and Mogensen [58] the large size ratio between the particles in that study may rather be a suggestion to enhance the electrolyte surface during cell fabrication by applying a coarse layer of YSZ grains before the anode cermet is deposited.

5.6.3 Electronic conduction

An electronic percolation path is needed from the TPB to the interconnect for the anode to be electron conducting. The nickel particles must be well connected with each other to obtain low resistance electronic paths through the anode. The electronic conductivity therefore increases with increasing Ni content. However, as mentioned by Dees et al. [52], the nickel content should be kept as low as possible due to the high thermal expansion coefficient of nickel compared to YSZ.

A percolation threshold of 30-40 vol% Ni has been established [52],[55],[56]. Below this limit the Ni-YSZ cermet shows predominantly ionic conductivity since the YSZ phase must facilitate the charge transfer and the ohmic resistance of the composite increases significantly. The electronic conductivity of the anode then drops to that of the YSZ

phase which is in the order of one fifth of that of nickel [52]. Above the percolation threshold the anode shifts to primarily electronic conductance through the nickel phase. The percolation threshold has, however, been found to be influenced by factors such as porosity, pore size, size distribution, size of raw powders and the contiguity of each component [54]. Dees et al. [52] found no connection between YSZ particle size and the percolation limit.

5.6.4 Preparation

To be able to optimise the microstructure of the finished SOFC, the starting powders and fabrication method must be optimised. The particle sizes of the starting powders dictate the particle sizes of the finished anode cermet. The YSZ particle size of the finished cermet is additionally influenced by the pre-calcination temperature and the sintering temperature determines the Ni particle size [48]. Kawada et al. [56] found the characteristics of the electrodes to be affected by preparation conditions such as nickel content, pre-calcination temperature and baking temperature. They found that the NiO and YSZ particles should be pre-calcined at 1700K and finally baked at 1800K. The high baking temperature was in this work believed to cause improved sintering of the YSZ particles and thus lower the ionic resistivity of the YSZ phase. Pre-calcination of the electrode material is furthermore believed to prevent nickel particle sintering and the subsequent performance degradation of the electrode [53]. Shrinking of the electrodes during firing may lead to reduced gas permeability and significant shear stresses at the interfaces to the electrolyte [60].

As studied in detail by Vels Jensen [61] the purity of the starting powders is essential. Impurities present in the initial Ni and YSZ powders and contamination during processing and operation may aggregate at the TPB thus reducing the TPB length. This may cause a significant increase in the interfacial resistance between anode and electrolyte. The impurities are typically oxides of Si, Al, Fe and Na. Removal of the impurities represents an additional cost and the silicate and alumina may also be deliberately added to improve sintering of zirconia. As suggested by Brown et al. [57], the impurities may also increase the activation energy of the anode reactions thus further limit the operating cell voltage.

5.7 Cathode

The cathode must provide reaction sites for the electrochemical reduction of oxygen to oxygen ions. As for the anode, the electrochemically active part of the cathode is the three-phase boundary between cathode material, electrolyte and gaseous oxygen. The microstructure of the cathode is important and optimisation of porosity, tortuosity and pore size is essential.

The cathode operate in a highly oxidising environment preventing the use of base metals as electrode material. In addition, the use of noble metals are eliminated due to cost aspects. Semiconductive oxides have therefore been chosen as cathode materials. The state-of-the-art cathode material is Sr-doped lanthanum manganite (LSM) typically $La_{0.8}Sr_{0.2}O_3$ [62]. The dopant increases the electronic conductivity and limits phase transitions. The TPB may, as for on the anode side, be extended into the cathode material by incorporation of YSZ as is the practice in the planar Jülich cells [63].

5.8 Electrolyte

The state-of-the art electrolyte in SOFCs is the metallic oxide yttria-stabilised zirconia (YSZ). Zirconia (ZrO_2) may exist in three different stable structures. The monoclinic structure is stable at room temperature and is transformed to tetragonal at 1170^{o}C. The phase transformation to the cubic structure occurs at 2370^{o}C [64]. The monoclinic structure is mainly an electronic conductor, and is therefore not usable as electrolyte. The tetragonal phase is unstable in moist atmospheres. Therefore, the cubic zirconia structure is the preferred one. The cubic structure may be obtained even at low temperatures by addition of yttria (Y_2O_3) at around 8 mol% (8YSZ). The addition of yttria also leads to oxygen ion vacancies and this defect structure enhances the ionic conductivity of the electrolyte material [65].

The YSZ composition of 8 mol% yttria and 92 mol% zirconia (8YSZ) has normally been used in the SOFC application since the ionic conductivity shows a maximum around this ratio [64],[66],[67]. The mechanical strength of the YSZ, on the other hand, decreases with increasing yttria content but is found to be nearly constant in the interval between 7.7 and 8.5 mol% [66]. Above 9.5 mol% the flexural strength of the YSZ decreases by 50% compared to that at around 8 mol%.

Although an yttria content of 8 mol% is often assumed to be sufficient to stabilise the cubic structure down to room temperature, there is evidence that contradicts this assumption e.g. in the work by Gibson et al. [66] and Haering et al. [68]. The latter reported that the conductivity of 8YSZ decreases significantly at 1000^{o}C as a function of operation time, and may thus after some time be lower than that of the more stable 10YSZ (10mol% yttria). This, according to the authors, may be due to a change in the nanostructure of the electrolyte material, most likely a change in the defect structure. Gibson et al. [66] suggests that the conductivity decrease over time experienced for 8YSZ yttria is caused by precipitation of the less conductive tetragonal phase.

Appel et al. [69] studied the effect of addition of small amounts of Mn in YSZ. The rationale for the study is based on the fact that Mn from the state-of-the-art LSM cathode may diffuse into the electrolyte during operation [70]. Appel et al. [69] found that at 1000^{o}C the addition of more than 2 mol% Mn to a 7.9YSZ (7.9 mol% yttria) stabilised the cubic structure of the YSZ electrolyte. However, at lower operating temperatures the stabilising effect of Mn was found to diminish and at all temperatures decreased the ionic conductivity of the electrolyte. It may therefore be concluded that Mn diffusion into the electrolyte at all temperatures should be avoided when considering the electrolyte's conductivity, but that a Mn content above 2 mol% may reduce the degradation rate of the electrolyte material in high temperature operation.

5.9 Interconnect

The interconnect material must be stable in reducing and oxidising atmospheres. It must also show high electronic conductivity at high temperatures and should not react with the electrodes. The required electronic conductivity suggests the use of metallic interconnects. However, at high operating temperatures metals are easily oxidised on the air side.

Since the 1970s, the perovskite lanthanum chromite ($LaCrO_3$) has been used as interconnect material in the SOFC. By adding dopants such as Sr phase transition is avoided, and at a doping of 20 mol% the thermal expansion coefficient of the material is close to that of YSZ. Interaction between the interconnect material and especially glass-based

sealants may, however, occur. Furthermore, doped $LaCrO_3$ may expand in hydrogen rich atmospheres producing cracks in large interconnect plates.

For systems operating at lower temperatures, ferritic metal alloys such as stainless steel may be used as interconnect materials. Sulzer Hexis uses chromium based alloys with small amounts of iron and yttria in their small scale residential combined heat and power units. The thermal expansion coefficient of this alloy is close to that of YSZ. The metallic interconnects are cheaper to produce than the perovskites and have better thermal conductivity.

5.10 Performance loss mechanisms

As mentioned in Section (5.3) there are several loss mechanisms involved in SOFC operation causing the cell not to operate at the theoretical maximum voltage. If the gas leakages and fuel and air crossover are insignificant, the theoretical OCV (Open Circuit Voltage) may be obtained in SOFC operation. However, as current is drawn through the cell, the voltage drops instantaneously. There are three main mechanisms causing this voltage drop; activation losses, ohmic losses and concentration losses. Each mechanism is most significant at different levels of current density as shown in Figure (5.6). This causes changes in the gradient of IV-curves (current-voltage curves) at different levels of current density. In high temperature operation, the activation losses may not be visible in the IV-curves, but the mechanisms causing these losses are nonetheless contributing to the overall voltage drop as current passes through the cell.

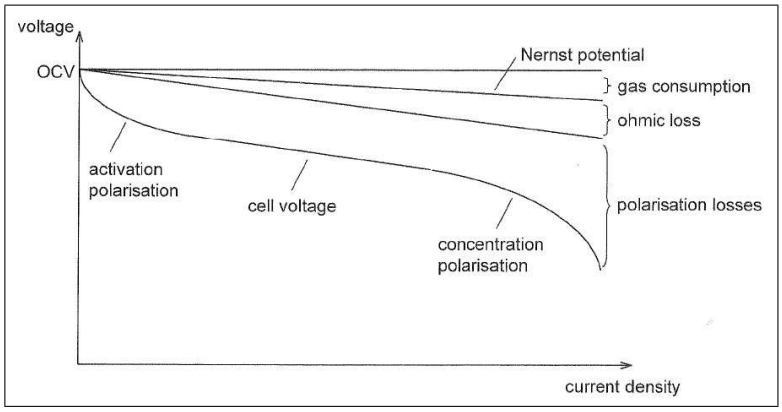

Fig. 5.6: IV curve showing loss mechanisms relevant for SOFC operation (from Singhal & Kendall [62]).

Throughout the literature several terms are used for the observed voltage losses. This is to many readers a source of confusion and even misunderstanding. The electrochemically correct term is overvoltage, overpotential or polarisation/polarisation resistance. The thermodynamic society probably prefers irreversibilities. Loss or voltage drop may be too vague, but at least describes the results of the mechanisms visually on a IV-curve. The term polarisation is preferred in the following as this is the one mainly used in the literature presented below.

During operation, the cell performance may decrease over time due to increased polarisation. For the state-of-the-art SOFC important mechanisms increasing the polarisation are nickel agglomeration and nickel loss, contact resistance, chemical reactions and diffusion between the different cell layers and the interconnects, carbon deposition

due to direct conversion of hydrocarbon fuels and sulphur poisoning of the anode [54], [71]. Additionally, thermal cycling, i.e. cool-down and subsequent heat-up may decrease the SOFC performance due to changes in the cell structure. The level of fuel or oxidiser utilisation also has an influence on the SOFC operating voltage and may thus be regarded an additional loss mechanism; as the level of gas consumption increases, the Nernst potential decreases and the cell voltage thus decreases. A fuel cell running on 100% fuel utilisation would therefore operate at zero voltage. In practical fuel cell stacks a maximum level of fuel utilisation of 80-90% is practised.

In the following sections the polarisation mechanisms and the other performance degrading mechanisms are presented.

5.10.1 Polarisation

The term polarisation is used to describe voltage losses or electrode overpotential as a function of current density. Normally, throughout the literature these are divided into three main mechanisms:

- activation polarisation
- ohmic polarisation
- concentration polarisation

Based on these three mechanisms, the following expression for the cell voltage can be deduced i.e. the useful voltage output of an operating SOFC:

$$U_{cell} = E_{rev} - IR - \eta_{activation} - \eta_{concentration} \tag{5.9}$$

where

I = current passing through the cell

R = ohmic resistance of the cell

$\eta_{activation}$ = activation polarisation of both electrodes

$\eta_{concentration}$ = concentration polarisation due to mass transport limitations

Activation polarisation is caused by resistance towards charge transfer in the electrochemical reactions involved and may thus be considered a reaction resistance. As the electrochemical reactions occur at the TPB, the activation polarisation is directly connected to the length of the TPB. Although dominating at low operating temperatures and low current densities, activation polarisation is related to the whole operating interval.

Ohmic polarisation is caused by the ohmic resistance of the cell materials and is linearly dependent on current and current path. Both electrodes contribute through their resistance towards electron conduction and the electrolyte contributes through its resistance towards ion transport.

Concentration polarisation is voltage loss due to resistance towards diffusion of the gaseous species in the electrodes. The gases entering the SOFC normally flow over the electrodes in a laminar manner. Diffusion therefore must take care of the transport of the reacting species through the electrodes to and from the TPBs. At high current densities the relatively slow diffusion processes may limit the electrochemical conversion. Additionally, as the electrochemical reactions proceed, the reaction products formed at the anode dilute the fuel and the diffusion resistance increases.

Activation polarisation

Activation polarisation describes voltage losses caused by charge transfer at the reaction zones of the fuel cell and thus depends on the electrode-electrolyte interface. At the cathode TPB, electrons coming from the external circuit are transferred from the electrode material to the oxygen which is then reduced to oxygen ions. At the anode TPB the oxygen ions are oxidised by liberating their electrons to the anode material. Although not fully understood, it is believed that these reactions involve processes such as surface adsorption, dissociation and surface diffusion [62].

Thus, the activation polarisation must depend on the electrode microstructure; the length of the TPB, hydrogen partial pressure (anode), oxygen partial pressure (cathode), oxygen vacancy concentration and mobility in the electrolyte, electron concentration in the electrocatalyst and temperature [62].

The activation polarisation, or voltage loss, is caused by limitations in the reaction rate as current is passing through the fuel cell. Assuming that the charge transfer step determines the kinetics, the Butler-Volmer equation may be used as an estimate to model the activation polarisation:

$$i = i_o\left[exp\left(\frac{\beta z F \eta_{activation}}{RT}\right) - exp\left(-\frac{(1-\beta) z F \eta_{activation}}{RT}\right)\right] \tag{5.10}$$

where

i = current density
i_o = exchange current density
β = transfer coefficient
z = number of electrons participating in the reaction
F = Faraday constant
$\eta_{activation}$ = activation polarisation
R = universal gas constant
T = temperature

Without going into detail, approximated expressions for $\eta_{activation}$ can be derived from the Butler-Volmer equation for the low and high current density regimes, respectively [62]:

$$|\eta_{activation,low}| \approx \frac{RT}{zFi_o} i = R_{ct} i \tag{5.11}$$

$$\eta_{activation,high} \approx \frac{RT}{\beta z F} ln(i_o) - \frac{RT}{\beta z F} ln(i) \tag{5.12}$$

In the low current density regime, the intrinsic charge transfer resistance R_{ct} can be defined (in Ω cm^2) as [51]:

$$R_{ct} = \frac{RT}{zFi_o} \tag{5.13}$$

R_{ct} is a function of the electrochemical properties of the electrode/electrolyte interface and the TPB length. However, in a composite electrode, e.g. LSM-YSZ or Ni-YSZ, the TPB is stretched out into the electrodes as discussed previously. Thus, the activation polarisation may be lower than that given by R_{ct}. There is therefore, as concluded by Tanner et al. [72] an effective charge transfer resistance R_{ct}^{eff} that is governed by the

ionic conductivity and thickness of the electrode and microstructural properties such as particle size and electrode porosity.

Norby et al. [73] found the charge transfer resistance, R_{ct}, to vary with approximately $(p_{H_2O})^{-1/2}$ at low p_{H_2}. Also, at moderate p_{H_2} it was found that R_{ct} decreased linearly with increasing TPB length. Their overall conclusion was that the anode impedance increases with increasing p_{H_2} and decreases with increasing p_{H_2O}.

Matsuzaki and Yasuda [74] studied the electrochemical oxidation of H_2 and CO in a H_2-H_2O-CO-CO_2 system at the interface between porous Ni-YSZ and YSZ electrolyte. They found that the polarisation resistance increased when the CO concentration ratio defined as $p_{CO}/(p_{H_2}+p_{CO})$ exceeded 0.2 and 0.5 at 750 and 1000^{o}C, respectively. The increase in polarisation was believed to be caused by an increase in charge transfer resistance and mass transfer resistance with increasing CO concentration. The latter include dissociative adsorption of active species on the electrode surface and the subsequent diffusion of the adsorbed species on the electrode surface. At the lower temperature investigated in this work, 750^{o}C, it was concluded that mass transfer resistance caused the differences in polarisation whereas at 1000^{o}C it was concluded that both mass transfer resistance and charge transfer resistance play a role.

Mizusaki et el. [75] found the electrode-electrolyte interfacial conductivity (σ_e) in H_2-H_2O atmospheres to be essentially independent of p_{H_2} below 850^{o}C. At 850^{o}C however, they found σ_e to be dependent of $(p_{H_2})^{-2}$ at low p_{H_2}. They also found σ_e to depend on p_{H_2O} except for at low p_{H_2} at temperatures below 750^{o}C. Additionally, it was found that σ_e increases linearly with increasing TPB length, suggesting that the rate determining processes take place around the TPB. In another work by Mizusaki et al. [49] it was found that σ_e was essentially independent of p_{H_2} at low p_{H_2O} but increased with increasing p_{H_2O} when p_{H_2O} was large. They further proposed a reaction mechanism and claimed that the reaction between oxygen adsorbed on nickel and gaseous hydrogen is the rate determining step:

$$H_2(g) + O_{ad} \rightarrow H_2O_{ad} \tag{5.14}$$

Mogensen and Skaarup [50] gave an overview on some of the reported literature on electrode kinetics. They commented that the literature on SOFC electrode performance testing is full of contradictions and that normally no information about the reaction kinetics is given. They further conclude that the details on the rate determining mechanisms for H_2 oxidation on Ni-YSZ anodes are not yet fully understood. At least three processes are probably involved of which one or two depends on the microstructure. Adsorption and surface diffusion of H_2 on the Ni particles are not likely the rate determining processes and the rate limiting process may therefore take place on the TPB or on the YSZ surface.

Ohmic polarisation

Ohmic polarisation is caused by the electronic resistivity of the electrodes and the ionic resistivity of the electrolyte. In addition there are ohmic interfacial resistances between the electrodes and electrolyte. This voltage loss increases linearly with increasing current

density and can be expressed as [62]:

$$\eta_{ohmic} = (\rho_e l_e + \rho_c l_c + \rho_a l_a + R_{contact})i \quad (5.15)$$

where

ρ_i = resistivity of electrolyte, cathode and anode
l_i = thickness of electrolyte, cathode and anode
$R_{contact}$ = contact resistance
i = current density

Due to the relatively high ionic resistivity of YSZ, the largest contributor to the ohmic resistance is the electrolyte. The ionic resistivity of YSZ at 800^{o}C is around 50Ω cm as compared to the cathode's (LSM) and anode's electronic resistivities in the orders of 10^{-2} and 10^{-4} Ω cm, respectively [62]. However, as the operating temperature increases, the conductivity of the YSZ is significantly improved [65]. Nonetheless, by the development of thin film electrolyte (5-30 μm), electrode supported cells the ohmic polarisation is significantly reduced and thus the performance increases. At present it is therefore common practice to produce electrode supported rather than electrolyte supported cells.

Concentration polarisation

As previously mentioned, the electrochemical reactions in the SOFC occur at the TPB i.e. in the zone where electrolyte, electrode and gas are present simultaneously. The gaseous species must therefore travel from the bulk flow through the porous structure of the electrodes to reach the reaction zone. Additionally, at the anode side, the reaction products must be transported from the TPB out to the bulk flow again. As the bulk gas flow is generally laminar, diffusion must take care of the gas transport through the electrodes.

Diffusion is not generally causing significant voltage losses, but becomes the limiting factor at high current densities. Thus, concentration polarisation, or diffusion polarisation, is a physical resistance to gas transport through the electrodes and is a function of diffusivity and partial pressures of the gases to be transported, electrode microstructure and current density [62]. It is therefore important to optimise microstructural factors of the electrodes such as porosity, pore size and tortuosity in order to minimise the concentration polarisation.

The binary diffusion coefficient for a mixture of oxygen and nitrogen is lower than that for hydrogen in steam (at room temperature $D_{O_2-N_2}$=0.22cm^2/s, $D_{H_2-H_2O}$=0.91cm^2/s). Virkar et al. [51] therefore suggests that for comparable microstructures and electrode thicknesses, the cathodic concentration polarisation would be larger than the anodic.

5.10.2 Fuel utilisation

As mentioned in Section (5.3), the operating voltage of the SOFC is governed by the Nernst equations (Eq. 5.6 and Eq. (5.7)). As current passes through a SOFC, H_2 and CO are electrochemically oxidised and liberate electrons as shown in Eq. (5.2) and Eq. (5.3), respectively. Considering, for simplicity, the hydrogen oxidation reaction only one may see that the number of electrons liberated at the anode is twice the number of hydrogen molecules consumed; the molar flow of electrons, $\dot{n}_e$, is twice the molar flow of

hydrogen, $\dot{n}_{H_2}$:

$$\dot{n}_e = 2\,\dot{n}_{H_2} \tag{5.16}$$

The current drawn through the fuel cell is thus seen to be a direct, but simple, measure on the fuel consumption or fuel utilisation, U_f. Fuel utilisation may be expressed in terms of the molar flow of hydrogen entering ($\dot{m}_{H_{2,in}}$) and leaving ($\dot{m}_{H_{2,out}}$) the fuel cell:

$$U_f = 1 - \frac{\dot{m}_{H_{2,out}}}{\dot{m}_{H_{2,in}}} \tag{5.17}$$

At low fuel utilisation i.e. when the fuel flow is large compared to the current drawn, the fuel gas is essentially unaltered leaving the cell. In this case the Nernst potential is the same over the entire fuel cell area and can be calculated based on the inlet gas composition.

However, as the fuel utilisation increases the gas composition is changed by the production of H_2O and CO_2. The Nernst potential of the cell thus decreases as the increasingly diluted gas travels over the cell area. This mixing effect therefore represents a voltage loss as shown in Figure (5.6). In the extreme case of 100% fuel utilisation, the cell voltage would drop to 0 V. A maximum fuel utilisation of 80-90% in operating fuel cell stacks is therefore normal practice [62].

5.10.3 Cell degradation

The achievement and demonstration of durability and long life time of the SOFC technology is one essential remaining step towards commecialisation of the technology. The commercially required cell life time is by Badwal and Tanner [76] suggested to lie in the order of 40.000-50.000 hours. It therefore seems clear that the cell degradation rate must be small. The cell degradation appears as an increase in cell resistance and a consequently lower operating voltage due to changes in the structure and composition of the cell components.

Both electrodes as well as the electrolyte and the interfaces between may contribute to the cell degradation. The mechanisms and mutual contributions may not be fully known. However, anode-related mechanisms such as nickel agglomeration and depletion of Ni at high p_{H_2O} have been reported [54], [71]. Degradation of the YSZ electrolyte may involve ordering of the oxide vacancies thus reducing the ionic conductivity [78].

Nickel having a low melting temperature, may agglomerate at the electrolyte interface and change shape during the initial reduction from NiO and the subsequent operation [54]. Thus, as the Ni particles are coarsened or agglomerated, both the TPB and the electrical conductivity of the anode may be reduced [60]. Furthermore, nickel particles are high surface-area solids. Thermodynamically, there is therefore an additional driving force towards agglomeration i.e. minimisation of the free energy by minimising the surface area [60]. Nickel agglomeration is therefore thought to be caused by the poor wettability between the nickel and YSZ phases [71]. Additionally, as reported by Mogensen and Skaarup [50], the nickel atoms are quite mobile even at an as low temperature as 700°C. This certainly have an influence on the ability to maintain a very fine cermet structure over time.

By careful design of the anode microstructure, nickel agglomeration may be prevented or at least reduced [60]. The solution may be a binary mixture of coarse and fine YSZ particles thus constructing a network of coarse YSZ particles connected by fine YSZ

particles. This construction has been suggested by Mogensen and Skaarup [50] among others. The Ni agglomeration has been found to be accelerated by the presence of steam in the fuel gas as reported by Zhu and Deevi [54]. At high steam partial pressures, nickel may additionally be lost from the anode by evaporation and subsequent transport of the evaporated species by the anode fuel gas as reported by Gubner et al. [79]. The most significant specie in this respect is the volatile hydroxide, $Ni(OH)_2$. This process is increasingly important at higher operating temperatures and higher gas flow rates. At low p_{H_2O} the effect of nickel depletion by $Ni(OH)_2$ transport is expected to be insignificant [78]. High steam partial pressures however, reduces, as presented in Section (5.10.1) the polarisation losses at the anode-electrolyte interface [49] and is needed for hydrocarbon reforming as mentioned in Section (5.3).

Primdahl and Mogensen [78] reported that the cell degradation versus time in terms of an increased anode-related polarisation at 1000^oC was found to be $10m\Omega\ cm^2$ per 1000 hours. At 850^oC the polarisation was found to increase at a rate of $100m\Omega\ cm^2$. In both cases the current density was $300mA\ cm^{-2}$. In this work it was also concluded that the degradation rate did not seem to be affected by applying a graded anode structure. The grading studied in this case was on the weight ratio between NiO to YSZ and not on particle sizes. The total cell resistance was in this work reported to decrease during the first 2-400 hours of operation. This might be due to better adhesion between the cell layers thus reducing the contact resistance.

Iwata [80] reported an increase in anode degradation of 14 μV/h at a current density of 300 mA cm^{-2} for an anode supported planar SOFC. The cell was operated on 50:50 H_2: N_2 for about 1000 hours at around 1000^oC. The degradation rate was calculated for the operation period between 600 and 1000 hours. The cathodic polarisation decreased during the first 100 hours of operation maybe due to an increase in the cathode/electrolyte interfacial conductivity. After this initial polarisation decrease the cathodic polarisation was stable during the rest of the experimental period. The anodic polarisation, on the other hand, increased more or less constantly through the whole experimental period. Another cell was run at approximately 900^oC and did not experience any increase in the anodic polarisation during the first 70 hours. This is ascribed to a lower nickel agglomeration rate at the lower operating temperature. Furthermore, post-experimental analysis showed that the initial pore radius distribution was significantly shifted during the 1000 hours of operation. The initial pores of radius around 10 to 200 nm were close to non-existent after the run. It was concluded that these pores seems to be related to the TPB, and that their growth into larger pores affects the anodic polarisation. The post-experimental analysis also showed that the nickel particle size changed from 0.1 to 1 μm initially to 1 to 10 μm after the run. The dispersion of the particles was in addition significantly narrowed. The anode degradation was thus found to be caused by Ni sintering reducing the specific nickel surface area and the contact area between anode and electrolyte.

The tubular cathode supported SOFC of Westinghouse (now Siemens Westinghouse) has been reported to be operated continuously up to 69000 hours with a performance degradation rate of less than 0.5% per 1000 h [81]. In their next generation cathode supported cells, the cell degradation rate was reduced to 0.2% per 1000 h during operation up to 13000 hours. Global Thermoelectric's anode supported planar cells were reported to degrade at a rate of 2.2% per 1000 hours during the first 5000 hours of operation, after which the degradation rate was reduced to 0.53% [82]. These degradation rates are, however, extrapolated values from a 800 hours test assuming a second order trend in the degradation rate.

Stolten et al. [83] reported data on long-term tests on single cell planar SOFCs and stacks. Single cells are reported to be operated for nearly two years at an average degradation rate of 1.4% per 1000 hours. A 10-cell stack was operated for 6000 hours at a degradation rate of 0.8% per 1000 hours and two 40-cell stacks were operated for 5000 hours degrading at an average rate of 0.3% per 1000 hours. The cell composition is, however, not clearly indicated in this work, but there was "some" alumina added to the YSZ electrolyte and "some" ceria in the Ni/zirconia anode. The cathode is made of Ca-doped lanthan manganite. Thus, the reported degradation rates may not be directly compared to those reported on the more common LSM/YSZ/Ni-YSZ SOFCs.

Cathode side ageing effects include reaction with the electrolyte forming a thin layer of low-conductive $La_2Zr_2O_7$ [77] and pore formation and pore movement causing increases in polarisation resistance [60]. In addition, when using chromium containing alloys as interconnect materials, evaporation of chromium and subsequent precipitation of Cr_2O_3(s) at the cathode-electrolyte interface may severely degrade the cathode TPB.

Chen et al. [84] found that the interaction between the LSM cathode and YSZ electrolyte resulted in formation of both $SrZrO_3$ and $La_2Zr_2O_7$. The processes was found to be temperature dependent and that both processing and operating temperature should be kept below 800^{o}C to prevent the formation of these low-conducting phases.

At an operating temperature of 1000^{o}C the 8YSZ electrolyte may not be stable and the conductivity may therefore decrease as a function of operating time [68]. As mentioned previously, this may be caused by changes in the defect structure or a partly change from the cubic phase to the less conductive tetragonal phase. A compromise between the highest initial conductivity and long term stability must therefore be made. Gibson et al. [66] found, however, the conductivity of 8.5YSZ (8.5mol% yttria) to be nearly constant over time at an operating temperature of 1000^{o}C. The experimental time in this work was only around 80 hours, and may therefore not be representative at long-term operation.

5.10.4 Thermal cycling

Rapid thermal cycling may increase the possibility for crack formation and delamination of the cells. This may also be caused by large temperature gradients over the cell.

Primdahl and Mogensen [78] ran a SOFC anode through nine thermal cycles from 1000 to below 100^{o}C at 100^{o}C h^{-1}. Over the first two cycles the anode-related polarisation was found to increase by about 15mΩ cm^2 per cycle. No degradation was found during the next seven cycles.

Hsiao and Selman [77] investigated the cathode and anode impedance before and after a thermal cycle from 950^{o}C to room temperature and up to 950^{o}C again. Even at the slow cooling and heating rate reported in this work (1^{o}C min^{-1}), the thermal cycle caused and increase in the cathode-electrolyte interfacial resistance. The thermal cycle was also reported to probably cause microstructural changes on the Ni/YSZ interface on the anode side of the SOFC. This is suggested to be caused by a loss of contact area between Ni and YSZ due to thermal expansion induced cracking or due to coalescence of nickel particles.

Singhal [81] reported that the Siemens Westinghouse tubular SOFC could withstand 100 thermal cycles from ambient temperature to 1000^{o}C within 5 hours without signs of mechanical damage or performance degradation.

5.10.5 Carbon layer

Methane may be reformed directly on the anode surface if steam is present. Dry oxidation of methane and reforming of higher hydrocarbons may cause carbon depositions on the anode surface which eventually blocks the porous structure. The following three reactions may contribute in carbon formation on the SOFC anode:

$$2CO \leftrightarrow CO_2 + C \tag{5.18}$$

$$CH_4 \leftrightarrow 2H_2 + C \tag{5.19}$$

$$CO + H_2 \leftrightarrow H_2O + C \tag{5.20}$$

Partial oxidation (POX) is an alternative for hydrocarbon reforming if steam is not available. The process represents understoichiometric combustion of the fuel and the fuel gas entering the SOFC has therefore a lower energy content. Thus, CO_2 and H_2O is produced via combustion, and the steam may subsequently be utilised for steam reforming of the remaining methane according to Eq. (5.4).

5.10.6 Sulphur poisoning

Sulphur, as H_2S, is normally present in natural gas and its influence on SOFC performance has therefore to some extent been investigated. From the literature on steam reforming, it is well known that sulphur degrades the performance of nickel based catalysts. Sulphur may chemisorb on the catalyst surfaces and thus block the reaction sites needed for the reforming reactions. The coverage has been found to depend on the ratio p_{H_2S}/p_{H_2} and temperature as studied by e.g. Alstrup et al. [85]. It may therefore be necessary to remove sulphur from the fuel gas when utilising hydrocarbon fuels in a SOFC system in order to maintain the reforming reactions and prevent coking of the anode.

There is also evidence that sulphur increases the polarisation losses at the anode-electrolyte interface. Dees et al. [59] studied the effect of adding up to above 100 ppm H_2S on SOFC performance when fueled by H_2/H_2O mixtures. It was found that the interfacial resistance between anode and electrolyte increased when sulphur was introduced to the fuel mixture. Matsuzaki and Yasuda [86],[87] found that the lower limit of detectable sulphur effects on the SOFC performance was 0.05, 0.5 and 2 ppm at 750, 900 and 1000^{o}C, respectively. In addition, they reported that the interfacial resistance regained its initial level after removal of the sulphur in the fuel gas. Geyer et al. [88] reported a doubling of the anode polarisation as 5 ppm H_2S was introduced in a H_2/H_2O fuel gas mixture to a SOFC operating at 950^{o}C. Primdahl and Mogensen [89] reported an increase in the anode/electrolyte interfacial resistance by 60% as 35 ppm H_2S was added to a similar fuel gas at 850 and 1000^{o}C. They found the effect to be reversible but independent of operating temperature and current density.

Singhal [90] reported that the tubular Siemens Westinghouse SOFC operating at 1000^{o}C experienced a 10% voltage drop during the first 24 hours when as little as 1 ppm H_2S was added to the fuel gas (H_2/H_2O). On removal of the sulphur from the fuel gas most of the voltage loss was recovered. Stolten et al. [83] reported a 2% drop in power output upon addition of up to 10 ppm H_2S at 950^{o}C.[3]

Petrik et al. [91] reported sulphur tolerance and stable operating at a H_2S concentration of 300 ppm. The extreme tolerance in this case may be due to that the quoted

[3] As mentioned in Section (5.10.3) the planar cell in this case is not completely a state-of-the-art SOFC, but is nonetheless a Ni-Zr based one.

sulphur-tolerant pre-reformer absorbs a significant portion of the sulphur prior to introduction to the SOFC.

Biomass gasification producer gases may, as shown in Paper I in this thesis, contain high levels of sulphur, mainly as H_2S. A study on the SOFC performance at high sulphur concentrations has therefore been performed. The main results are presented in Paper III.

5.10.7 Other losses

As mentioned in Section (5.6.4), contaminants from the cell fabrication materials as well as from fabrication processes and cell operation may cause a significant increase in the interfacial resistance between the anode and electrolyte as studied by Vels Jensen [61] and Mogensen et al. [92]. These impurities are typically oxides of Si, Al, Fe and Na. Although no results are published yet, it seems reasonable to assume that if such species are present in the fuel gas utilised in a SOFC, a further increase in the interfacial resistance over time may be expected.

Singhal [90] reported that 1 ppm HCl did not have any detectable effect on the SOFC performance at 1000^oC.

As shown in Paper I, biomass gasification gases may contain significant amounts of alkali metals and chlorine and compounds of these. Their influence, if any, on SOFC performance is not known and should therefore be investigated.

5.11 SOFC performance versus gas composition

The SOFC is able to electrochemically oxidise H_2 and CO and to some extent light hydrocarbons such as methane. There is some debate in the SOFC community regarding the importance of CO oxidation. As discussed below, the kinetics of the CO oxidation may be slower than the water-gas shift reaction. Thus, if water is present hydrogen may be the only fuel component taking part in the anode reactions. Furthermore, steam must be added when utilising hydrocarbon fuels, at least if Ni-YSZ is used as anode material. The steam reformed hydrocarbon gas mixture consists essentially of CO and H_2. Also in this case, H_2 may therefore be the only contributor to the anode oxidation reactions.

However, since CO is not a poison to the anode material, and at least to some extent may be electrochemically oxidised, the state-of-the art SOFC is highly fuel flexible. The limitation towards direct utilisation of hydrocarbon fuels is overcome by adding steam to the hydrocarbon fuel gas. The hydrocarbon fuel is thus reformed to CO and H_2 either in a separate normally nickel based pre-reformer or internally in the SOFC anode.

The most important overall reactions for the SOFC are, as presented in Section (5.3), the oxidation reactions of H_2 (Eq. 5.21) and CO (Eq. 5.22) (and CH_4 (Eq. 5.23)) in addition to the steam reforming reaction of methane (Eq. 5.24) and the water-gas-shift reaction (Eq. 5.25):

$$H_2 + 1/2O_2 \leftrightarrow H_2O \tag{5.21}$$
$$CO + 1/2O_2 \leftrightarrow CO_2 \tag{5.22}$$
$$CH_4 + 2O_2 \leftrightarrow 2H_2O + CO_2 \tag{5.23}$$
$$CH_4 + H_2O \leftrightarrow CO + 3H_2 \tag{5.24}$$
$$CO + H_2O \leftrightarrow H_2 + CO_2 \tag{5.25}$$

Matsuzaki and Yasuda [74] studied the electrochemical oxidation of H_2 and CO at the interface between a porous Ni-YSZ anode and a YSZ electrolyte in various mixed atmospheres of H_2, H_2O, CO and CO_2. They found the polarisation resistance to increase above a certain CO concentration ratio (i.e. $p_{CO}/(p_{H_2}+p_{CO})$) as mentioned in Section 5.10. Furthermore, they found the electrochemical oxidation rate of H_2 to be 1.9-2.3 and 2.3-3.1 times higher than that of CO at 1023 and 1273K, respectively. Indications of comparable kinetics in reformed CH_4 and in a H_2-H_2O system were quoted. Additionally, it was found that the shift reaction (Eq. 5.25) is so rapid compared to the kinetics of the oxidation reactions that it can be assumed to be in equilibrium. Consequently, the H_2 oxidation is dominating, and the anode performance is essentially the same for a H_2-H_2O mixture as for a fuel mixture of reformed methane.

Primdahl and Mogensen [89] found the SOFC performance at 1000^{o}C to increase with increasing p_{H_2}. This is not surprising when considering the Nernst equation (Eq. 5.6) governing the cell voltage in terms of the partial pressures of the gaseous components. However, in this work it was found that above a p_{H_2} of 0.2 atm, the activation polarisation decreased with increasing hydrogen partial pressure. Thus, in addition to an increase in the cell voltage with increasing p_{H_2}, the anodic polarisation also decreases. In a later work by Brown et al. [57], the anode related resistance was found to be relatively constant with p_{H_2} in the interval between 0.03 and 0.97 atm. The resistance was in this work found to decrease with increasing p_{H_2O}.

Onuma et al. [93] studied the electrochemical reaction rates in a CH_4-H_2O system. An in-house made tubular electrolyte supported SOFC was operated between 600 and 900^{o}C on varying mixtures of CH_4 and H_2O. The anode was prepared as Pt paste deposited on the YSZ electrolyte, meaning that the results presented may differ from those obtained using a Ni-YSZ cermet anode.[4] However, they concluded that the H_2 electrochemical oxidation reaction is the dominating one between 600 and 900^{o}C. Furthermore, it was found that the rates of both the H_2 and CO oxidation reactions were enhanced in a CH_4-H_2O system compared to pure H_2-H_2O and CO-CO_2 systems, respectively. These phenomena were proposed to be related to the differences in adsorbed species at the TPB.

In a recent work by Costa-Nunes et al. [94] the performance of a planar SOFC operated at 700^{o}C on H_2, CO and a syngas consisting of H_2, CO and N_2 was compared. When operating on CO, the maximum power density obtained was only 50% of that obtained when operating on H_2. The performance was essentially the same when operating on syngas and H_2. This, according to the authors, demonstrates that when operating on the syngas, only hydrogen is being electrochemically oxidised. In contrast to the work by Primdahl and Mogensen [89] mentioned above, no significant change in the anode polarisation was found as p_{H_2} was varied between 0.1 and 0.97 atm. The addition of 0.5 atm H_2O was by Costa-Nunes et al. [94] found to cause a decrease in the current density at a given voltage at current densities above a certain level (175 mA cm^{-2}). A negative influence on the H_2 reaction kinetics by steam is suggested. At 800^{o}C the effect of adding 0.5 atm H_2O on the cell performance was, however, heavily reduced.

[4] According to Mizusaki et al. [75] one main difference between a Pt-system and a Ni-system is the reaction kinetics; the reaction rates in a Pt-system is one order of magnitude larger that those in a Ni-system. The cited results from the work by Onuma et al. may therefore be qualitatively valid for a Ni-based anode as well.

5.11.1 Reported fuel flexibility

Since the SOFC does not require pure hydrogen to work, several fuel options have been investigated throughout the literature. The fuel flexibility is also beneficial in an economical point of view as hydrogen production is expensive. The use of natural gas has been studied extensively through the years, and there is therefore a significant amount of published papers covering this. In the following some of the works on other SOFC fuels are presented.

Fossil fuel derivates

Pastula et al. [82] at Global Thermoelectric Inc. have tested a system of a 1kW$_e$ SOFC stack utilising natural gas as fuel. The natural gas was first desulphurised in a separate filter and reformed in a nickel-based pre-reformer.

Sulzer Hexis has been running several 1 kW$_e$ field test units on natural gas and modified versions of these fueled by home heating oil [95]. The version running on home heating oil used a Rh-based steam pre-reformer. Sulphur removal was found to be necessary to prevent degradation of the pre-reformer. The SOFC stack was built up by planar cells delivered by ECN/InDEC.

Westinghouse has performed long term tests with its tubular SOFC running on natural gas and reformed logistic fuels (DF-2 diesel and JP-8 jet fuel) [81]. The performance was reported to be similar for all three fuels over time, and the performance did not degrade over a total of nearly 6000 hours of operation. The JP-8 fuel has also been investigated at TMI by Petrik et al. [91]. They reported that by using a steam pre-reformer a 25-cell stack was operated for 1600 hours.

By utilising a Ru-based pre-reforming catalyst, Tompsett et al. [96] were able to run micro-SOFCs on a mixture of propane and butane. The system, including a co-generating gas burner, was suggested to be used as a leisure CHP system or to run micro-hybrid vehicles. Sammes et al. [97] studied internal reformation of butane by adding oxygen to the fuel stream. An oxygen-to-butane ratio of 1.7 was found to be sufficient to avoid coking in the SOFC anode at an operating temperature of 900^{o}C.

Zhan et al. [98] studied propane-air mixtures as fuel for in-house made anode-supported SOFCs. By keeping the oxygen-to-propane ratio above 1.75, stable power output was obtained without coking on the anode. Liu and Barnett [99] of the same group also studied utilisation of humidified (3% H_2O) methane and natural gas. At 800^{o}C the SOFC performance in terms of power density was slightly higher when using methane and natural gas compared to hydrogen. However, at open-circuit conditions carbon was rapidly deposited at 800^{o}C. At lower temperatures the carbon deposition rate decreased. A two-step reaction mechanism was proposed in this work; methane cracking followed by electrochemical oxidation of the resulting carbon.

Ahmed et al. [100] studied the use of reformed liquefied petroleum gas (LPG) as fuel for SOFCs. These gases have high propane and butane contents, but can be reformed to mixtures of CH_4, H_2 and CO_2. A 1kW SOFC stack was operated successfully on commercial LPG.

Stolten et al. [83] at Daimler-Benz/Dornier reported data on single cell SOFC performance operating on synthetic coal gas and a mixture of 2/3 H_2, balance H_2O. The long-term operation (4000 h) showed a significantly lower performance on the unspecified synthetic coal gas compared to the H_2/H_2O mixture.

Saunders and Kendall [101] and Saunders et al. [102] found that methanol, methanoic acid and formic acid can be used directly as fuel for SOFCs. By adding small amounts of

water or air, carbon formation on the anode was prevented. Also, by mixing iso-octane, ethanol, octanol and formic acid, their small tubular SOFC was found to be able to operate longer (4 h) than on iso-octane, ethanol or octanol alone [101]. However, carbon deposition occurred even in the mixed fuel case.

Thermodynamically, ethanol may also be directly reformed in the SOFC by adding appropriate levels of water as shown in [103]. It was shown that the minimum amount of water needed to prevent carbon formation decreases with increasing temperature. No experimental verification was reported.

Biomass derived fuels

Certain bacteria may metabolise organic matter under anaerobic conditions producing mainly methane and carbon dioxide. Stainforth and Kendall [104] studied the use of such gases as fuel for small tubular SOFCs. It was found that the CO_2 content of the biogas aided internal reforming of methane, but that addition of air to the gas was needed to prevent carbon deposition. The cell performance was reported to be almost equal to that of using hydrogen as fuel.

Stainforth and Kendall [105] also operated a tubular SOFC on landfill gas with a initial gas composition of 56 vol% CH_4, 26 vol% CO_2 and 18 vol% N_2. Apart from desulphurisation they found that addition of some oxygen to the fuel stream was needed in order to achieve complete reforming of the methane.

Ammonia is produced commercially, but may also be a significant component in some biogases. Wojcik et al. [106] studied cracking of ammonia and the subsequent electrochemical conversion of hydrogen in a specially designed tubular SOFC. By using an iron catalyst incorporated in a silver anode, the cell performance was similar when fueled by ammonia compared to pure hydrogen. In addition, it is noted that also nickel may act as a catalyst for cracking of ammonia to form H_2 and N_2, making ammonia a potential fuel component even for the state-of-the-art SOFC.

5.12 Conclusions

Even though the SOFC has been developed for more than a century, there are still problems connected to production methods, cost and long term operational stability. Production of the planar cells is easier and thus potentially cheaper than that of the tubular cells. However, a fully working assembly line for mass production of even the planar cells have proven difficult to establish. The cells produced at a specific site are therefore not fully standardised in the sense that the composition and performance of individual cells may be different from different production batches.

The SOFC performance is furthermore highly dependent on the quality and particle distribution of the starting powders. Impurities present in the starting powders may have a significant negative influence on the cell's performance. The cell performance is furthermore influenced by the mixture of the different species in the starting powders and the particle size distribution of the powders. The nickel content in the anode material must be over a certain limit to ensure proper electronic conduction from the three-phase boundary to the interconnect thus minimising the anodic ohmic polarisation. The ionic conductivity and thus the ohmic polarisation of the electrolyte is governed by the amount of dopant (yttria), and has been found to be minimised at around 8 mol% yttria (8YSZ). Incorporation of YSZ into the anode and cathode material may help broadening

the TPB; by applying two different YSZ particle sizes the TPB may be further increased and the activation polarisation is thus reduced.

The different loss mechanisms, the polarisations, are thus highly influenced by the microstructure of the two electrodes and the electrolyte. However, the microstructure may be altered during operation causing performance degradation. Nickel agglomeration may to some extent be retarded by applying the above mentioned binary YSZ particle mixture in the anode, but has been found to be accelerated by the presence of steam. At high temperatures steam may furthermore cause evaporation of nickel. On the other hand, steam has been found to reduce the polarisation at the anode-electrolyte interface and may furthermore be needed to reform hydrocarbon fuels.

Although there are several mechanisms causing cell degradation over time, long-term operation has been successfully demonstrated. By further improving the cell structure and operational stability, and reducing the production cost, SOFCs may increase its market attractiveness and thus become an option in future power production.

One of the most significant advantages of the SOFC is the high fuel flexibility. The SOFC is therefore the fuel cell type that is most suitable for utilising carbon containing fuels; hydrocarbon fuels may be internally reformed in the presence of steam and CO may be electrochemically oxidised. The high operating temperature is a further advantage in combined heat and power applications due to the simultaneous production of high temperature heat in addition to power. High overall efficiency is possible, particularly if the surplus heat is utilised in a bottoming cycle or other heat demanding processes.

A future system of heat and power production from biomass materials may be based on biomass gasification and SOFC. Steam gasification may be particularly suitable as it produces a gas rich in hydrogen. The level of hydrocarbons is low compared to natural gas, and there is also steam present that may be used for reforming internally in the SOFC. Based on the main gas composition, gasifier producer gases are therefore suitable as fuel for SOFC. An experimental comparison of the SOFC performance when utilising natural gas and gasifier gases should, however, be performed.

Biomass materials additionally contain other trace species such as sulphur, chlorine and alkali metals. When biomass materials are gasified these species may follow the gas stream. A detailed knowledge on the composition of the trace species in the SOFC operating temperature interval is needed. The influence these species may have on SOFC performance is furthermore not fully known. Sulphur is known to reduce the performance of steam reforming catalysts and the electrochemical performance of the SOFC. Most of the reported literature has, however, been related to sulphur levels relevant for utilisation of natural gas as fuel. The levels of sulphur in gasifier producer gases may be significantly higher. A detailed study on the SOFC performance at high sulphur levels should therefore be performed. Additionally, a study on the influence the alkali metals and chlorine and compounds of these may have on SOFC performance should be performed.

6. COMPOSITION OF BIOMASS GASIFICATION PRODUCER GASES

Gases from gasification of biomass consist mainly of H_2, CO, H_2O, CO_2, N_2 and light hydrocarbons. In addition there are minor species present such as compounds containing K, Na, S and Cl. The amount and speciation of the minor species varies with varying fuel composition, temperature and main gas composition.

Biomass gasifier producer gases are, due to the significant amounts of the combustibles H_2 and CO, suitable as fuel for the Solid Oxide Fuel Cell (SOFC). However, the impact from the minor species on the SOFC performance has not yet been thoroughly investigated. Prior to such experiments, a detailed knowledge on the composition and typical concentrations of the minor species is needed.

Due to the presence of alkali metals in gasifier producer gases, there is a risk of condensation of alkali rich carbonate phases. The temperature at which the condensation occurs depends on the amount and distribution of the alkali metals. Any condensation on the SOFC anode must be avoided as this will block the porous anode structure and therefore cause a significant decrease in cell performance. If methane is present and internally reformed in the SOFC, an endothermic process, the temperature may be lowered at the fuel gas inlet. In any case, the SOFC must be operated well above the condensation limit. In Section (6.2) the condensation limit as a function of the amount of alkali metals is further investigated.

Results from equilibrium calculations on two typical biomass gasifier producer gases are presented in Paper I; one from air blown downdraft gasification of wood pellets and one from steam gasification of wood chips. In both cases a parameter study has been performed. The parameters that have been varied are: the amount of the minor species, K, Na, S and Cl, the operating temperature and the level of fuel conversion (i.e. oxygen is added thus simulating an increasing level of oxidation of the combustibles). Thus, typical levels and the speciation of the minor components in biomass gasification gases have been modelled in a broad range of conditions relevant for SOFC operation.

6.1 FactSage

The calculations presented in this chapter have been performed using the program FactSage [46],[107]. In this chapter the Equilib module in FactSage has been used. This module calculates the chemical equilibrium of any given system containing the chosen species based on minimisation of the Gibbs free energy. For a given temperature, pressure and composition the total Gibbs energy can be represented as:

$$G = \sum_i n_i \mu_i \tag{6.1}$$

Here n is amount, μ is chemical potential and the sum is over all chemically distinct species of the system [107].

When the elements or compounds are specified, FactSage calculates the concentration of the chemical species after the initial elements have reacted or partially reacted to reach a state of chemical equilibrium [46].

FactSage databases consist of two different types, compound databases (for pure substances) and solution databases. The compound databases are for solid, liquid and gaseous species, whereas the solution databases are for solid and liquid alloys, carbides, nitrides and carbonitrides, concentrated aqueous solutions, ceramics, salts, mattes, etc. FactSage also permits user defined databases [46]. The following built-in databases are available in the FactSage version used here:

- Compound databases:
  - FACT - F*A*C*T 5.0 compound database
  - SGPS - SGTE pure substances database
  - SGSL - SGTE intermetallic compounds
- Solution databases:
  - FACT - F*A*C*T 5.0 solution database
  - SGSL - SGTE alloy database

6.2 Condensation limits

The temperature at which condensation starts depends mainly on the amount of potassium present. Thus, for different compositions of biomass material, the condensation temperature varies, assuming that all alkali metals initially present in the material follow the gas flow.

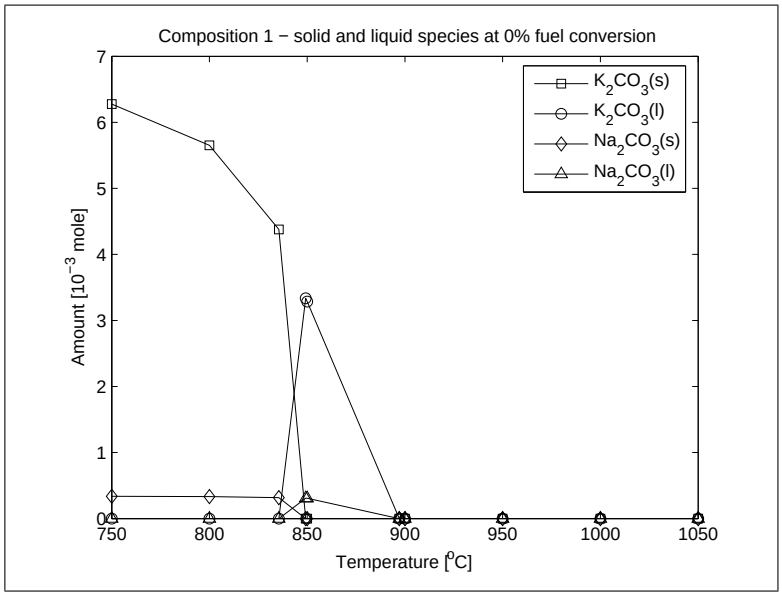

Fig. 6.1: Solid and liquid species at 0.014 mol% K, 0.0034 mol% S, 0.0007 mol% Cl and 0.0007 mol% Na (see Paper I for details).

For the gas compositions presented in Paper I, a condensation temperature of just below 900°C was found in all cases were potassium was present, as exemplified in Figure

(6.1). The constant dew point temperature is not, however, very surprising since only two levels of potassium concentrations were investigated, 0 and 0.0014 mol%. The most important condensed phases in these cases were solid and liquid potassium and sodium carbonates (K_2CO_3 and Na_2CO_3).

A more detailed investigation into the factors determining the condensation limit is given in the following sections. The composition of the main gaseous components (H_2, CO, H_2O, CO_2, CH_4 and N_2) is the same as that used in Paper I, i.e. a typical biomass gasification producer gas from a gasifier using air as oxidising agent. Variations of the concentration of K, S and Cl and their influence on the condensation of liquid and solid phases are studied. Na is normally low in biomass materials and is therefore kept low and constant throughout the calculations.

The molar concentrations presented below are related to the concentration in the modeled gasifier producer gas. As mentioned in Paper I, the modeling work presented here is based on the assumption that all matter initially present in the biomass material is gasified, including the trace species investigated. The concentration of the trace species in the gas can be related to the carbon content of the gas and thus to the carbon content of the solid fuel material (i.e K/C in the gas phase equals K/C in the original fuel). It is therefore possible to correlate the gas phase concentrations presented here to the trace specie content of raw biomass materials. The investigated ranges of gas phase mole fractions and the corresponding weight fractions in the solid fuel are given in Table 4 in Paper I.

6.2.1 Variations in the potassium content

For a given temperature and constant levels of the other species investigate (S, Cl and Na), the condensation limit, or dew point, depends heavily on the level of potassium present in the gasifier producer gas. As shown in Figure (6.1), in a gas containing 0.014 mol% K, 0.0034 mol% S and 0.0007 mol% Cl and Na, condensed K- and Na-carbonates are expected to be found below 900^{o}C. Keeping all but the level of potassium constant, the K-level should therefore be kept below 0.015 mol% to prevent condensation at 900^{o}C as shown in Figure (6.2)

By repeating the calculation above at 850^{o}C, it is clearly seen that both the amount of condensed phases increase, and that the condensation starts at a significantly lower K concentration. As can be seen in Figure (6.3) now both liquid and solid carbonates may be present as the K concentration increases. The lower limit of condensation is in this case a modest 0.002 mol% potassium.

It therefore seems clear that SOFC operation below 900^{o}C utilising gases containing alkali metals, requires significant upstream filtering.

Further calculations not presented here showed that at 800^{o}C and the same composition of trace species as above, condensed phases are expected at as low potassium concentrations as 0.0002 mol%, i.e. at one tenth of that at 850^{o}C. The condensation limits at 950 and 1000^{o}C were correspondingly found to be 0.05 and 0.15 mol% K, respectively.

6.2.2 Variations in the sulphur content

By introducing more sulphur to the gas composition than above and thus simulating a more sulphur rich biomass material, the condensation limit changes slightly. In the calculations presented in Figure (6.4), the sulphur content of the gas is four times that

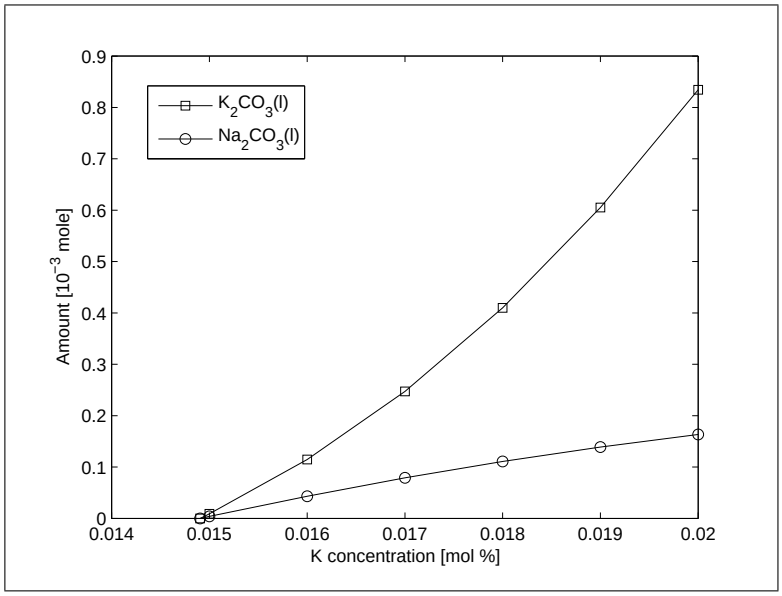

Fig. 6.2: Condensed phases as a function of the K concentration at 900°C; 0.0034 mol% S, 0.0007 mol% Cl and 0.0007 mol% Na.

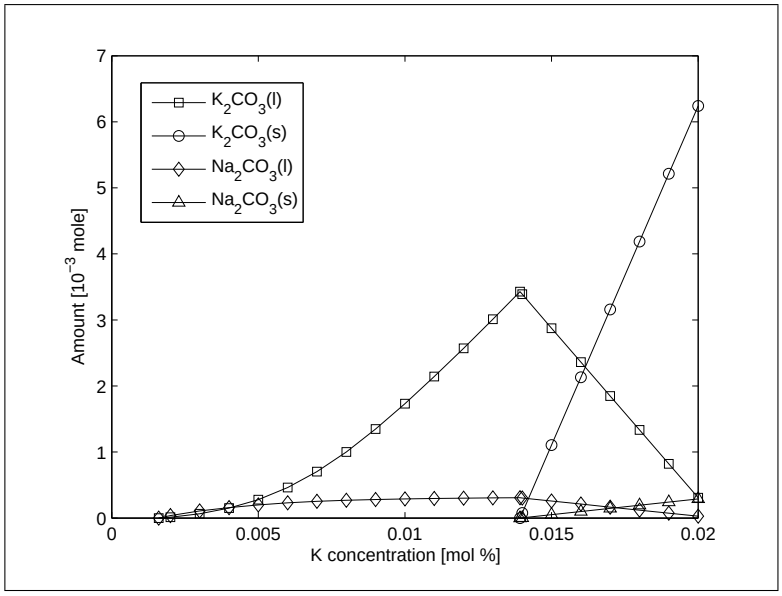

Fig. 6.3: Condensed phases as a function of the K concentration at 850°C; 0.0034 mol% S, 0.0007 mol% Cl and 0.0007 mol% Na.

in the calculations presented above.

The limit at which condensed phases appear is here slightly reduced to around 0.014 mol% potassium. In addition to K_2S (l) now appearing, the gas phase H_2S level is also expected to be four times higher as shown in Paper I. Not shown here, a doubling of the sulphur content correspondingly reduces the condensation limit to somewhere between 0.015 and 0.014 mol% potassium. At 850, 950 and 1000° there are correspondingly slight reductions in the condensation limit in terms of potassium concentration as the sulphur concentration is multiplied by four.

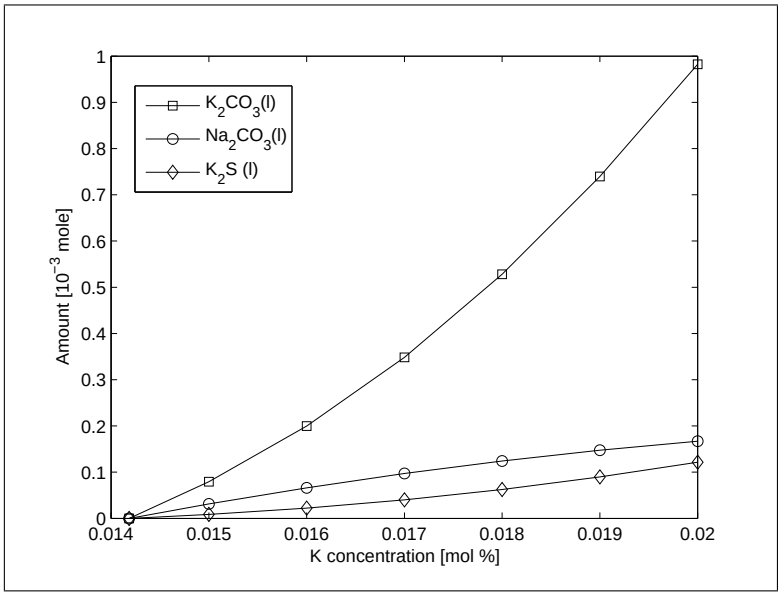

Fig. 6.4: Condensed phases as a function of the K concentration at 900°C; 0.014 mol% S, 0.0007 mol% Cl and 0.0007 mol% Na.

6.2.3 Variations in the chlorine content

An increased chlorine concentration, on the other hand, significantly increases the limit of potassium concentration at which condensation occurs. By introducing four times as much chlorine and keeping the sulphur and sodium levels constant, the condensation limit at 900°C increases from 0.015 to nearly 0.018 mol% potassium as shown in Figure (6.5).

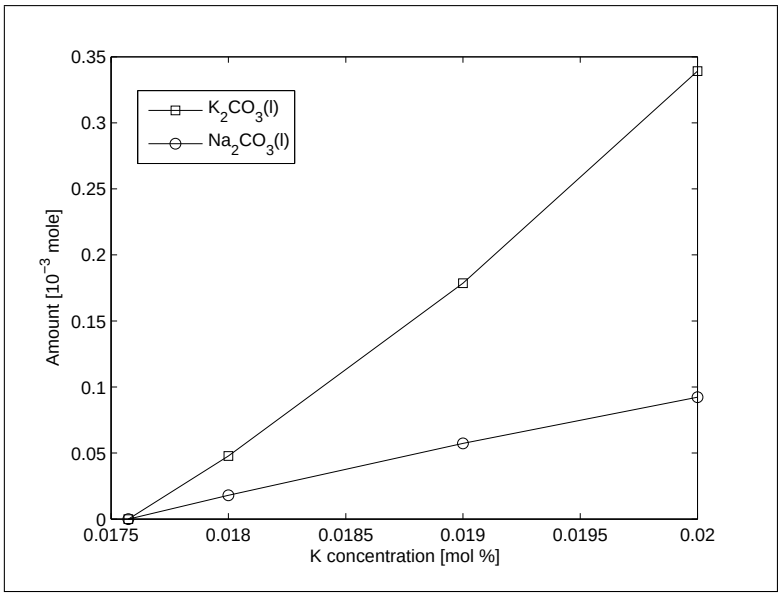

Fig. 6.5: Condensed phases as a function of the K concentration at 900°C; 0.0034 mol% S, 0.003 mol% Cl and 0.0007 mol% Na.

Compared to the results in Figure (6.2) it is clear that both the limit of condensation increases as more chlorine is introduced and, consequently, the amount of condensed phases at any given K concentration is significantly lower. As the Cl content increases,

the concentration of particularly gaseous KCl is, however, expected to increase as presented in Paper I. The influence KCl might have on SOFC performance is not yet known.

At 850^{o}C an increased level of chlorine also increases the K-level at which condensation occurs. As shown in Figure multiplying the Cl-concentration by four increases the condensation limit to around 0.005 mol% K as opposed to 0.002 mol% K (Figure 6.3).

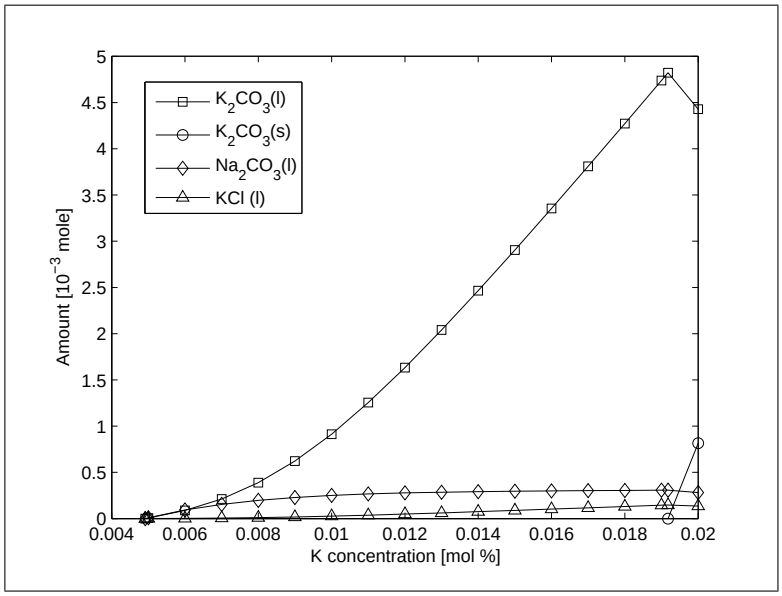

Fig. 6.6: Condensed phases as a function of the K concentration at 850^{o}C; 0.0034 mol% S, 0.003 mol% Cl and 0.0007 mol% Na.

However, increasing the Cl-concentration this much also increases the possibility for condensation of KCl as shown in Figure (6.6).

At 950^{o}C a slight increase in the condensation limit in terms of K-concentration is expected and at 1000^o the addition of four times more chlorine essentially makes no difference.

6.2.4 Conclusions

The most important factor determining the condensation limits for gases containing alkali metals, sulphur and chlorine is the potassium concentration in the gas phase. By increasing the K-concentration the temperature at which no condensation is expected to occur increases. Consequently, by lowering the gas temperature, the K-concentration at which condensation is expected to start decreases.

High sulphur concentrations in the gas may further lower the limit of condensation; at a given temperature condensed phases may exist at a lower K-concentration as more sulphur is introduced. Additionally, a condensed K_2S phase may exist in equilibrium with the gasifier gas at higher levels of sulphur.

Chlorine may significantly increase the level of potassium concentration at which condensation begins and consequently decrease the amount of condensed phases at a given K-concentration. High chlorine concentrations may, however, lead to the formation of a condensed KCl phase.

The most important condensed species that may be present in gases containing alkali metals are potassium and sodium carbonates.

7. PAPER I - EQUILIBRIUM CALCULATIONS OF THE COMPOSITION OF TRACE COMPOUNDS FROM BIOMASS GASIFICATION IN THE SOLID OXIDE FUEL CELL OPERATING TEMPERATURE INTERVAL

Submitted for publication in FUEL.

Equilibrium calculations of the composition of trace compounds from biomass gasification in the Solid Oxide Fuel Cell operating temperature interval

Arnstein Norheim[a], Daniel Lindberg[b], Johan E. Hustad[a], Rainer Backman[c]
[a]Department of Energy and Process Engineering, Norwegian University of Science and Technology, Kolbjørn Hejes Vei 1A, 7491 Trondheim, Norway
[b]Process Chemistry Centre, Åbo Akademi University, Biskopsgatan 8, 20500 Turku, Finland
[c]Energy Technology and Thermal Process Chemistry, Umeå University, 90187 Umeå, Sweden

Abstract

The Solid Oxide Fuel Cell (SOFC), operated at 750-1000°C, is suitable to be fuelled by biomass gasification gases as it may utilise both CO and H_2 in the electrochemical oxidation to produce electricity and heat. None of the main gas components from biomass gasification (CO, CO_2, H_2, H_2O, N_2 and light hydrocarbons) will harm the SOFC. However, other minor components such as compounds of S, Cl, Na and K may form species which degrade the SOFC fuel electrode and thus have a negative influence on the SOFC performance. Knowledge on the composition of the minor components and the expected level of these compounds is thus of great importance in order to be able to perform a detailed experimental study and an evaluation of the SOFC performance fuelled by biomass gasification gases. This work comprises results from equilibrium calculations of the composition of biomass gasification gases from two types of biomass gasifiers, one using air as gasifying agent and one using steam, in the SOFC operating temperature interval (750-1000°C). The amounts of the trace species S, K, Cl and Na have been varied thus simulating different biomass fuels.

1. Background

Gasification of biomass produces a gas consisting mainly of H_2, H_2O, CO, CO_2, N_2, CH_4 and other light hydrocarbons. The fractions of the different components differ depending on the biomass used, gasification medium and technology, and process temperature. Gasification processes using air as gasification medium produces in general a gas rich on N_2 (up to 50 vol-% d.b. [1]). Steam gasification, on the other hand, may produce a gas low in N_2 but rich in H_2 (35-45 vol-% d.b. [2]). In addition to the main gas components, there are other minor components present in the gas from biomass gasification, such as sulphur, chlorine and alkali metals. Typical levels present in different biomass materials are given in Table 1.

Fuel	Ultimate analysis (wt % d.b.)								Ref
	C	H	O	N	K	S	Cl	Na	
Wood	51.6	6.3	41.5	-	-	0.1	-	-	[3]
Wood	49.1	6.0	44.3	0.5	-	0.01	0.1	-	[4]
Verge grass	48.7	6.4	42.5	1.9	-	0.14	0.4	-	[4]
Sawdust	48.0	6.0	45.4	0.2	-	0.05	-	-	[5]
Olive residue	52.4	6.8	38.0	0.8	1.8	0.1	0.002	0.02	[6]
Willow	48.7	5.9	44.5	0.9	-	0.05	0.02	-	[7]
Chip board	50.3	5.9	42.3	1.4	-	0.08	0.09	-	[7]
Park wood	51.5	5.7	41.3	1.2	-	0.25	0.03	-	[7]
Pine sawdust	50.5	7.1	41.1	0.2	-	0.57	-	-	[8]
Wood pellets	50.7	6.9	42.4	0.3	-	-	-	-	[1]

Table 1 Ultimate analysis of different biomass materials.

The Solid Oxide Fuel Cell (SOFC) is a high temperature fuel cell operated at 750-1000^{o}C. H_2, CO and steam reformed hydrocarbons may all be electrochemically oxidised in this type of fuel cell [9], [10]. In addition to power, generated at efficiencies exceeding 50%, high temperature steam is produced. The SOFC has been proposed to be used in several concepts and configuration, and is especially suited in a combined heat and power system [11] - [18]. The state-of-the art SOFC fuel electrode (anode) is made of a porous cermet of nickel and ytria-stabilised zirconia (Ni-YSZ), whereas the electrolyte is made of dense YSZ and the air side electrode (cathode) is made of Sr-doped $LaMnO_3$ [9].

Due to the composition of the gas from biomass gasification, the gas is well suited to be fed to the SOFC [19]. However, the influences of the trace species such as S, Cl, Na and K on the SOFC have not been fully investigated. To be able to perform detailed experimental investigations on the influence the trace elements might have on the SOFC performance, and to choose which components should be included in such experiments, a detailed knowledge on the composition of trace components in typical gasifier gases is needed. This work comprises a modelling study of the composition of trace species in typical gasifier gases with focusing on the potential harmful species containing S, Cl, Na and K.

2. Method

The aim of this work is to establish a reasonable composition of gases from biomass gasifiers focusing on the minor species containing sulphur, chlorine, potassium and sodium. The main gas composition used here is taken from a work done on a downdraft, air blown gasifier [1] in addition to steam gasifier [2]. The gas compositions are shown in Table 2. These gases are investigated in the temperature range (750 – 1000^{o}C) by equilibrium calculations performed by the program package FactSage [20]. Of particular interest are the changes in gas composition as different parameters, such as temperature, fuel conversion and the content of sulphur, chlorine and alkali metals, change.

Species	Air gasification	Steam gasification
	Vol-%, w.b.	Vol-%, w.b.
N_2	41.0	1.8
CO	21.2	14.6
CO_2	8.3	17.7
H_2	13.8	20.3
CH_4	1.4	9.7
H_2O	14.3	36

Table 2 Main gas components from air and steam gasification

Calculation of thermodynamic equilibrium is based on minimisation of the Gibbs free energy. If a state of chemical equilibrium is to be achieved in a system of chemical species, the total Gibbs energy of the system has to be minimised. For a given temperature, pressure and composition the total Gibbs energy can be represented as:

$$G=\sum_i n_i \mu_i \qquad \textbf{Eq. 1}$$

Here, n is the amount of the species involved, μ is chemical potential of the species and the sum represent all chemically distinct species of the entire system [20].

The thermodynamic data for the stoichiometric compounds used in the calculations was taken from the FACT database [20],[21] and the thermodynamic data for the solution phases were taken from [22] -[23].

Table 3 shows the molar fractions of the main elements, C, H, O and N in the producer gas from the air blown gasifier at different levels of fuel conversion. At 40 and 80% fuel conversion the composition is calculated under the assumption that 40 and 80%, respectively, of the original CO, H_2 and CH_4 is oxidised. The oxygen needed for this conversion is added to the original composition as this would be supplied to the anode chamber from the cathode in a real SOFC operation. Table 3 thus shows a decrease in the mole fractions of carbon, hydrogen and nitrogen as the level of fuel conversion increases due to the addition of oxygen.

Fuel conversion	0 %	40 %	80 %
Element	Mole fraction	Mole fraction	Mole fraction
C	13.6	12.7	11.9
H	27.2	25.4	23.8
O	23.0	28.1	32.6
N	36.2	33.8	31.7

Table 3 Molar fractions of the main elements in the examined gas at different levels of fuel conversion

Equilibrium calculations have been performed at all three levels of fuel conversion shown in Table 3 i.e. for all three compositions of the main elements C, H, O and N. The trace elements, S, Cl, K and Na, have been investigated in the range of concentrations shown in the column in Table 4 named "Air gasification". When performing the calculations, the amount of the trace species are related to the carbon content in the raw fuel and then it is assumed that all the carbon is gasified and all the S, Cl, Na and K is either gasified or entrained in the gas flow. Thus, under this assumption, a range of compositions of the biomass material as shown in the last column in Table 4 has been investigated. Additionally, some of the calculations have been repeated using an equal trace specie-to-carbon factor but using the gas composition from the steam gasifier in Güssing, Austria [2]. The composition of this gas on a molar basis, and the range of the trace species are shown in the column in Table 4 named "Steam gasification". It is seen that as the molar fraction of carbon is lower in the steam gasification case, the molar fractions of the trace species are also lower. The results reported below are from the air-gasification case if not stated otherwise.

Element	Mole fraction (% w.b.) Gas composition		Weight fraction (% d.b.) Ultimate analysis fuel
	Air gasification	Steam gasification	
C	13.6	8.8	50.4
H	27.2	58.8	6.9
O	23.0	31.6	42.2
N	36.2	0.8	0.3
K	0-0.0136	0-0.0088	0-0.16
S	0.00068-0.0136	0.00044-0.0088	0.007-0.13
Cl	0.00034-0.0136	0.00022-0.0088	0.004-0.15
Na	0-0.00068	0-0.00044	0-0.005

Table 4 Range of concentration of trace species in gas composition and in raw fuel

3. Results and discussions

3.1 Major gaseous species

The equilibrium composition of the main gas components (N_2, CO, H_2, H_2O and CO_2) in the temperature interval between 750 and 1050^{o}C is shown in Fig. 1 and Fig. 2 for 0 and 80% fuel conversion, respectively.

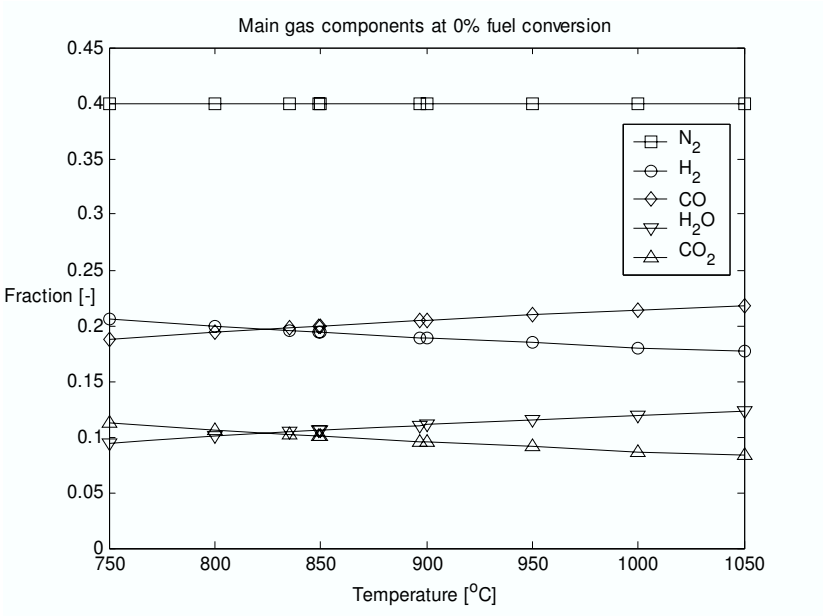

Fig. 1 Molar fractions of main gas components at 0% fuel conversion

For both levels of fuel conversion it is seen that as the temperature increases, the level of CO and H_2O increases. This can be explained by the water-gas shift reaction (Eq. 2). As the temperature increases from 750 to 1050°C, the equilibrium of the reaction is shifted to the left.

$$CO+H_2O \Leftrightarrow CO_2+H_2 \qquad \textbf{Eq. 2}$$

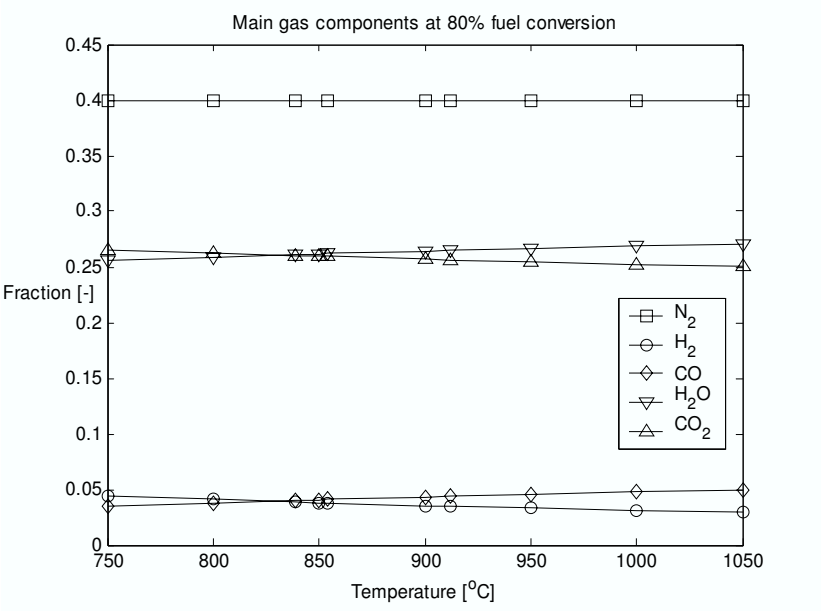

Fig. 2 Molar fractions of main gas components at 80% fuel conversion

3.2 Gaseous trace elements

3.2.1 Sulphur

In the temperature interval investigated, essentially all the sulphur is in the form of H_2S and a doubling of the sulphur content in the fuel gas leads to a doubling of the H_2S level. This is shown in Fig. 3 and Fig. 5 with H_2S levels at 1000°C of 72 and 144 ppm, respectively.

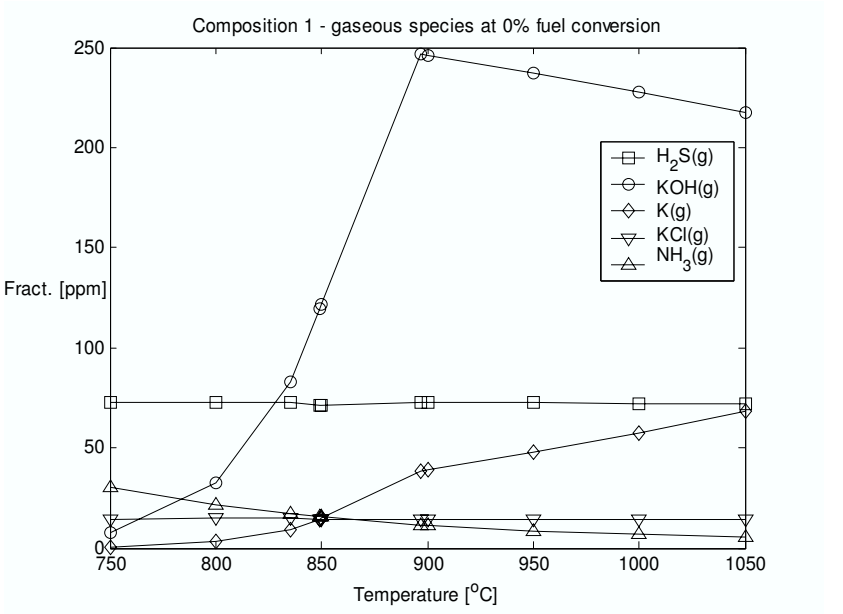

Fig. 3 Gaseous species at 0% fuel conversion; K = C/1000, S = C/4000, Cl = C/20000, Na = 0.05K

Sulphur in the form of H_2S is known to cause performance losses for the SOFC. Even at as low levels as 1-5 ppm the losses are reported to be significant [25] but reversible i.e. the SOFC performance recovers after removing the sulphur from the fuel flow. As the H_2S level increases above 100 ppm the performance losses are reported to be irreversible [26]. However, it has been reported that the tolerance towards H_2S poisoning increases with increasing operating temperature [25].

For the same level of sulphur in the fuel, related to the carbon content in the fuel, the ppm level of H_2S is lower in the steam gasification case, as shown in Fig. 4. This is due to the fact that the carbon content in the fuel gas is lower than for the air gasification case. However, the H_2S level is also in this case stable throughout the temperature interval, and essentially all the sulphur is here also found as H_2S.

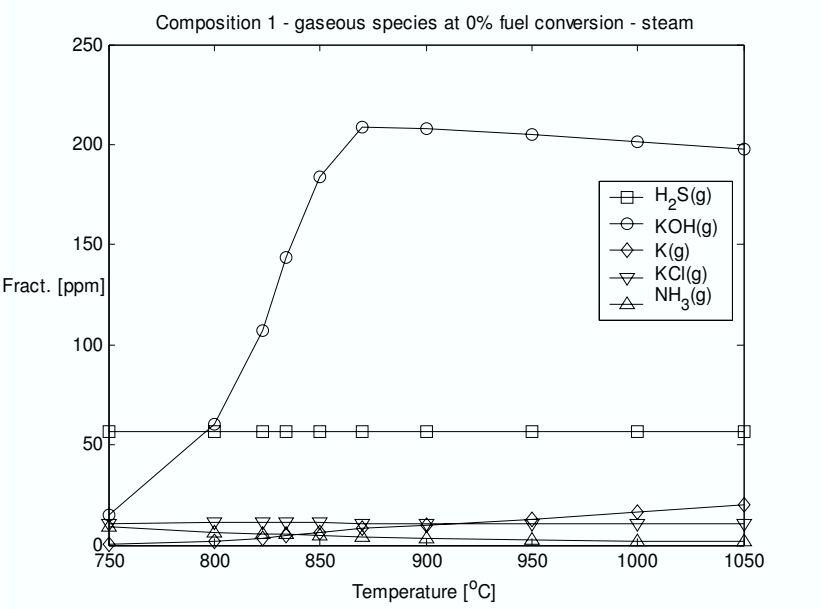

Fig. 4 Gaseous species at 0% fuel conversion – steam gasification; K = C/1000, S = C/4000, Cl = C/20000, Na = 0.05K

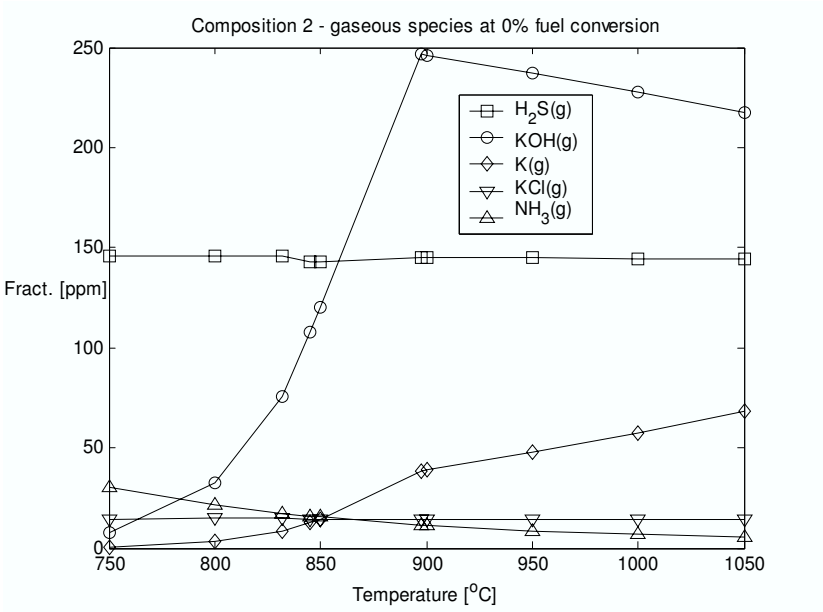

Fig. 5 Gaseous species at 0% fuel conversion; K = C/1000, S = C/2000, Cl = C/20000, Na = 0.05K

Returning to the air gasification case, one can see that at high levels of fuel conversion (80%) some SO_2 is present at temperatures above 950°C as shown in Fig. 6. At high levels of fuel conversion more H_2O and CO_2 is present in the gas as shown previously in Fig. 1 and Fig. 2.

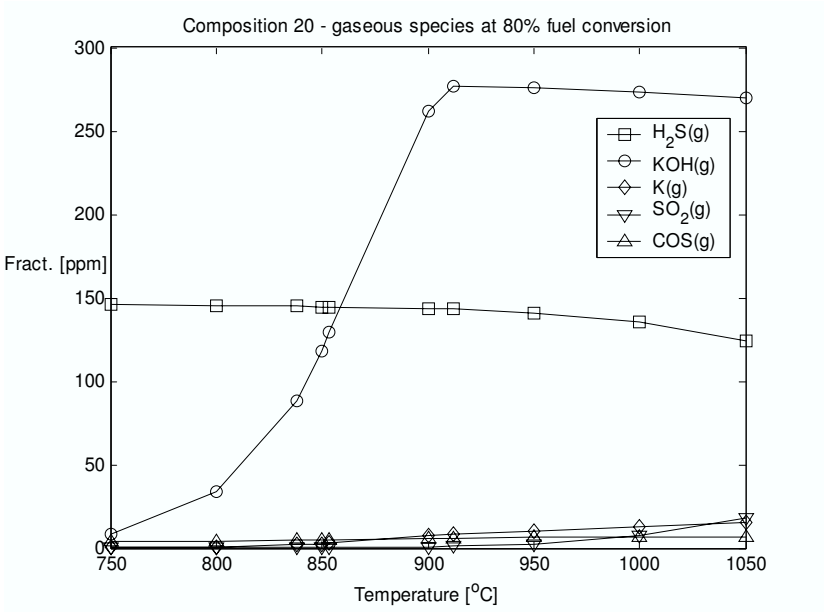

Fig. 6 Gaseous species at 80% fuel conversion; K = C/1000, S = C/2000, Cl = C/20000, Na = 0.05K

A third sulphur component, COS, is present throughout the whole temperature interval at very low levels from approximately 3 to 7 ppm. As for SO_2 the level of COS is greatest at high total sulphur contents, high temperatures and high levels of fuel conversion.

3.2.2 Potassium

Gaseous KOH shows a similar trend in almost all the calculations performed; from a low level of 7-8 ppm at 750°C, the level increases steeply up to 220-280 ppm at 900°C as the solid and liquid potassium containing components evaporate. Above 900°C the level of KOH(g) decreases as shown in Fig. 3 and Fig. 5. The reduction of the level of KOH(g) above 900°C is balanced by an increasing amount of K(g). At higher levels of fuel conversion, i.e. when more oxygen is available, more KOH is produced and thus the level of gaseous K decreases as shown in Fig. 5 and Fig. 6 for 0% and 80% fuel conversion, respectively. In the steam gasification case at 0% fuel conversion, the level of gaseous K is low, and almost all the gaseous potassium is in the form of KOH as seen in Fig. 4. This may be understood by looking at the oxygen fraction at 0% conversion for steam gasification in Table 4 and that for air gasification at 80% fuel conversion in Table 3. The oxygen fractions are essentially equal in the two cases. However, KOH shows a similar trend in the steam gasification case, but the peak level is shifted to a slightly lower temperature. This can be explained by the fact that the solid and liquid components are evaporated at a lower temperature in the steam gasification case.

Potassium also reacts with chlorine to produce KCl. At higher Cl-content in the gas the KOH and, consequently, the K level decrease as can be seen by comparing results from Fig. 3 and Figs. 8 and 9.

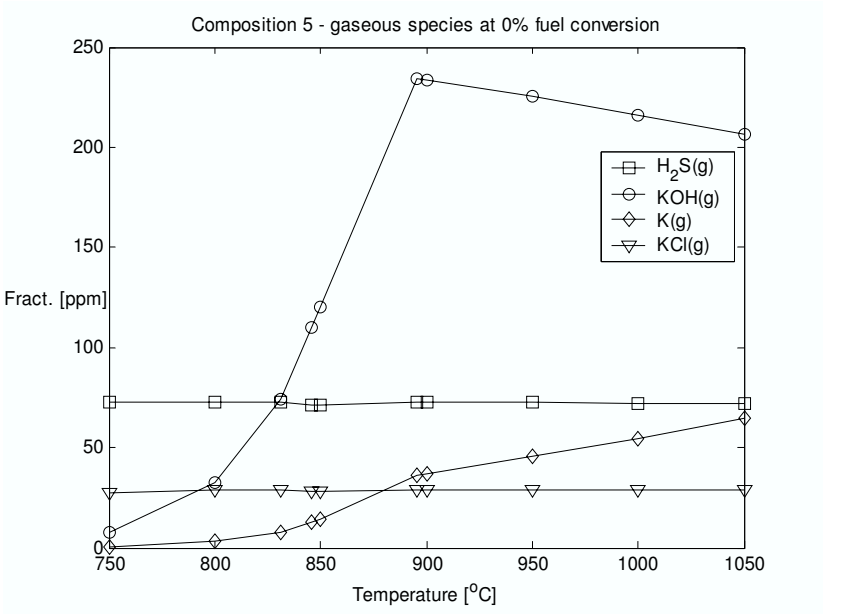

Fig. 7 Gaseous species at 0% fuel conversion; K = C/1000, S = C/4000, Cl = C/10000, Na = 0.05K

Alkali compounds may promote corrosion of the material in SOFC anode and thus decrease the cell performance. If the nickel in the SOFC anode is partly or completely oxidised the catalytic properties of the nickel are reduced and the anode will lose its electrical conductivity.

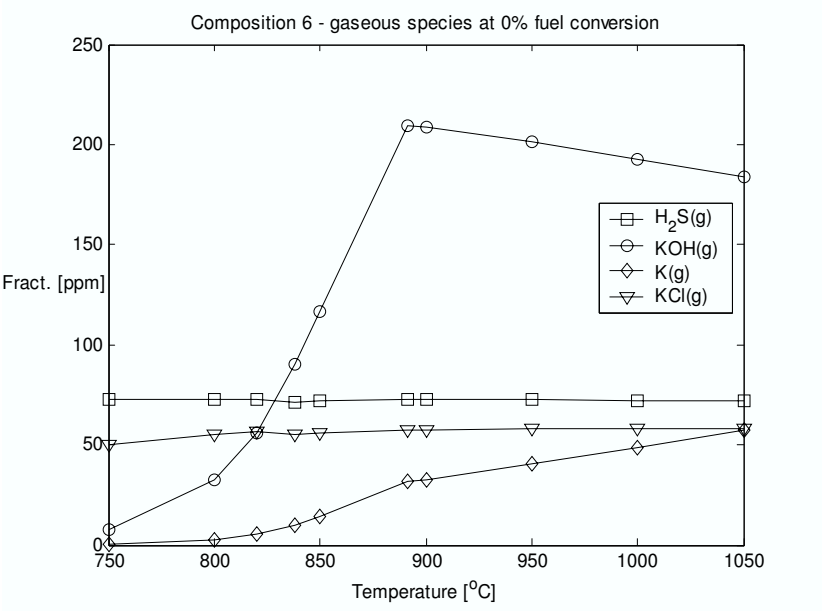

Fig. 8 Gaseous species at 0% fuel conversion; K = C/1000, S = C/4000, Cl = C/5000, Na = 0.05K

In the temperature interval investigated, the level of gaseous potassium containing species increase with increasing temperatures up to around 900°C. This is caused by the evaporation of solid and liquid carbonate (K_2CO_3) as shown in Fig. 13.

3.2.3 Chlorine

As long as there is potassium available chlorine reacts to produce gaseous KCl. The KCl level increases in these cases proportional to the Cl content in the fuel, as discussed above. Additionally, in cases of high chlorine content $(KCl)_2$ is formed, the level decrease with increasing temperatures as shown in Fig. 9.

In one of the compositions investigated, there is no potassium and sodium present. Chlorine reacts in this case with hydrogen to produce HCl as shown in Fig. 10.

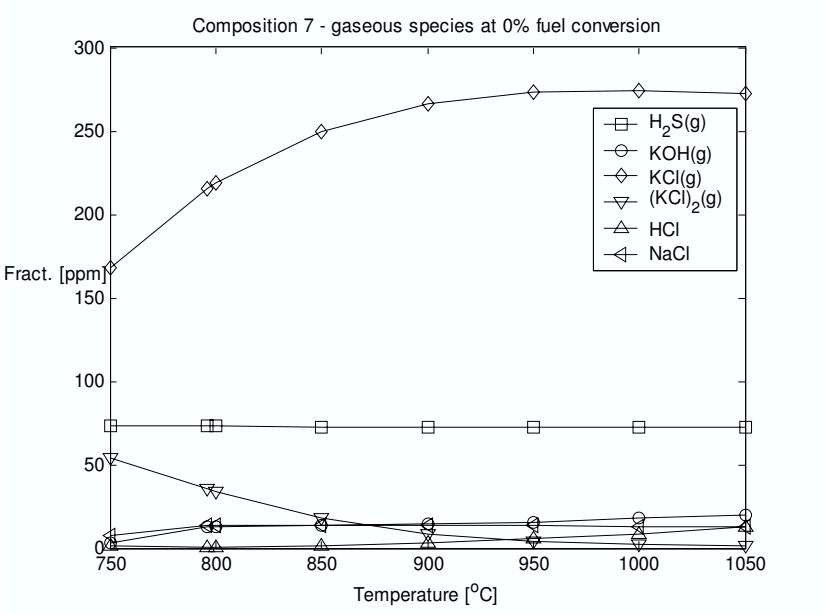

Fig. 9 Gaseous species at 0% fuel conversion; K = C/1000, S = C/4000, Cl = C/1000, Na = 0.05K

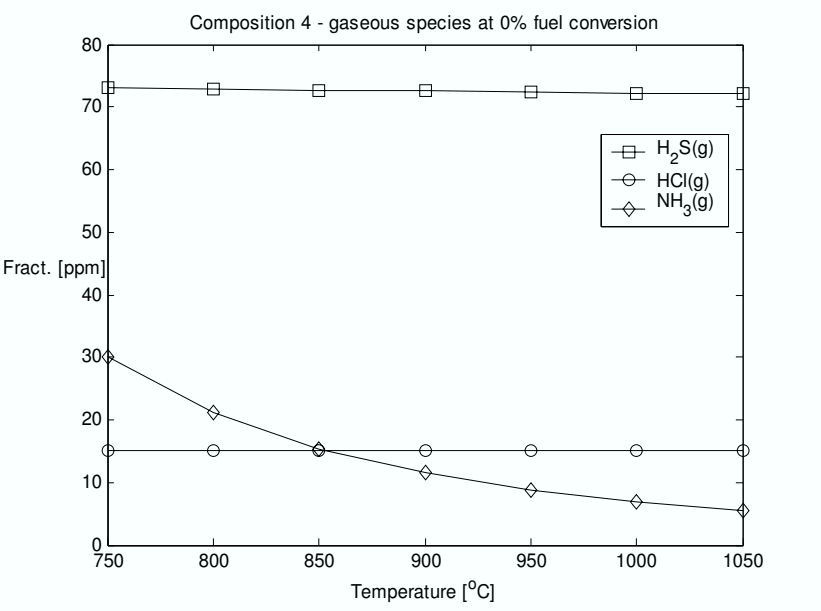

Fig. 10 Gaseous species at 0% fuel conversion; K = 0, S = C/4000, Cl = C/20000, Na = 0

3.2.4 Sodium

The sodium level investigated is low, 0.05 times the potassium level in all cases investigated. However, three sodium containing species are found: Na, NaOH and NaCl.

Both gaseous Na and NaOH are in general nearly nonexistent up to a temperature of 850°C. Above this temperature and up to 900°C the Na and NaOH levels increase up to about 7 ppm. Above this temperature the Na level increases further (1-2 ppm) up to 1050°C whereas the NaOH level decreases an equivalent amount, as shown in Fig. 11.

The NaCl level is in general low (1-2 ppm) and stable throughout the temperature interval investigated. A maximum level of 13-14 ppm is found in the composition with the highest chlorine level (Cl=C/1000). In this case the NaOH and Na levels are low (around 1 ppm).

The levels of the different Na containing species do not seem to be influenced by the level of fuel conversion. This may be due to that oxygen and hydrogen are not limiting the distribution of Na among Na(g) and NaOH(g) even at 0% fuel conversion. Addition of even more oxygen at the higher levels of fuel conversion does not alter this distribution. Thus, the level of chlorine only seems to have any influence on the level of the different gaseous Na components.

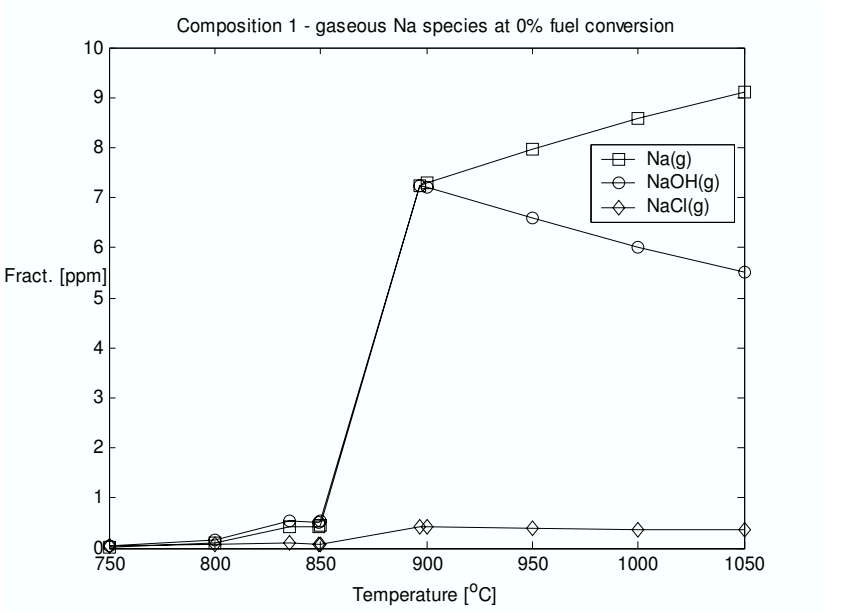

Fig. 11 Gaseous Na-species at 0% fuel conversion; K = C/1000, S = C/4000, Cl = C/20000, Na = 0.05K

3.3 Liquid and solid trace compounds

The molar amount of liquid and solid species is low compared to the amount of gaseous species in all calculations performed. For the case shown in Fig. 12 there is a maximum of 0.007 moles of solids at 750°C and of 0.004 moles of liquids at 850°C. In comparison the amount of gaseous species in this case is constant throughout the temperature interval at a value of 45 moles. The other calculation results do not differ significantly from this general picture except the one with no sodium and potassium present. In that case there is no solid or liquid species present in the temperature interval investigated.

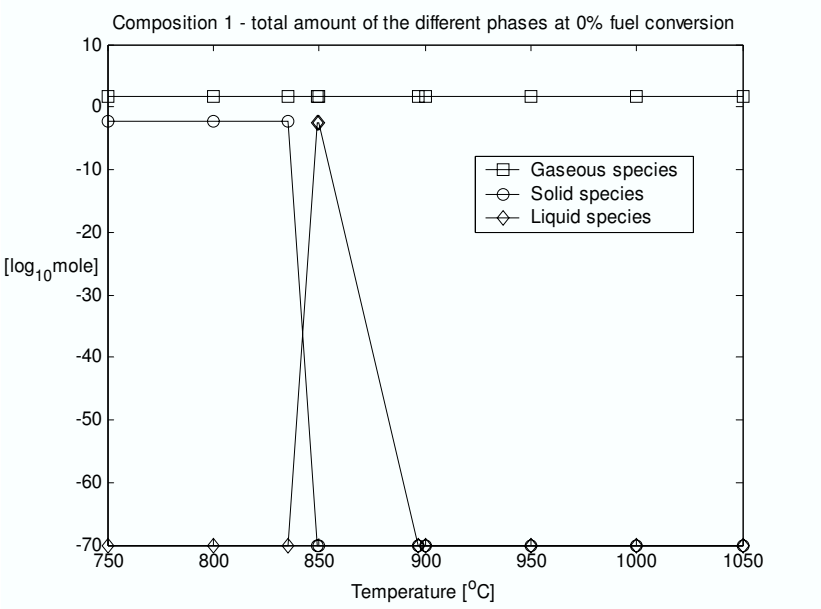

Fig. 12 Molar amounts of the different phases at 0% fuel conversion; K = C/1000, S = C/4000, Cl = C/20000, Na = 0.05K

Liquid or solid components may have a negative influence on the SOFC performance as the porous anode may be partly or completely blocked. If so happens the gas diffusion through the anode layer may be reduced or stopped. Additionally, alkali melts such as Na_2CO_3 and KCl have been reported to oxidise nickel [27], [28] and melted NaOH has been reported to cause formation of stable phases of nickel and alkali metal e.g. $NaNiO_2$ [29]. Thus, operating the SOFC below 900°C may cause severe performance losses and cell degradations if alkali metals are present in the gas.

3.3.1 Sulphur

Small amounts of liquid K_2S and Na_2S are present in the temperature interval between 830 and 900°C. The molar amount of K_2S, being approximately 5% of the total amount of liquid species, is in general ten times larger than the amount of Na_2S. The amounts of these two species increase proportional to the sulphur content in fuel.

3.3.2 Potassium

As can be seen in Fig. 13 potassium carbonate (K_2CO_3) is the dominating solid and liquid specie in this case and also in the other cases investigated. The amount of solid carbonate decreases from 750°C until it reaches zero close to 850°C. This is partially due to melting

as there is formed some liquid K_2CO_3 from 840°C, but also due to evaporation of the carbonates as discussed previously (see Fig. 3).b

3.3.3 Chlorine

In the case with the highest chlorine content (Cl=C/1000) no solid species are present in the temperature interval investigated and all liquid species are completely evaporated at 800°C. Liquid KCl is the dominating specie in this case with a maximum level at 750°C of 54 mol-% of the total amount of liquid components. However, in general the amount of KCl is only in the order of 1-3% of the total amount of liquid species. Additionally, liquid NaCl is present at a level approximately one tenth of that of KCl. No solid chlorine containing species are stable in the investigated temperature interval.

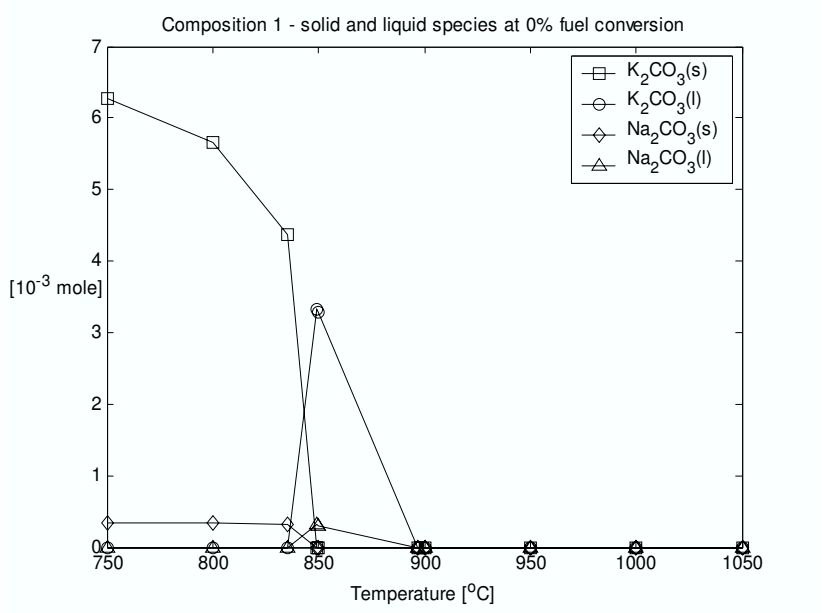

Fig. 13 Solid and liquid species at 0% fuel conversion; K = C/1000, S = C/4000, Cl = C/20000, Na = 0.05K

3.3.4 Sodium

The most significant solid and liquid sodium specie in these calculations is sodium carbonate, Na_2CO_3. The level of solid carbonate is low and nearly constant in the temperature interval between 750 and 830°C. From this temperature level and up to

around 850°C the solid carbonate melts. Thus liquid Na_2CO_3 appears, the level showing a peak at 850°C and then decreases to zero around 900°C as shown in Fig. 13.

In addition to the carbonate and the sulphide and the chloride (as discussed above), some NaOH is present. Its amount and dependence on temperature seem to be similar to that of Na_2S i.e. a small amount in the temperature interval between 830 and 900°C only.

4. Conclusions

The major trace components present in the gas from gasification of biomass have been identified for several levels of sulphur, potassium, chlorine and sodium in the SOFC operating temperature interval.

Sulphur is present mainly as H_2S(g) whereas potassium is mainly present as KOH(g) and to some extent K(g) depending mainly on the temperature. High chlorine content in the fuel favours KCl(g) production. Cl is also found as HCl(g) in some cases, especially if there is limited or no potassium present in the gas. The calculations show very limited molar amounts of liquid and solid species present. However, in the temperature interval between 750 and 900°C there is a small amount of carbonate-rich liquid phase and solid carbonates in equilibrium with the gasifier gas. The temperature at which the potassium salts condense depends on the amount of potassium present in the fuel gas. Thus, if the potassium level is lowered, the temperature at which the salts condense is also in general lowered.

The calculations show in general that steam gasification is favourable compared to air gasification concerning the level of most of the minor species because they are related to the carbon content in the gasification gas which in steam gasification is lower than in air gasification.

Acknowledgements

The Nordic Graduate School of Biofuel Science and Technology has funded this work.

References

[1] Barrio M. Ph.D. thesis Norwegian University of Science and Technology, Norway 2002
[2] Hofbauer H, Veronik G, Fleck T, Rauch R, Mackinger H, Fercher E. Developments in Thermochemical Biomass Conversion 1997;2:1016-1025.
[3] McKendry P. Bioresource Technology 2002;83:37-46.
[4] Faaij A, van Ree R, Waldheim L, Olsson E, Oudhuis A, van Wijk A, Daey-Ouwens C, Turkenburg W. Biomass & Bioenergy 1997;12:387-407.

[5] Turn S, Kinoshita C, Zhang Z, Ishimura D, Zhou J. Int. J. Hydrogen Energy 1998;23:641-648.
[6] Ollero P, Serrera A, Arjona R, Alcantarilla S. Biomass & Bioenergy 2003;24:151-161.
[7] van der Drift A, van Doorn J, Vermeulen JW. Biomass & Bioenergy 2001;20: 45-56.
[8] Lv PM, Xiong ZH, Chang J, Wu CZ, Chen Y, Zhu JX. Bioresource Technology 2004;95:95-101.
[9] Minh NQ, Takahashi T. Science and Technology of Ceramic Fuel Cells. Elsevier 1995.
[10] Larminie J, Dicks A. Fuel cell systems explained. Wiley 2000.
[11] Riensche E, Achenbach E, Froning D, Haines MR, Heidug WK, Lokurlu A, von Andrian S. Journal of Power Sources 2000;86:404-410.
[12] Dokiya M. Solid State Ionics 2002;152-153:383-392.
[13] Ahmed K, Gamman J, Föger K. Solid State Ionics 2002;152-153:485-492.
[14] Sammes NM, Boersma R. Journal of Power Sources 2000;86:98-110.
[15] Van herle J, Maréchal F, Leuenberger S, Favrat D. Journal of Power Sources 2003;118:375-383.
[16] Wojcik A, Middleton H, Damopoulos I, Van herle J. Journal of Power Sources 2003;118:342-348.
[17] Schuler A, Zähringer T, Doggwiler B, Rüegge A. Proceedings of the fourth European SOFC forum 2000;1:107-114.
[18] Dicks A, Larminie J. Proceedings of the fourth European SOFC forum 2000;2:927-936.
[19] Norheim A, Hustad JE, Byrknes J, Vik A. Paper submitted to Science in Thermal and Chemical Biomass Conversion, Victoria, BC, Canada 2004.
[20] Bale CW, Chartrand P, Degterov SA, Eriksson G, Hack K, Ben Mahfoud R, Melancon J, Pelton AD, Petersen S. Calphad 2002;26(2):189-228.
[21] Center for Research in Computational Thermochemistry, www.crct.polymtl.ca
[22] Sangster JM, Pelton AD. In: Cook LP, McMurdie HF, editors. Phase diagrams for ceramists. The American Ceramic Society 1989.
[23] Backman R, Enestam S, Zevenhoven R. In: Liekki 2, Hupa M, Matinlinna J, editors. Technical review 1993–1998, Åbo Akademi University, Turku, Finland 1998;1073-94.
[24] Eriksson G, Hack K. Metallurgical Transactions B 1990;21.
[25] Matsuzaki Y, Yasuda I. Solid State Ionics 2000;132:261-269.
[26] Dees DW, Balachandran U, Dorris SE, Heiberger JJ, McPheeters CC, Picciolo JJ. Proceedings of the 1st International Symposium on Solid Oxide Fuel Cells (SOFC-I) 1989:318.
[27] Li YS, Niu Y, Wu WT. Materials Science & Engineering A 2003;345:64-71.
[28] Hara M, Shinata Y, Hashimoto S. Corrosion Science 1997;39(4):627-638.
[29] Komath M. Materials chemistry and physics 1996;45:171-175.

8. EXPERIMENTAL INVESTIGATIONS OF SOLID OXIDE FUEL CELL PERFORMANCE

As presented in Chapter (5), there has been a significant effort in the SOFC community to optimise the SOFC structure and to investigate reaction mechanisms involved. Factors limiting and degrading the SOFC performance are thus partly well known. Much of this work has, however, been performed on a rather fundamental scale. Microstructural aspects are therefore well studied and to some extent understood. Half-cell experiments have particularly revealed information on fundamentals of electrode and electrode/electrolyte mechanisms and performance limiting factors. Commercial actors have also contributed with particularly performance data and success stories of long term operation. These data are, however, often of limited value due to the level of secrecy and confidentiality these companies live under.

There is therefore a lack of single cell SOFC or stack performance data available in the published literature. Laboratory specifics further complicates comparison of performance data published by different authors. Most laboratories and commercial actors have their own experimental setup that normally is all but well described. In addition there is no standard SOFC fabrication procedure and materials selection even in the case of the state-of-the-art LSM/YSZ/Ni SOFC. This can, however, not be expected, but certainly adds to the problems of comparing performance data from different authors.

The best way to compare performance data may therefore be to perform a comparative study on one single setup using a single cell SOFC. Two or more data series that are to be compared should additionally be performed within a limited period of time to prevent time induced effects to influence on the results.

8.1 Summary of Paper II

Due to the limited amount of single cell SOFC performance data and the difficulties of comparing data from different authors, an experimental series was initiated. The aim was to compare single cell performance as the composition of the fuel gas fed to the cell was altered. The setup used in both Paper II and Paper III is described in Section (8.3). In the experiments performed in connection with Paper II, the single cell SOFC was operated at 975^{o}C at low fuel and air utilisation.

First, the H_2 and CO partial pressures (p_{H_2} and p_{CO}) were varied and IV-curves (current-voltage curves) were established for each fuel gas mixture. The CO_2 partial pressure (p_{CO_2}) in the inlet fuel gas was kept constant at 0.1 atm. p_{H_2} and p_{CO} was varied keeping the sum of the two constant at 0.9 atm ($p_{H_2} + p_{CO} = 0.9$ atm). The OCV (open circuit voltage) was seen to increase with p_{H_2} and, consequently, p_{CO} reduction. The most significant effect was seen when p_{H_2} was increased from 0 to 0.4 atm whereafter the increase in OCV flattened out (Figure 1 in Paper II). The cell voltage at any given current also increased as p_{H_2} increased as shown in Figure 2 in Paper II. In addition, the total cell resistance increased with p_{CO} in accordance with the work by Matsuzaki

and Yasuda [74] and Sasaki et al. [108]. The most significant increase in cell resistance occurred when p_{CO} increased to above 0.7 atm and p_{H_2} consequently decreased to below 0.2 atm. The cell resistance was around 20% lower when using a fuel mixture of 90:10 H_2/CO_2 than when using a mixture of 90:10 CO/CO_2.

In the next part, p_{H_2} was kept constant at 0.5 atm (at room temperature) and p_{N_2} and p_{CO_2} were varied between 0 and 0.5 atm keeping the sum of the two constant at 0.5 atm ($p_{N_2} + p_{CO_2} = 0.5$ atm). It was seen, as presented in Figure 4 and Figure 5 in Paper II, that as p_{CO_2} increased and consequently p_{N_2} decreased, both the OCV and the operating voltage at all current levels decreased. This may be due to an equilibration of the water-gas shift reaction (Eq. 5.25) when CO_2 is present thus causing CO to be present in the fuel gas. However, the cell resistance was higher when using a mixture of 50:50 H_2:N_2 than when using a mixture of 50:50 H_2:CO_2. It is not clear what caused this change in cell resistance, but an enhancement of the reaction rates when CO_2 is present is possible and this would seem to be in accordance with the work of Onuma et al. [93]

There is essentially no data available in the open literature regarding SOFC performance when using biomass gasifier producer gases. In the last part of the experimental series presented in Paper II the SOFC performance when using producer gas and reformed natural gas was therefore compared. All gas compositions were mixed from gas bottles. The results do consequently not present performance data of using real natural gas and gasifier gas. At thermodynamic equilibrium the compositions are, however, representative of reformed natural gas and producer gas from steam gasification.

Based on the results, presented in Figures 5 and 6 in Paper II, it was concluded that the gases from biomass gasification are suitable as fuel for the SOFC. Additionally, the SOFC performance is essentially the same when using steam reformed natural gas and gasifier producer gas.

8.2 Summary of Paper III

As mentioned in Section (5.10) H_2S is known to degrade the SOFC performance both in terms of a reduction in the reforming capabilities of the Ni-catalyst and an increase in the anode related resistance. Most results published are based on half-cell experiments and at relatively low sulphur concentrations.

An experimental series was therefore performed aiming at revealing the SOFC performance at higher sulphur levels. In gasifier producer gases the H_2S concentration may be well above 200 ppm and the literature published so far does not include performance data for such high sulphur concentrations. The fuel gas was mixed from gas bottles to simulate the expected producer gas composition from biomass steam gasification. H_2S was introduced at concentration ranging from 5 to 240 ppm. The single cell SOFC setup was the same as that used in connection with the experiments presented in Paper II. The cell was operated at 800 and 850°C.

The performance data are presented in Paper III. Since no methane or other hydrocarbons were present in the fuel gas, the results represent the influence sulphur has on the electrochemical performance of the SOFC. The influence these high sulphur concentrations have on the reforming reactions was thus not revealed here.

It was found that the total cell resistance increased significantly at all levels of H_2S concentrations investigated. Additionally, above a certain H_2S concentration, the increase in cell resistance was stabilised; further increasing the sulphur concentration did not seem to cause any additional increase in the cell resistance. No clear correlation

between operating temperature and the effect of sulphur poisoning was found.

The experiments lasted for more than three weeks. During the first 400 hours, the cell resistance at 0 ppm H_2S decreased significantly i.e. the cell performance increased. This also influenced the results obtained for the initial sulphur concentrations investigated. Thus, the performance at e.g. 5 ppm H_2S was poorer than the performance at 10 ppm H_2S as can be seen in Figure 2 in Paper III. This certainly makes it difficult to quantify the sulphur effect during this initial 400 hours period. However, during the last experiments, the cell performance at 0 ppm H_2S was stable. It was therefore possible to draw clearer conclusions regarding the cell performance at 80, 120 and 240 ppm H_2S than at the lower sulphur concentrations.

8.3 Setup

The experiments leading up to Paper II and Paper III were performed at the laboratory of Prototech, Bergen. The single cell used was a planar anode supported LSM/YSZ/Ni state-of-the-art SOFC delivered by Forschungszentrum Jülich. The details on these cells can be found in the work by Basu et al. [63]. The cells were delivered as quadratic 10 x 10 cm plates and were thereafter cut in a circular shape to fit in the setup. On both electrodes interconnects which also acted as gas flow distributors were placed as shown in Figure (8.1).

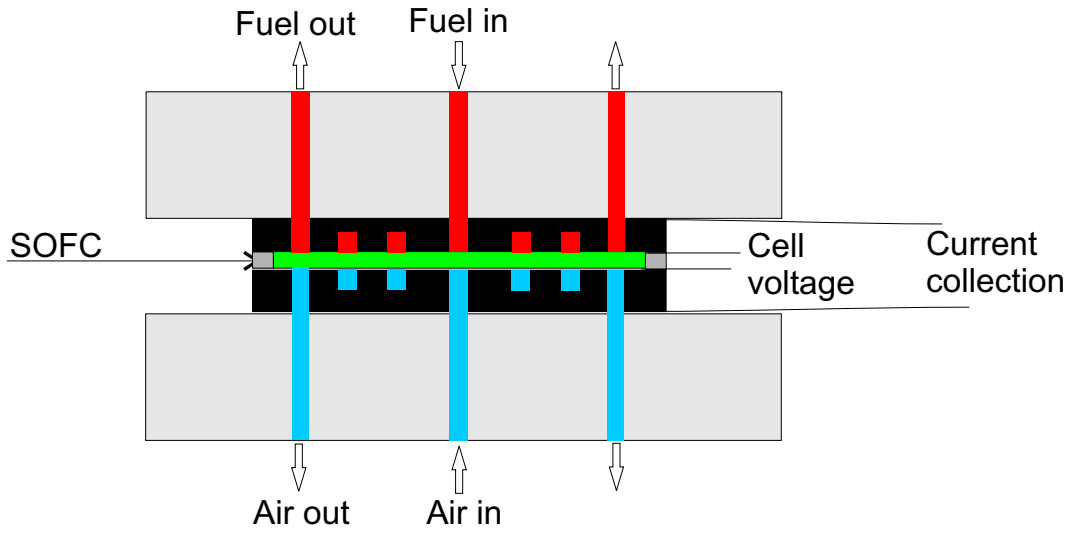

Fig. 8.1: Detail of the single cell setup (not to scale).

In the setup used in connection with Paper II, the cell diameter was 40 mm. Sealing was accommodated by a 0.27 mm Pt-film wrapped around the interconnect perimeter. This solution may cause fuel crossover to the cathode through the anode perimeter and may thus decrease the cell performance. The setup was slightly modified before the H_2S experiments described in Paper III were started. Here, the cell diameter was reduced to 30 mm and a sheet gasket was used to seal the setup. The cathode was grind down approximately 0.05 mm 2 mm in along the perimeter to be able to place a sheet gasket there in order to seal the setup as well as possible as shown in Figure (8.2). The active cell area was thus approximately 5 cm^2.

Fig. 8.2: Exploded view showing details of cell sealing (not to scale).

In the setup used for Paper II, current collection and voltage measurement were accommodated by placing 0.27 mm Pt-films directly on the electrodes. Pt-wires were welded onto the Pt-films and could thus be connected to the data-logging equipment. In the modified setup used for Paper III, current collection was done by placing Pt-films on the interconnects on the side opposite to the electrodes. Voltage measurement was done by placing Pt-wires directly on the electrodes. These wires were isolated from the interconnects.

The cell assembly was put into a larger setup schematically shown in Figure (8.3). The setup consists of alumina tubes for gas inlet and outlet and alumina stretch rods connected to a pressure cylinder situated in the lower part of the setup. Thus, the cell assembly could be held firmly together, ensuring contact between current-collectors, interconnects and the fuel cell.

The setup was placed in an electrically heated oven and heated to the desired temperature. Cell temperature, cell voltage and current were measured by a LabView FieldPoint unit. Fuel composition and fuel and air flow were controlled by Bronkhorst mass flow controllers.

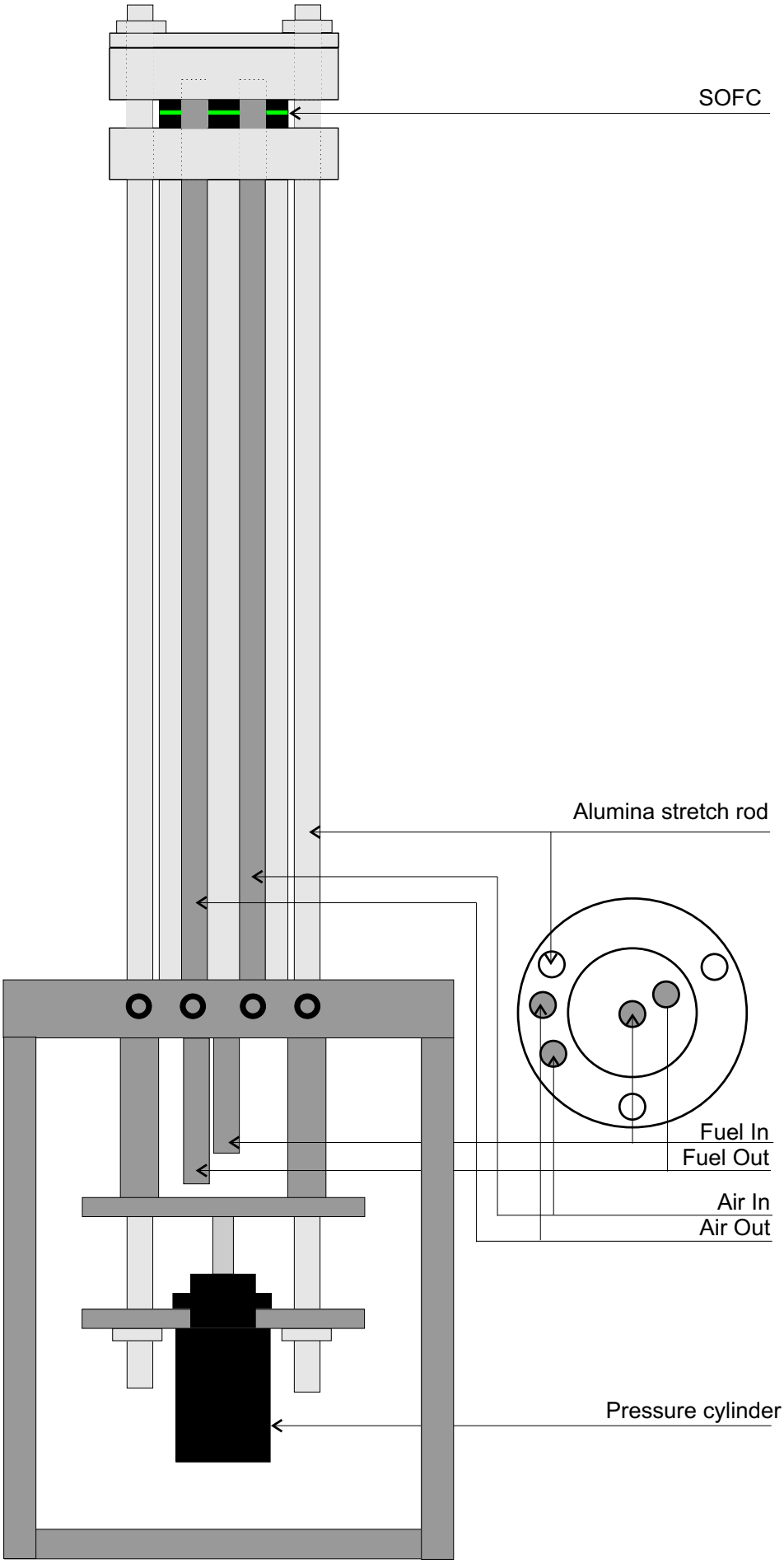

Fig. 8.3: Schematic of the single cell setup.

9. PAPER II - COMPARISON OF PERFORMANCE DATA OF A SOLID OXIDE FUEL CELL USING BIOMASS GASIFICATION GAS AND NATURAL GAS

To be published in the proceedings from Science in Thermal and Chemical Biomass conversion, Vancouver Island, BC, Canada, Aug./Sept. 2004.

Comparison of performance data of a Solid Oxide Fuel Cell using biomass gasification gas and natural gas

Arnstein Norheim and Johan E. Hustad
Norwegian University of Science and Technology, Department of Energy and Process Engineering, N-7491 Trondheim, Norway
Jan Byrknes and Arild Vik
Prototech AS, P.O.Box 6034, Postterminalen, N-5892 Bergen, Norway

ABSTRACT: Gasification of biomass produces a gas consisting mainly of H_2, CO, CO_2, H_2, N_2, CH_4 and other light hydrocarbons. The composition of the gas mixture differs depending on the biomass used, gasification process conditions and technology. Gasification processes using air as gasification medium produce a diluted fuel gas, with high nitrogen content, up to 50 % (vol). Steam gasification on the other hand, will give a gas richer in hydrogen and carbon monoxide and with only 3-5 % (vol) N_2. The hydrogen content can be as high as 35-45 % (vol) and CO typically 20-30 % (vol). The Solid Oxide Fuel Cell (SOFC) is a high temperature fuel cell operating at 750-1000^{o}C. H_2, CO and reformed hydrocarbons may all be electrochemically oxidised in this type of fuel cell making the SOFC highly fuel flexible. The SOFC has a relatively high electrical efficiency, more than 50% is achievable, and high temperature heat is produced in the cell. The SOFC is thus suitable for combined heat and power plants. A single cell SOFC setup was made at the laboratory of Prototech, Norway. A planar, anode supported circular shaped SOFC with a diameter of 40 mm was put between two flow distributor/current collector plates, one on each electrode. Gas flow, cell temperature, cell voltage and current drawn from the cell were logged by a computer. Experiments have been performed with various compositions of H_2 and CO diluted with CO_2 and N_2. Open Circuit Voltage (OCV) and current-voltage curves (IV-curves) were established for the various gas compositions. The effect of replacing hydrogen with CO as fuel and further the effect of increasing the N_2 and CO_2 concentration thus simulating a more dilute gas is shown. The results are compared with results using natural gas (CH_4) as fuel in the fuel cell. Thus the performance loss of the SOFC fuelled by dilute gases is estimated.

BACKGROUND

The Solid Oxide Fuel Cell (SOFC) is a high temperature fuel cell operating at 750-1000^{o}C. H_2, CO and reformed hydrocarbons may all be electrochemically oxidised in this type of fuel cell. The SOFC has thus proven to be very fuel flexible and various concepts have been proposed [1-6, 19, 20].

In addition to power, produced at efficiencies exceeding 50%, high temperature heat is produced in the cell which makes the SOFC suitable in a combined heat and power plant.

The state of the art SOFC anode is made of a porous cermet of nickel and Y_2O_3-stabilised ZrO_2 (Ni-YSZ) whereas the porous cathode is made of Sr-doped $LaMnO_3$. The electrolyte placed between the two electrodes is made of dense Y_2O_3-stabilised ZrO_2 (YSZ) [7-10].

Gasification of biomass produces a gas consisting mainly of H_2, CO, CO_2, H_2O, N_2, CH_4 and other light hydrocarbons. The composition of the gas mixture differs depending on the biomass used, gasification technology and temperature. Gasification processes using air as gasification medium produces a gas rich in nitrogen, up to 50 % (vol) [17]. Steam gasification on the other hand, may give a gas with only 3-5 % (vol) N_2 and a H_2 and CO content of 35-45 % (vol) and 20-30 % (vol), respectively [16]. Steam gasification of biomass would therefore be especially well suited as a supplier of fuel gas for a SOFC in an integrated system. Other gasification technologies should also be considered as they all produce a gas containing H_2, CO and CH_4 which take part, directly or indirectly, in the electrochemical reactions in an SOFC.

This work aims at investigating, experimentally, the SOFC performance under varying inlet gas composition. Any potential performance loss or cell degradation due to trace components such as sulphur, chlorine and alkali metals found in a gasifier producer gas, has not been investigated here. However, it is known that sulphur has a negative effect on the SOFC performance even at very low levels [21, 22]. The potential effects of alkali metals and chlorine are not known, but should be investigated in the future.

THEORY

As mentioned previously, H_2 and CO can be electrochemically oxidised in a SOFC. The main overall reactions on the SOFC anode side are the oxidation reactions of H_2 and CO:

$$H_2 + O^{2-} \Rightarrow H_2O + 2e^- \quad \text{(Eq. 1)}$$

$$CO + O^{2-} \Rightarrow CO_2 + 2e^- \quad \text{(Eq. 2)}$$

At the cathode the following reaction occurs:

$$O_2 + 4e^- \Rightarrow 2O^{2-} \quad \text{(Eq. 3)}$$

Thus the overall cell reactions are as follows:

$$H_2 + 1/2O_2 \Rightarrow H_2O \quad \text{(Eq. 4)}$$

$$CO + 1/2O_2 \Rightarrow CO_2 \quad \text{(Eq. 5)}$$

The cell voltage is governed by the partial pressures of the gases in the mixture fed to the anode and the partial pressure of oxygen fed to the cathode. The Nernst equation gives the theoretically obtainable voltage for the two above reactions.

$$E_N = E_G - \frac{RT}{nF} \ln K \qquad \text{(Eq. 6)}$$

Here E_G is the Gibbs voltage, R is the universal gas constant, T is the temperature in Kelvin, n is the number of electrons transferred in the reaction, F is the Faraday constant and K is the equilibrium constant for the reaction. The equilibrium constant, K, is calculated using the partial pressures of the gases involved in the reaction. For (Eq. 4) and (Eq. 5), respectively, this becomes

$$K_4 = \frac{p_{H_2O}}{p_{H_2}\sqrt{p_{O_2}}} \qquad \text{(Eq. 7)}$$

$$K_5 = \frac{p_{CO_2}}{p_{CO}\sqrt{p_{O_2}}} \qquad \text{(Eq. 8)}$$

The Nernst voltages at 975°C for equal mixtures of H_2/H_2O and CO/CO_2 (all partial pressures are 0.5) are E_{NH2} = 0.882 V and E_{NCO} = 0.856 V for the H_2 reaction (Eq. 4) and CO reaction (Eq. 5), respectively.

The actual operating voltage is lower than the theoretical Nernst voltage. This is due to loss mechanisms internally in the cell itself and in the surrounding equipment. At low current densities the voltage drops linearly with increasing current i.e. the losses are ohmic. At high current densities the gas transport through the anode and cathode becomes the limiting factor and the voltage drops more rapidly with further increasing loads. However, at the levels of current densities investigated in this work the voltage shows a clear linear relationship to the current drawn from the fuel cell.

When fuelled by natural gas, hydrocarbons are normally reformed to CO and H_2 by reaction with H_2O. This is done to prevent carbon layer formation on the anode and the consequent deactivation of the cell [11,18]. Steam reforming may be done either in a separate pre-reformer, internally in the fuel cell anode or as a combination of the two [7,8,12,13]. In either case the reforming reaction is essentially carried out over a supported nickel catalyst [11] with steam-to-carbon (S/C) ratios ranging from 1.5 to 8 [7,8,14,15].

It has been reported that thermodynamic equilibrium of the reforming reaction (Eq. 9) and the water-gas shift reaction (Eq. 10) is achieved over nickel catalysts at elevated temperatures (above 500°C) [18-20].

$$CH_4 + H_2O \Rightarrow CO + 3H_2 \qquad \text{(Eq. 9)}$$

$$CO + H_2O \Rightarrow CO_2 + H_2 \qquad \text{(Eq. 10)}$$

EXPERIMENTAL SETUP

A single cell SOFC setup was made at the laboratory of Prototech, Norway. A planar, anode supported circular SOFC was put between two alumina flow distribution plates, one on each electrode. The cell diameter was 40 mm and the anode thickness 600 µm. A thin Pt-film (0.27 mm) was placed directly on the electrodes i.e. between the electrodes and flow distribution plates for current collection and voltage measurements. This assembly was pressurised with springs to ensure good electrical contact and to reduce gas leakages. Additionally, the cell was sealed off along the outer rim of the cell. Thus the diffusion of especially hydrogen and the subsequent burning outside the cell was minimised.

Ceramic (alumina) tubes were connected to the cell/flow distribution plate assembly before the whole setup was put into an electrically heated oven. The Pt-films for current and voltage measurements were connected via Pt-wires to a NI Field Point^{TM} unit. Additionally an S-type thermocouple placed close to the anode was connected to the Field Point unit.

Fuel composition, fuel flow and air flow was controlled by a Bronkhorst flow control system.

RESULTS AND DISCUSSIONS

In all experiments performed in this work, the total fuel flow entering the anode is 200 ml/min and the air flow to the cathode is 200 ml/min. The maximum current drawn from the fuel cell is 0.5 A which corresponds to a maximum H_2 or CO utilisation of around 4 ml/min. Thus, these experiments are performed with a large fuel and air excess and the gas composition is essentially constant over the electrodes. All partial pressures mentioned in this section are related to a total gas pressure of 1 atm.

CHANGING THE H_2/CO RELATIONSHIP, CONSTANT CO_2

Fig. 1 shows the open circuit voltage (OCV) for a series where the partial pressures of H_2 and CO (p_{H2} and p_{CO}) are varied. Throughout this series $p_{CO} = 0.9 - p_{H2}$ and p_{CO2} is constant at 0.1. It is seen that as CO is replaced with H_2 the OCV increases systematically. This is in accordance with the theoretical expression for the cell performance as previously stated.

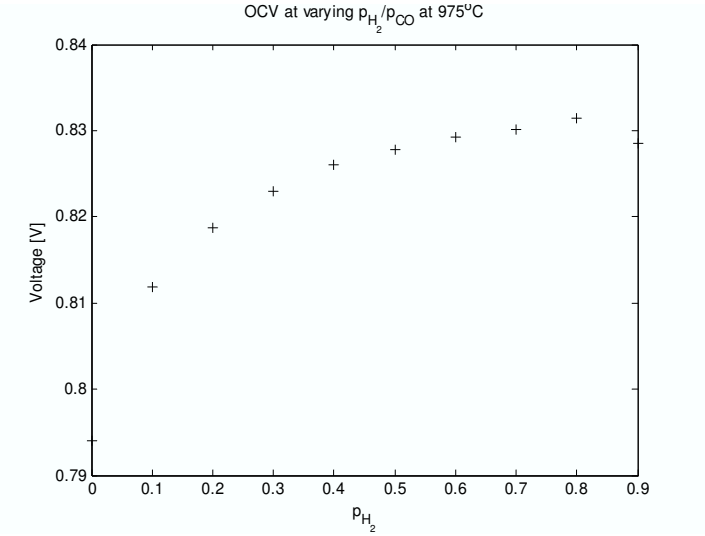

Fig. 1 Open circuit voltage at $p_{CO} = 0.9\text{-}p_{H2}$ and $p_{CO2} = 0.1$ at 975°C.

The OCV is the cell voltage when no current is drawn from the fuel cell. To investigate the cell performance at a given input gas composition, current-voltage curves (IV-curves) are established. This is done by adjusting the current flowing through the cell and measure the corresponding cell voltage. Fig. 2 shows IV curves for four of the gas compositions from Fig. 1. It is seen that as H_2 is replaced in an equal amount with CO, the cell voltage at all levels of the current drawn from the cell decreases. The sum of the partial pressures of the combustibles H_2 and CO is constant in all four series.

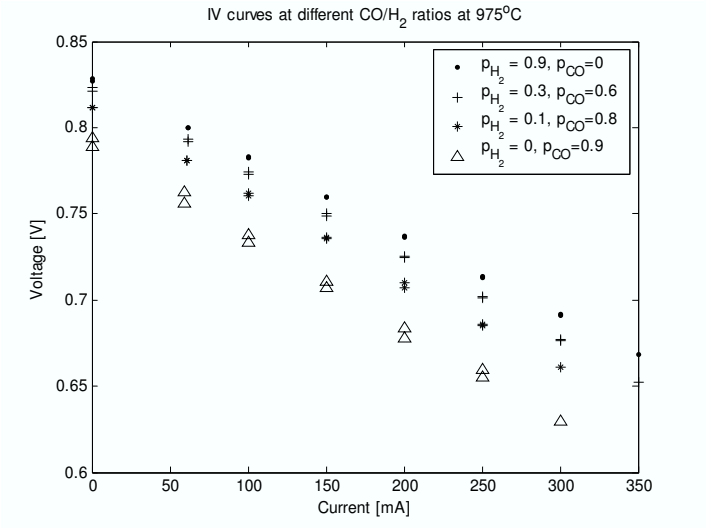

Fig. 2 IV curves at varying p_{H2}/p_{CO} ratio (p_{CO} = 0.9-p_{H2} and p_{CO2} = 0.1) at 975°C.

The average linear voltage drop has been calculated for the cases investigated in these experiments. For the case with H_2 only fed to the anode, the linear voltage drop is 0.46 V/A. As the fuel gas mixture is switched to CO only, the linear voltage drop increases to 0.55 V/A, which implies that the cell performs poorer as more CO is used compared to H_2.

CHANGING THE CO_2/N_2 RELATIONSHIP, CONSTANT H_2

In this series the aim was to investigate whether the water-gas shift reaction (Eq. 10) reaches thermodynamic equilibrium or not in the SOFC anode. Fig. 3 shows the OCV values for a series with a constant H_2 partial pressure of 0.5 in the gas fed to the cell at room temperature. Going from left to right in Fig. 3 N_2 is replaced with equal amounts of CO_2. Thus, if no equilibration occurs, the OCV should remain constant, as the partial pressure of H_2 in that case would be constant. However, as can be seen in the figure, the OCV decreases significantly as N_2 is replaced with CO_2. The reason is that more CO and H_2O are produced as more CO_2 is introduced to the gas mixture. When CO replaces H_2, the cell performance is reduced as seen in Fig. 1. In addition, the equilibrium ratio of both pH_2/pH_2O and pCO/pCO_2 decreases as more CO_2 is introduced. Since the cell voltage is directly proportional to these ratios, this indicates that equilibrium is close to achieved and that the cell voltage should in fact decrease.

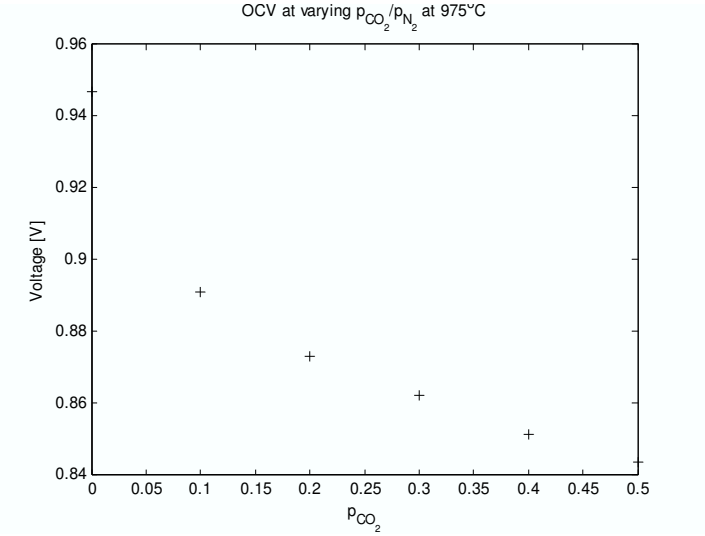

Fig. 3 Open circuit voltage at $p_{N2} = 0.5\text{-}p_{CO2}$ and $p_{H2} = 0.5$ at 975°C.

The linear voltage drop for the case with N_2 present is 0.46 V/A, whereas for the case with CO_2 present the voltage drop is 0.41 V/A as can be seen in Fig. 4. But the lower operating voltage when CO_2 is the only diluent present, gives a poorer cell performance throughout the conditions investigated here.

It can be concluded that a dilution with CO_2 decreases the cell performance compared to dilution with N_2.This is due to the in-situ conversion of H_2 to CO and that more reaction products (H_2O and CO_2) are added or produced by dilution with CO_2. Dilution with N_2 on the other hand, leaves the gas composition unchanged. The total amount of the combustibles, H_2 and CO, however, remains the same regardless of the diluent introduced to the gas mixture.

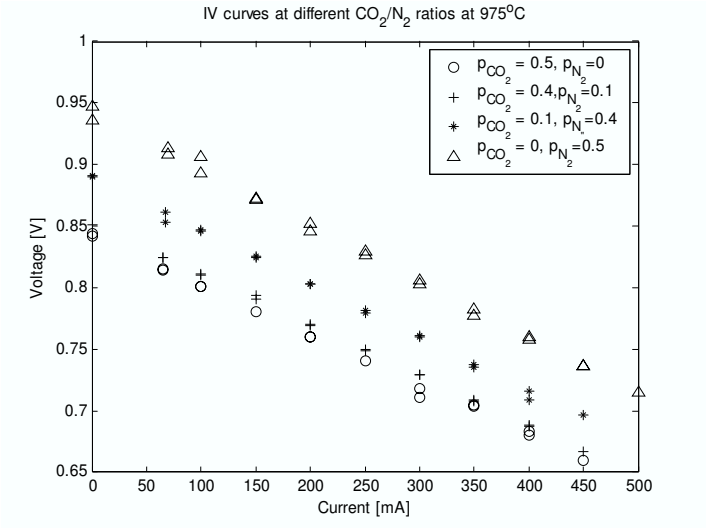

Fig. 4 IV curves at varying p_{CO2}/p_{N2} ratio (p_{N2} = 0.5-p_{CO2} and p_{H2} = 0.5) at 975°C.

COMPARING NATURAL GAS AND BIOMASS PRODUCER GAS

In this series of experiments the performance of the SOFC fuelled by reformed North Sea pipeline natural gas [213] is compared to the performance using a producer gas from a steam gasification plant [16]. For the natural gas cases investigated syngases are mixed in accordance to the pre-reformer outlet equilibrium compositions for different steam-to-carbon ratios (S/C). For the gasification gases the gas composition reported from the Güssing steam gasification plant [16] using wood chips and wood pellets as fuels are used. The different fuel compositions investigated are given in Table 1. It is seen that as the S/C ratio for the pre-reforming of natural gas increases the volume fraction of the reactants H_2 and CO decreases and the fractions of the products H_2O and CO_2 increases. It is therefore expected that the SOFC performance decreases slightly with increasing S/C ratio. The differences in the gas composition for gasification of the two different biomass fuels are mainly due to the different water content in the two fuels. At present time the gasifier in Güssing is fed by wood chips.

Table 1 Gas composition of natural gas at different steam-to-carbon ratios (S/C) and gasifier gas.

	Natural gas					Gasifier gas	
S/C	Unreformed	1.8	2.0	2.2	2.5	Wood chips	Wood pellets
CH_4	88.1	0	0	0	0	0	0
C_2H_6	6.2	0	0	0	0	0	0
C_3H_8	2.0	0	0	0	0	0	0
H_2	0	62.0	60.0	58.0	55.2	37.1	43.1
H_2O	0	17.0	20.0	22.8	26.6	31.2	14.0
CO_2	3.1	3.1	2.5	3.9	4.3	10.3	6.9
CO	0	17.5	16.5	15.3	13.8	20.2	34.6
N_2	0.5	0.1	0.1	0.1	0.1	1.7	1.5

Fig. 5 shows that the voltage is slightly lower for the gasified wood chips case compared to natural gas and wood pellets. The gasified wood pellet case and the four natural gas cases have essentially the same voltage and voltage drop throughout the conditions tested.

The single cell SOFC performance changes from one experimental series to another due to long-term instabilities in the experimental setup. This does not, however, have any influences on the results within each series as these are of relatively short durations. The cell performance was verified to be the same before and after each series by feeding the cell by a reference gas mixture.

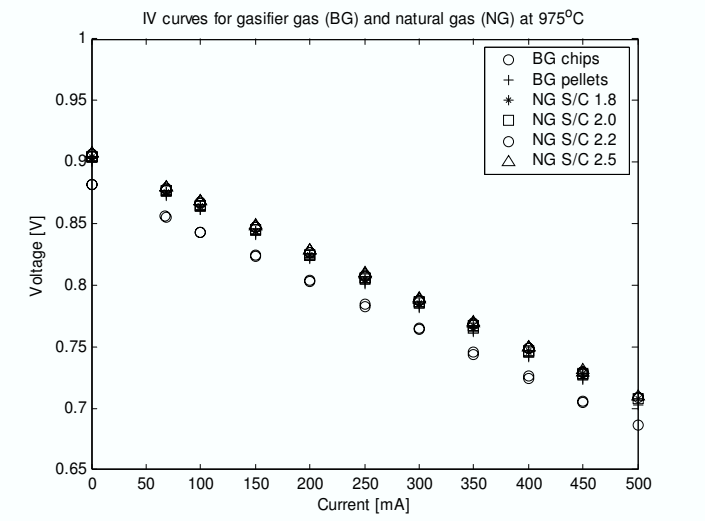

Fig. 5 IV curves for gasifier gas and reformed natural gas.

The power yield in the six test cases investigated here are therefore essentially the same. A small difference is, however, observed for the gasified wood chips case as shown in Fig. 6. The SOFC seems to perform almost equal when fuelled with biomass gasifier gas compared to reformed natural gas.

One point should be noted here: The single cell setup essentially offers the possibility to study the operating conditions at a full-sized fuel cell inlet. This can be explained by considering the large fuel and air excess which these experiments are performed at and the fuel conversion in the cell is very low even at the highest loads. As a consequence, the fuel composition fed to the cell leaves the cell almost unchanged, i.e. the conditions are nearly constant over the whole anode area. In a real-sized cell running at high fuel conversion, the gas conditions changes radically from the gas inlet to the gas outlet and more products (H_2O and CO_2) are formed. Regardless of fuel feed, the amount of products formed then will be more similar than in the excess feed experiments. Thus, the performance differences between the different fuel compositions reported in this work will be even smaller in a large-scale fuel cell with more realistic fuel utilisation.

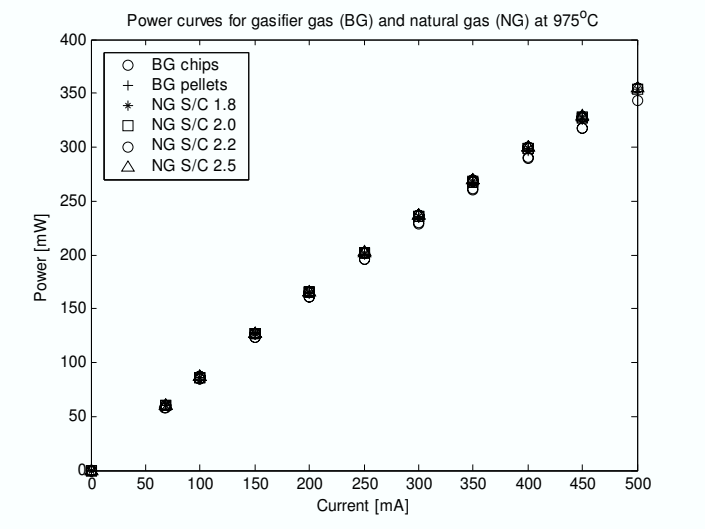

Fig. 6 Power curves for gasifier gas and natural gas.

CONCLUSIONS

The SOFC is well suited to run on gas from biomass gasification and the performance will be comparable to that of natural gas. The operating principle and the governing reactions for the performance of the SOFC results in that as more reaction products (H_2O and CO_2) are mixed into the

fuel gas or formed in the cell, the cell operating voltage and thus the performance decreases. Mixing nitrogen to the fuel gas has no negative influence on the cell performance as this does not change the mutual relationship between reactants and products. However, the energy content in the fuel gas decreases, and consequently the volume gas flow must be increased to achieve equal power production.

It is derived from the experiments that thermodynamic equilibrium is close to achieved at the SOFC anode and nickel particles are acting as catalysts to approach the equilibrium. Predicting the SOFC performance for any given gas, the equilibrium gas composition should thus be considered.

ACKNOWLEDGEMENTS

The Nordic Graduate School of Biofuel Science and Technology has funded this work.

REFERENCES

1 Riensche E. et al. (2000) Clean combined-cycle SOFC power plants. Journal of Power Sources, vol 86, 404-410.
2 Dokiya M (2002) SOFC system and technology. Solid State Ionics, vol 152-153, 383-392.
3 Ahmed K. et al. (2002) Demonstration of LPG-fueled solid oxide fuel cell systems. Solid State Ionics, vol 152-153, 485-492.
4 Sammes N.M. & Boersma R. (2000) Small-scale fuel cells for residential applications. Journal of Power Sources, vol 86, 98-110.
5 Van herle J. et al. (2003) Energy balance model of a SOFC cogenerator operated with biogas. Journal of Power Sources, vol 118, 375-383.
6 Wojcik A. et al. (2003) Ammonia as a fuel in solid oxide fuel cells. Journal of Power Sources, vol 118, 342-348.
7 Minh N.Q. & Takahashi T. (1995) Science and Technology of Ceramic Fuel Cells. Elsevier.
8 Larminie J. & Dicks A. (2000) Fuel cell systems explained. Wiley.
9 Bossel U. G. (1992) Final report on SOFC Data – Facts & Figures. Swiss Federal Office of Energy.
10 Yamamoto O. (2000) Solid oxide fuel cells: fundamental aspects and prospects. Electrochimica Acta, vol 45, 2423-2435.
11 Finnerty C.M et al. (1998) Carbon formation on and deactivation of nickel-based/zirconia anodes in solid oxide fuel cells running on methane. Catalysis Today, vol 46, 137-145.
12 Hiei Y. et al. (1996) Partial oxidation of methane for internally reformed solid oxide fuel cell. Solid State Ionics, vol 86-88, 1267-1272.
13 Meusinger J. et al. (1998) Reforming of natural gas in solid oxide fuel cell systems. Journal of Power Sources, vol 71, 315-320.
14 Achenbach E. & Riensche E. (1994) Methane/steam reforming kinetics for solid oxide fuel cells. Journal of Power Sources, vol 52, 283-288.
15 Ødegård R. et al. (1995) Methane reforming on Ni/Zirconia SOFC anodes. Proceedings of the 4th International Symposium on Solid Oxide Fuel Cells, 810-819.

16 Hofbauer H., Rauch R., Bosch K., Koch R., Aichernig C. (2002) Biomass CHP Plant Güssing – A Success Story. Renet-Austria, Austria.
17 Barrio M. (2002) Experimental investigation of small-scale gasification of woody biomass. PhD thesis Norwegian University of Science and Technology, Norway.
18 Clarke S.H. et al. (1997) Catalytic aspects of the steam reforming of hydrocarbons in internal reforming fuel cells. Catalysis Today, vol 38, 411-423.
19 Schuler A. et al. (2000) Sulzer Hexis SOFC running on home heating oil. Proceedings of the fourth European SOFC forum, vol 1, 107-114.
20 Dicks A. & Larminie J. (2000) Reforming of fossil fuels (Status survey). Proceedings of the fourth European SOFC forum, vol 2, 927-936.
21 Matsuzaki Y. & Yasuda I. (2001) Effect of a sulphur-containing impurity on electrochemical properties of a Ni-YSZ electrode. Proceedings of the 7th International symposium on Solid Oxide Fuel Cells, 769-782.
22 Singhal S.C. (2000) Advances in solid oxide fuel cell technology. Solid State Ionics, vol 135, 305-313.
23 Gas composition from Hydro's Heimdal laboratorium, November 2002.

10. PAPER III - EXPERIMENTAL STUDIES ON THE INFLUENCE OF H_2S ON SOFC PERFORMANCE

Submitted for publication in Journal of Power Sources.

Experimental studies on the influence of H_2S on SOFC performance

Arnstein Norheim[a], Jan Byrknes[b], Markus Broström[c], Johan E. Hustad[a], Arild Vik[b]
[a]Department of Energy and Process Engineering, Norwegian University of Science and Technology, Kolbjørn Hejes vei 1A, 7491 Trondheim, Norway, email: Norheim: arnstein.norheim@ntnu.no Hustad: johan.e.hustad@ntnu.no
[b]Prototech AS, Postboks 6034, Postterminalen, 5892 Bergen, Norway, email: Byrknes: jan@prototech.no, Vik: arild@prototech.no
[c]Energy Technology and Thermal Process Chemistry, Umeå University, 901 87 Umeå, Sweden, email: Broström: markus.brostrom@chem.umu.se

Abstract

The change of performance in a single cell planar Solid Oxide Fuel Cell (SOFC) has been investigated as different H_2S concentrations were mixed into the anode fuel gas. At an operating temperature of 800°C the H_2S concentrations investigated were in the range from 5 to 240 ppm. Two H_2S concentrations, 40 and 80 ppm, were additionally investigated at 850°C. The results indicate that the sulphur poisoning of the anode was close to completed at an H_2S concentration of 10 ppm. Increasing the H_2S concentration further only caused a marginal additional performance loss. Increasing the temperature did not seem to have any clear effect on the SOFC's tolerance towards H_2S. The cell resistance at 800°C increased by 0.14 and 0.13 Ω cm^2 to 1.21 and 1.20 Ω cm^2 at 120 and 240 ppm H_2S, respectively. The current density was 200 mA cm^{-2}. Even at these H_2S concentrations the cell performance was found to be restored as the sulphur was removed from the gas mixture.

1. Introduction

The Solid Oxide Fuel Cell (SOFC) may be fuelled by a variety of fuels such as natural gas [1-4], oil derived gases and liquids [5-8], pure ammonia [9] and synthesis gases from coal and biomass gasification [7, 10-12]. This is possible mainly due to the high operating temperature (600-1000°C) enabling the SOFC to both internally reform light hydrocarbons and electrochemically oxidise CO in addition to hydrogen.

A recent study [13] showed that the SOFC performance is essentially unaltered when switching from a typical gas composition of steam reformed natural gas to that of steam gasified biomass. There are, however, trace components such as compounds of sulphur, chlorine and alkali metals present in most biomass materials and therefore also in biomass gasification producer gases. In natural gas, some sulphur is normally present either from the raw gas or added by the gas utility company for safety purposes. Thus, due to the historic interest in natural gas as SOFC fuel, the impact of sulphur on the SOFC performance has been investigated, especially in the low ppm range (1-50 ppm H_2S). The sulphur level may be significantly higher in biomass gasification gases. The Güssing steam-gasifier producer gas, for example, is reported to contain 20-40 ppm H_2S even after the gas cleaning system [14]. Unfiltered biomass gasifier producer gases may therefore, although not frequently reported, contain H_2S at levels well above the concentrations normally investigated in the SOFC literature.

Several researchers have studied the effect of sulphur on SOFC half-cells i.e. an experimental setup designed to investigate the effects on the anode/electrolyte interface only. Matsuzaki and Yasuda [15, 16] studied the poisoning effect of sulphur at levels up to 15 ppm in a mixture of 79/21 % (vol.) H_2/H_2O at 750, 900 and 1000°C. Their electrolyte was made of Y_2O_3-stabilised ZrO_2 (YSZ). NiO and Pt-paste were used as anode and cathode, respectively. They found that the lower limit of detectable sulphur poisoning is 0.05, 0.5 and 2 ppm at 750, 900 and 1000°C, respectively. The time needed for the poisoning effect to stabilise was found to be 12 and 9 ks at 750 and 900°C, respectively and between 3.6 and 4.8 ks at 1000°C. After removing the sulphur impurity, the interface resistance regained its initial level in all cases investigated; the time needed being 360, 9 and 3.6 ks at 750, 900 and 1000°C, respectively. At 1000°C it was found that 2 ppm H_2S increased the anodic overpotential by 2 mV whereas 15 ppm increased the overpotential by 74 mV. The anodic overpotential did not increase linearly with increasing H_2S concentration.

In an earlier work by Dees et al. [17] the interfacial resistance between a Nickel-YSZ (Ni-YSZ) anode and YSZ electrolyte was investigated at H_2S levels up to 105 ppm in a fuel gas mixture of 97/3 % (vol.) H_2/H_2O at 1000°C. At 105 ppm H_2S the area specific resistance of the interface had increased to 0.446 Ω cm^2 from the initial level at no H_2S of 0.271 Ω cm^2. However, it was concluded that at 105 ppm H_2S the cell degradation was irreversible due to the fact that nickel is not thermodynamically stable at that sulphur level. Additionally, it was proposed that the irreversibility at 105 ppm H_2S may be caused by sulphur being incorporated into the electrolyte.

Geyer et al. [18] found that addition of 5 ppm H_2S in a fuel gas mixture of 97/3 % (vol.) H_2/H_2O at 950°C caused a doubling of the electrode polarisation. Primdahl and Mogensen [19] investigated the effect on the interfacial resistance between Ni/Ni-YSZ anodes and YSZ electrolytes when 35 ppm H_2S was added in a similar gas mixture at 850 and 1000°C. It was concluded that the electrode resistance increased by 60% upon addition of the sulphur impurity irrespective of anode type, operating temperature and an anodic current of 0 or 100 mA cm^{-2}. Additionally, it was concluded that the poisoning effect was completely reversible.

The available literature on the performance of a complete SOFC cell or stack fuelled by gases containing sulphur is sparse and at least not as systematic as the references sited above. Most work is done on the state-of-the art SOFC configuration, namely Ni-YSZ anode, YSZ electrolyte and Sr-doped $LaMnO_3$ (LSM) cathode. Singhal [20] reports that the tubular Siemens Westinghouse SOFC operating at 1000°C experiences a 10% voltage drop, presumably at a given load, upon addition of 1 ppm H_2S to a fuel mixture of 89/11 % (vol.) H_2/H_2O.

Petrik et al. [8] reported that their SOFC was able to tolerate high-sulphur containing military fuels referred to as JP-8 and F-76. The SOFC was reported to be stable at a 300 ppm H_2S spiked composition. Furthermore, it is in this work stated that similar results were obtained for H_2S concentrations up to 2000 ppm. Additionally, a 25-cell stack was reported to operate continuously on steam reformed JP-8 fuel with an unspecified H_2S concentration for 1600 hours. This setup, however, also included a steam pre-reformer that is reported to be sulphur tolerant. Since the H_2S level in the fuel gas leaving the pre-reformer is not reported in this work, it may be difficult to draw any clear conclusions on the actual sulphur tolerance of this SOFC stack.

Stolten et al. [21] reported that their cell experienced a reversible 2% drop in power output for H_2S concentrations below 10 ppm at 950°C. The SOFC used was a planar 10 x 10 cm^2 cell. The anode material is reported to be Ni, zirconia and some ceria, the electrolyte was made of YSZ with some alumina and finally the cathode was made of Ca-doped $LaMnO_3$. From data presented in [21, (Fig.8.p92)], one can find that at a fuel mixture of 67/33 % (vol.) H_2/H_2O and a constant current density of 150mA cm^{-2}, addition of 0.5, 1.5, 2, 3 and 10 ppm H_2S reduced the cell voltage by approximately 10, 15, 20, 20 and 25 mV, respectively. For a different gas mixture (78/22 % (vol.) undefined coal gas/H_2O) and the same current density, addition of 1 and 4 ppm H_2S reduced the cell voltage by 10 and 15 mV, respectively, again based on data from the figure.

One may conclude, based on the presented literature that the interfacial resistance between anode and electrolyte of the SOFC increases by between 60 and 100% as H_2S is introduced in the fuel stream. There does not seem to be any clear consensus between the different authors as to whether there is a temperature effect on the sulphur tolerance or not. However, the effect of H_2S on the cell performance seems to be heavily non-linear as the concentration increases. As the H_2S concentration increases from 0 to between 5 and 10 ppm, the voltage at a given load seems to drop more rapidly than above 10 ppm. It is further difficult to draw conclusions regarding the stability of the Ni-based SOFC anode at high sulphur levels based on the published literature.

The objective of the present study is to investigate in detail the influence of H_2S on the SOFC performance. This is motivated by the diversion in the previous published data on the effect of sulphur impurities, and the lack of systematic data on complete SOFC performance at high sulphur levels. The present study has relevance to ongoing work aiming at using biomass gasification gases as a fuel for SOFC's.

2. Experimental setup

A planar, anode supported SOFC delivered by Forschungszentrum Jülich, was cut into a circular shape with a diameter of 26 mm giving an active cell area of around 5 cm^2. The cell has an approximately 1.6 mm thick porous Ni-YSZ anode, a 5 µm thick dense YSZ electrolyte and a 55 µm thick porous LSM-YSZ cathode [22].

Fig. 1 shows, schematically, details of the single cell setup used in the present work. On each electrode, $LaCrO_3$-based interconnects were used for gas distribution and current collection. For current collection the two interconnects were connected via Pt-films and Pt-wires to an ampere-meter, a resistance and a current control unit. Cell voltage was measured by connecting Pt-wires from the electrodes to a voltmeter. Finally, cell temperature was measured by an S-type thermocouple placed close to the anode in the fuel inlet tube. The cell perimeter was sealed to minimise gas leakages and finally the setup was placed in an electrically heated oven and heated to 800°C at a rate of 60°C/h.

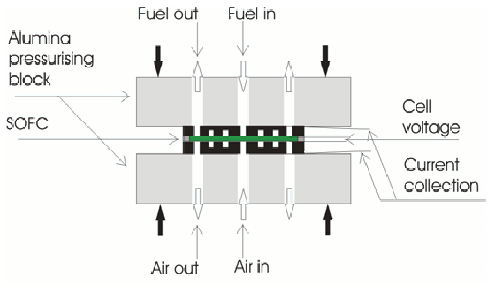

Fig. 1. Schematic detail of the single cell SOFC setup used in the present work.

The fuel mixture to the anode and air to the cathode was controlled by Bronkhorst mass flow controllers. In all the experiments presented here, a total fuel mixture flow rate of 300 ml/min was fed to the anode and an equal air flow was fed to the cathode. Thus, the fuel and air utilisation was kept low, and near homogeneous conditions over the entire cell are assumed.

The fuel gas mixture fed to the anode in all the experiments consisted of 2/3 H_2 and 1/3 CO_2 by volume at room temperature. This is a gas mixture that, when thermodynamically equilibrated at the operating temperature, is similar to that of biomass steam gasification producer gases.

H_2 and CO_2 were supplied by gas bottles of 2.5-quality. A premixed certified gas bottle containing 1000 ppm H_2S in CO_2 was used as H_2S supply. Thus, by adjusting the flow of the pure CO_2 and that of the H_2S containing CO_2, a range of H_2S concentrations could be obtained.

First, experiments of 5 to 80 ppm H_2S at 800^{o}C were performed. Thereafter, the temperature was increased to 850^{o}C and tests of 40 and 80 ppm H_2S were repeated. After reducing the temperature to 800^{o}C again, the 80 ppm H_2S test was repeated once more. Finally, the 120 and 240 ppm tests were performed.

Before and after each H_2S experiment, a reference experiment without H_2S was performed. This proved valuable as the cell performance increased significantly during the course of the experiments (24 days from start to stop).

Thus, the procedure was to first establish reference current-voltage curves (IV-tests) at 0 ppm H_2S. Then the desired H_2S concentration was introduced, the cell performance was allowed to stabilise and new IV-tests were performed. The H_2S was thereafter removed from the fuel gas mixture, the cell performance was once more allowed to stabilise and new reference IV-tests were performed. The cell was operated at a current density of 50 mA cm^{-2} between the IV-tests. Between each shift in H_2S concentration and cell performance stabilisation, there was a time period of approximately 24 hours.

After the experimental series the cell was analysed using environmental scanning electron microscope (ESEM) with an energy dispersive spectroscopy (EDS) detector, and X-ray diffractometry (XRD).

3. Results and discussion

3.1. Cell resistance versus H_2S concentration

Based on the IV-data, the total cell resistance was established for each level of H_2S concentration. This was done by measuring the voltage difference between the open circuit voltage (OCV) and the cell voltage at the maximum current level. This voltage drop was then divided by the current to produce the absolute cell resistance in ohms. Multiplying this number by the cell area (5 cm^2) gave the area specific cell resistance in $\Omega\ cm^2$.

The specific resistance at 0 ppm H_2S changed significantly during the experimental period of 24 days, as shown in Fig. 2. The IV-test before the first introduction of H_2S showed an area specific resistance of 2.16 $\Omega\ cm^2$ at a current density of 100 mA cm^{-2}. This was reduced to 1.17 $\Omega\ cm^2$ at the same load after the last experiment. The specific resistance at the different H_2S concentration also followed this declining trend (Fig. 2.). Thus, the highest cell resistance obtained was 2.36 $\Omega\ cm^2$ which was measured in the 5 ppm H_2S experiment. In all the following experiments smaller cell resistances were obtained, motivating the approach of studying the resistance change as the different H_2S concentrations were introduced, rather than comparing the specific resistances at the different H_2S concentrations.

The reduction in the resistance was not constant during the 24 days and was most pronounced during the experiments at 850^oC. During the last experiments of 80 to 240 ppm H_2S at 800^oC, the reduction in the resistance flattened out and finally increased slightly. This seems to be in accordance with the findings of Primdahl and Mogensen [23] as they in one case found the anode-related polarisation resistance to first stabilise after 300 h. They further report the changes in polarisation for different cells to be in the interval from -90 to 110 m$\Omega\ cm^2$ per 1000 h. In the present work, the cell resistance at 0 ppm H_2S is seen to stabilise around day 18 (Fig. 2.) i.e. after approximately 430 hours and then increase by a gradient of around 40 m$\Omega\ cm^2$ per 1000 h.

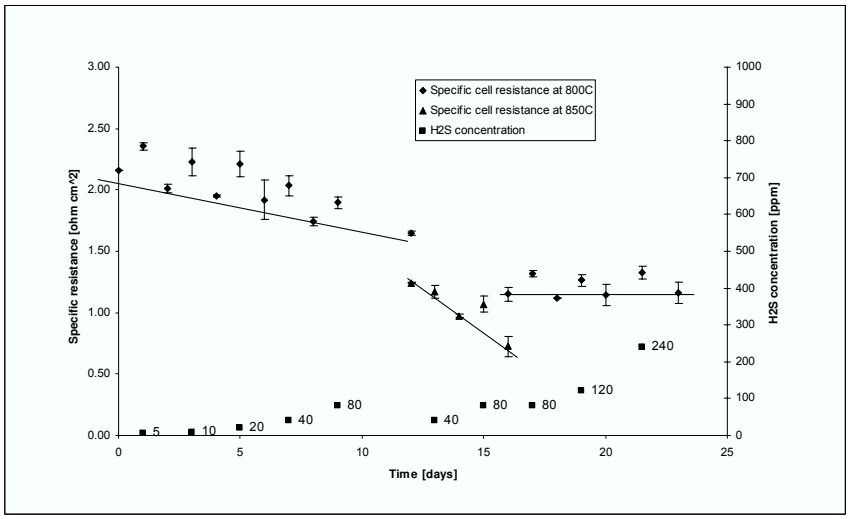

Fig. 2. Area specific resistance at a current density of 100 mA cm^2 versus time and H_2S concentration at - 800 and 850^{o}C.

The reduced area specific resistance may be due to better sintering of the anode/electrolyte interface causing a decrease in the interfacial resistance. The final slight increase in the resistance may be an effect of irreversible degradation of the anode material due to the high sulphur levels in agreements with the conclusions drawn by Dees et al. [17]. However, phase diagrams for Ni in an atmosphere of H_2 and H_2O at the actual operating temperature, clearly shows that the anode material is thermodynamically stable as Ni even at as high H_2S concentration as 300 ppm. Only at very high levels of fuel utilisation i.e. a hydrogen partial pressure well below 0.01 bar, one may expect Ni to be stable as NiS(s). This is shown in Fig. 3 calculated by using the program FactSage [24].

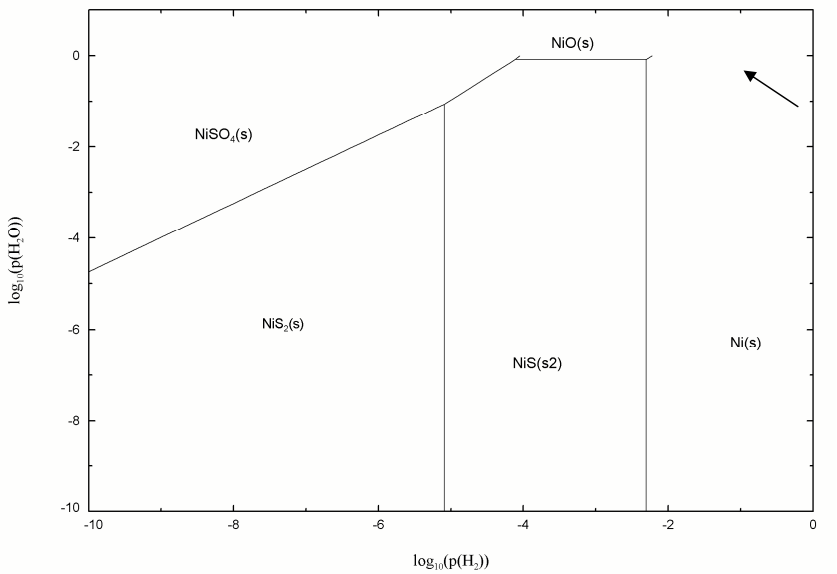

Fig. 3. Phase diagram of nickel in an atmosphere of H_2 and H_2O at 800°C and an H_2S concentration of 300 ppm. The SOFC operating interval is indicated in the upper right corner of the diagram (arrow).

Due to the steady decrease in cell resistance during the experimental period, two different values of the increase in cell resistance by introduction of H_2S were obtained; one compared to the cell resistance before introduction of H_2S and one compared to the cell resistance after removal of H_2S. It may be correct to assume that the cell resistance due to the time effect decreased at a nearly constant slope during the two days each experiment lasted. Thus, the increase in cell resistance caused by the actual H_2S concentration is given as the difference between the measured cell resistance at this H_2S concentration and the average of the measured cell resistances at 0 ppm H_2S before and after the H_2S experiment. For this to be correct, one must assume that the processes causing the decrease in cell resistance were constant during two days, and that the actual H_2S level caused no irreversible changes in the anode or anode/electrolyte interface.

In Table 1 the measured cell resistances are tabulated for all the different H_2S concentrations. In addition, the estimated, or averaged, cell resistances at 0 ppm H_2S and the estimated resistance increases due to the H_2S poisoning are given.

Table 1
Area specific cell resistances at given current densities at the different H_2S concentrations. The specific resistances at 0 ppm H_2S are given as an average of the measured ones before and after the actual H_2S experiment.

H_2S [ppm]	Temperature [^oC]	Maximum current density [mA cm^{-2}]	Specific resistance [Ω cm^2] Measured at H_2S level	Estimated at 0 ppm H_2S	Difference
5	809	100	2.355	2.085	0.270
10	810	100	2.230	1.980	0.250
20	810	100	2.215	1.935	0.280
40	809	100	2.035	1.833	0.203
80	810	100	1.900	1.718	0.182
40	853	100	1.170	1.108	0.063
80	853	100	1.070	0.848	0.223
80	809	100	1.320	1.135	0.185
80	810	200	1.215	1.070	0.145
120	809	100	1.265	1.133	0.133
120	810	200	1.205	1.078	0.128
240	809	100	1.330	1.155	0.175
240	811	200	1.200	1.080	0.120

Based on the results present here, it is difficult to quantitatively compare the effect of 5 ppm H_2S to that of 240 ppm H_2S due to the time effects. However, it seems clear that the cell resistance increase is not proportionally dependent on the sulphur concentration in the gas feed. Based on previously published literature and the present study, the sulphur poisoning of the SOFC anode seem to be nearly saturated at a relatively low H_2S concentration, probably in the order of 5-10 ppm. By further increasing the sulphur concentration, the cell resistance only increases marginally.

From the present results one may conclude that the specific cell resistance increases by 0.10-0.20 Ω cm^2 for H_2S concentrations in the range of 40-240 ppm. For the H_2S concentrations below 40 ppm one would expect a smaller increase in the cell resistance, but the initial time effect in these experiments disturbs the results too much to draw any clear conclusions.

3.2. Cell power versus H_2S concentration

The experiments at the highest H_2S concentrations were performed at the end of the experimental period, and are therefore, due to the mentioned time effect, the most quantitatively reliable ones. In Fig. 4 combined IV and power curves are presented for 0, 120 and 240 ppm H_2S. The area specific cell resistance at 0 ppm H_2S before the 120 ppm experiment and after the 240 were both 1.07 Ω cm^2 at a current density of 200 mA cm^{-2}. At 120 and 240 ppm H_2S the cell resistance increased to 1.21 and 1.20 Ω cm^2, respectively, at a current density of 200 mA cm^{-2}. This corresponds to a 13 and 12 % increase in cell resistance and voltage drop at 200 mA cm^{-2} for the 120 and 240 ppm case, respectively.

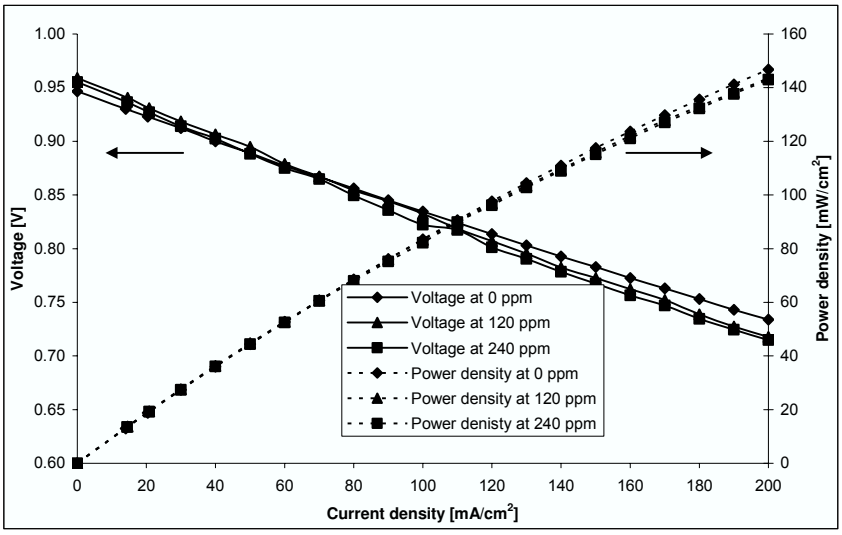

Fig. 4. Cell voltage (left axis) and power density (right axis) as a function of current density at 0, 120 and 240 ppm H_2S at 800^{o}C.

3.3. Voltage stability versus H_2S concentration

Between each shift in H_2S concentration, the cell was running at a constant current density of 50 mA cm^{-2} except during the IV tests used for resistance calculation. Current and cell voltage were continuously logged every 5 second during the complete experimental series, including the periods of constant load. By calculating the cell voltage's standard deviation for each hour during the periods of constant load, a measure of the cell voltage stability versus H_2S concentration is established. In Fig. 5., the hourly mean cell voltage at the constant load is shown for the series at 240 ppm H_2S and the subsequent series at 0 ppm H_2S in addition to the respective cell voltage's hourly standard deviation. Based on these data, and similar data obtained for the other sulphur concentrations, it is concluded that the stability of the cell voltage under load does not seem to be affected by H_2S concentrations up to 240 ppm.

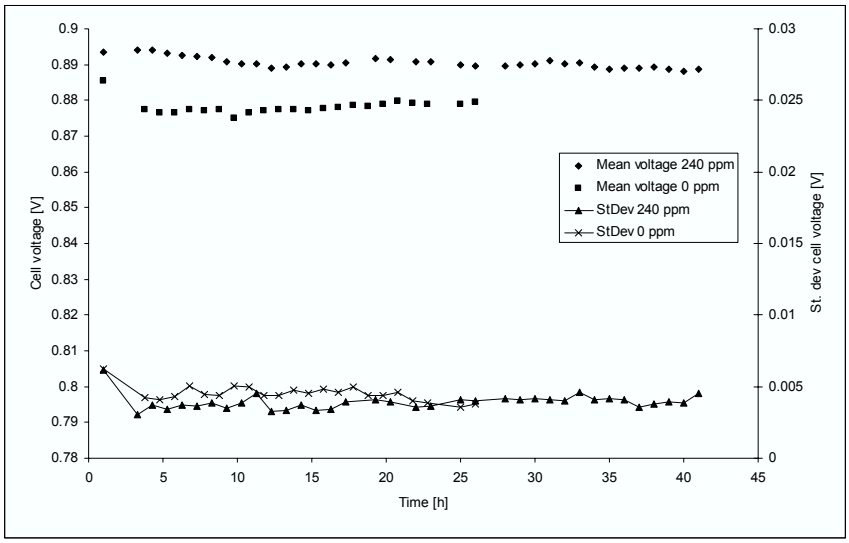

Fig. 5. Cell voltage (left axis) and standard deviation of cell voltage (right axis) at a constant load of 50 mA cm^{-2} versus time at 240 and 0 ppm H_2S at 800°C.

3.4. Temperature dependency

Temperature does not seem to have any consistent effect on the SOFC's sulphur tolerance. At 80 ppm H_2S at 850°C the cell resistance increased 0.22 Ω cm^2 at a load of 100 mA cm^{-2} compared to the 0.18-0.19 Ω cm^2 increase at 800°C (Table 1). The 40 ppm test at 850°C, however, shows a significantly smaller increase in cell resistance than the corresponding 800°C test. This may be due to a too early measurement of the cell resistance after the temperature step from 800 to 850°C giving a too high value of the cell resistance at 0 ppm before the 40 ppm H_2S experiment.

3.5. Open circuit voltage versus H_2S concentration

In Fig. 6 the measured OCV values for all experiments are shown. The OCV changed slightly in the reference experiments at 0 ppm H_2S over time, without any consistent trend. However, the OCV in all cases increased slightly when H_2S was introduced in the gas feed. This may be due to the fact that the increased resistance may reduce the inherent electron flow in the cell. Thus, the short circuit of the fuel cell is reduced causing a small rise in potential between the cathode and the anode.

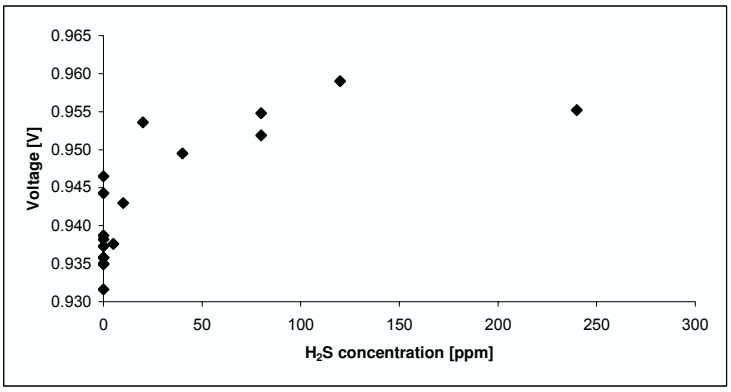

Fig. 6. Open circuit voltage at 800°C as a function of H_2S concentration.

A third effect of the introduction of H_2S is a consistent temperature rise of 1 to 2°C at all levels of H_2S, compared to the temperature at 0 ppm H2S. This has not been further investigated but may be due to the radiative heat absorption spectrum of H_2S or due to sulphur coverage of the thermocouple.

3.6. ESEM/EDS and XRD analysis

No sulphur (ESEM/EDS) or sulphur containing crystalline compounds (XRD) was found in the anode structure. This gives further reason to conclude that the cell performance degradation caused by up to 240 ppm H_2S is reversible and that sulphur does not, at this H_2S concentration, react chemically with the nickel catalyst in the SOFC anode.

4. Conclusions

SOFC performance losses at 800°C have been investigated as H_2S concentrations in the range from 5 to 240 ppm were mixed into the anode fuel gas. Two H_2S concentrations, 40 and 80 ppm, were additionally investigated at 850°C. The main gas composition in all experiments was 67% H_2 and 33% CO_2, by volume. This mixture is similar, when thermodynamically equilibrated at the SOFC operating temperature, to biomass steam gasification producer gases. The H_2S concentrations tested are in the range of the expected levels in such gases.

By introduction of H_2S to the fuel gas mixture, the total area specific cell resistance increased by 0.1 to 0.3 Ω cm^2. Due to processes occurring in the single cell SOFC during the first two weeks of the experimental series, it is difficult two accurately quantify the effect of e.g. doubling the H_2S concentration. The results indicate that the sulphur poisoning of the anode was close to completed at a H_2S concentration of 10 ppm. Increasing the H_2S concentration further only caused a marginal additional performance loss.

The cell was found to recover when H_2S was removed from the fuel gas in all the cases investigated here. Post experimental structure analysis showed no traces of sulphur in the anode layer.

The time needed for the cell resistance to stabilise after introduction and after removal of H_2S, was not accurately determined, but 24 hours seemed to be sufficient in all cases and at both temperatures investigated here.

Operational stability in terms of the stability of the operating cell voltage under load was not found to be affected by addition of sulphur to the fuel gas.

Increasing the temperature from 800 to 850^{o}C was not found to have any significant effect on the change in specific resistance caused by the introduction of H_2S.

Acknowledgements

The Nordic Graduate School of Biofuel Science and Technology has funded this work. Dan Boström, Energy Technology ant Thermal Process Chemsitry, Umeå University, is acknowledged for his work with the XRD analysis.

References

[1] R. Peters, R. Dahl, U. Klüttgen, C. Palm, D. Stolten, J. Power Sources, 106 (2002) 238-244.
[2] R. Peters, E. Riensche, P. Cremer, J. Power Sources, 86 (2000) 432-441.
[3] J. Meusinger, E. Riensche, U. Stimming, J. Power Sources, 71 (1998) 315-320.
[4] S.C. Singhal, Solid State Ion., 135 (2000) 305-313.
[5] K. Ahmed, J. Gamman, K. Föger, Solid State Ion., 152-153 (2002) 485-492.
[6] A. Schuler, T. Zähringer, B. Doggwiler, A. Rüegge, Proc. Fourth European Solid Oxide Fuel Cell Forum, 1 (2000), 107-114.
[7] A. Dicks, J. Larminie, Proc. Fourth European Solid Oxide Fuel Cell Forum, 2 (2000), 927-936.
[8] M.A. Petrik, C.E. Milliken, R.C. Ruhl, B.P. Lee, Proc. Fuel Cell Seminar, (1998) 124-127.
[9] A. Wojcik, H. Middleton, I. Damopoulos, J. Van herle, J. Power Sources, 118 (2003) 342-348.
[10] J. Van herle, F. Maréchal, S. Leuenberger, D. Favrat, J. Power Sources, 118 (2003) 375-383.
[11] T. Proell, R. Rauch, C. Aichernig, H. Hofbauer, Proc. ASME Turbo Expo, 2004, GT2004-53900.
[12] J. Stainforth, R.M. Ormerod, Catalysis Letters, 81 (2002) 19-23.
[13] A. Norheim, J.E. Hustad, J. Byrknes, A. Vik, Proc. STCBC, Victoria, BC, Canada, (2004). In Press.
[14] H. Hofbauer, R. Rauch, K. Bosch, R. Koch, C. Aichernig, in A.V. Bridgewater, Pyrolysis and Gasification of Biomass and Waste, CPL Press, Newbury, UK, (2003).
[15] Y. Matsuzaki, I. Yasuda, Solid State Ion., 132 (2000) 261-269.
[16] Y. Matsuzaki, I. Yasuda, in H. Yokokawa, S.C. Singhal (eds.), Proc. of the 7th Int. Symp. on Solid Oxide Fuel Cells, The Electrochemical Society, Pennington, NJ, Vol. 2001-16 (2001) 769-782.
[17] D.W. Dees, U. Balachandran, S.E. Dorris, J.J. Heiberger, C.C. McPheeters, J.J. Picciolo, in S.C. Singhal (ed.), Proc. of the 1st Int. Symp. on Solid Oxide Fuel Cells, The Electrochemical Society, Pennington, NJ, Vol. 89-11 (1989), 317-321.

[18] J. Geyer, H. Kohlmüller, H. Landes, R. Stübner, in U. Stimming, S.C. Singhal, H. Tagawa, W. Lehnert (eds.), Proc. of the 5th Int. Symp. on Solid Oxide Fuel Cells, The Electrochemical Society, Pennington, NJ, Vol. 97-40 (1997), 585-594.

[19] S. Primdahl, M. Mogensen, in M. Dokiya, S.C. Singhal (eds.), Proc. of the 6th Int. Symp. on Solid Oxide Fuel Cells, The Electrochemical Society, Pennington, NJ, vol 99-19 (1999) 530-540.

[20] S.C. Singhal, Solid State Ion., 135 (2000) 305-313.

[21] D. Stolten, R. Späh, R. Schamm, in U. Stimming, S.C. Singhal, H. Tagawa, W. Lehnert (eds.), Proc. of the 5th Int. Symp. on Solid Oxide Fuel Cells, The Electrochemical Society, Pennington, NJ, Vol. 97-40 (1997), 88-93.

[22] R.N. Basu, G. Blaß, H.P. Buchkremer, D. Stöver, F. Tietz, E. Wessel, I.C. Vinke, in H. Yokokawa, S.C. Singhal (eds.), Proc. Of the 7th Int. Symp. on Solid Oxide Fuel Cells, The Electrochemical Society, Pennington, Vol. 2001-16 (2001), 995-1001.

[23] S. Primdahl, M. Mogensen, J. Appl. Electrochem., 30 (2000), 247-257.

[24] C.W. Bale, P. Chartrand, S.A. Degterov, G. Eriksson, K. Hack, R. Ben Mahfoud, J. Melancon, A.D. Pelton, S. Petersen, Calphad, 26(2) (2002) 189-228.

11. CONCLUSIONS AND RECOMMENDATIONS FOR FURTHER WORK

11.1 Conclusions

The aim of this work has been to make initial steps towards a future system of combined heat and power production based on biomass gasification and Solid Oxide Fuel Cells. A literature study on biomass materials and thermal conversion of these together with a study on fuel cells in general and SOFC in detail, has been the basis for the present work. Although the main focus has been on the SOFC, a certain knowledge on the composition and quality of gasifier producer gases was needed in order to identify potential problems or bottlenecks regarding the operation of the SOFC. Three main aspects and potential problems have been studied in detail here:

1. The composition of typical gasifier producer gases focusing mainly on compounds formed from four trace species; sulphur, chlorine, potassium and sodium.

2. SOFC performance at varying fuel gas composition and the effect of adding inert gases, in addition to a comparison of the performance when using fuel gases similar to reformed natural gas and biomass gasification producer gases.

3. SOFC performance when using a fuel gas similar to biomass gasification producer gas with varying sulphur (H_2S) concentrations up to 240 ppm.

The modeling work was performed by using the program FactSage. The method used was calculation of thermodynamic equilibrium of the species present focusing mainly on four trace species present in biomass gasification gases, sulphur, chlorine, potassium and sodium. Important results were that sulphur is mainly found as H_2S and can be found at concentrations well above 200 ppm. Furthermore, alkali metals may be present at high concentrations mainly as KOH, K and KCl. Chlorine is thus found as KCl as long as potassium is present. Otherwise, chlorine may be found as HCl. The amount of especially potassium governs the temperature at which condensation of alkali rich carbonates occurs. Relating this knowledge to SOFC operation, the conclusions from this study are:

- SOFC performance degradation at high sulphur concentrations in the fuel gas need to be further investigated.

- SOFC performance at high levels of alkali metals and chlorine in the fuel gas need to be investigated.

- SOFC operation at temperatures below the condensation temperature should be avoided as this most probably would cause deposition of alkali rich carbonates on the anode surface.

The two experimental parts presented in this thesis were performed in the laboratory of Prototech, Bergen by using a small single cell SOFC in an in-house built setup. Fuel and air excess ratios were kept high throughout the experiments and fuel and air utilisation were consequently kept low. The first experimental series aimed at investigating the SOFC performance under varying fuel inlet gas composition. By keeping the CO_2 partial pressure constant at 0.1 bar and varying the H_2 and CO partial pressures, it was found that increasing the CO partial pressure and consequently reducing the H_2 partial pressure causes a reduced SOFC performance. The difference is significant, but the SOFC may be successfully operated at up to 90% CO and still produce electrical power. The SOFC therefore has high fuel flexibility. This experimental series further showed that the change in cell performance when switching from a synthetically mixed fuel gas similar to reformed natural gas and a similarly mixed biomass gasification producer gas is relatively small. It was therefore concluded that biomass gasification producer gases are suitable as fuel for SOFCs. This conclusion is so far only valid as long as the producer gases do not contain trace species such as sulphur, chlorine and alkali metals.

The second experimental series aimed at investigating the SOFC performance when using a fuel gas containing up to 240 ppm H_2S. The fuel gas was mixed from gas bottles to simulate, when thermodynamically equilibrated, producer gas from biomass steam gasification. The single cell SOFC was operated at 800^oC and H_2S was introduced at varying concentrations from 5 to 240 ppm. Two tests (40 and 80 ppm H_2S) were repeated at 850^oC in order to investigate whether the effect of sulphur is temperature dependent or not. The cell was operated for 24 hours at each sulphur concentration and current-voltage curves were established at the end of each exposure period to be able to calculate the total area specific cell resistance at the given sulphur level. Between each sulphur exposure period the cell was operated for 24 hours at 0 ppm H_2S in order to obtain a reference cell resistance before and after each sulphur test. The cell resistance at 0 ppm H_2S decreased during the initial 400 hours of operation. This made it difficult to interpret the results during this period. However, even at a sulphur concentration of only 5 ppm H_2S a significant increase in area specific cell resistance was observed. Furthermore, a doubling of the sulphur concentration did not seem to double the increase in cell resistance. This may indicate that the effect of sulphur poisoning of the SOFC anode is more or less stabilised at a rather low sulphur concentration and a further increase in sulphur concentration thus only marginally increases the cell resistance. Based on the results from these experiments, this saturation sulphur concentration seems to be in the order of 10-20 ppm H_2S. Temperature did not seem to have a significant influence on the effect of sulphur on the SOFC performance, but the results obtained at 850^o were somewhat obscured by the initial increase in cell performance. The most reliable results were those obtained after the initial 400 h period. These results include those at the highest sulphur concentrations; 80, 120 and 240 ppm H_2S. During these experiments, the cell resistance at 0 ppm H_2S was stable between each period of sulphur poisoning. The cell resistance at 80, 120 and 240 ppm H_2S were almost identical and the cell resistance regained its initial level after each exposure period. These results give additional reason to conclude that at above a certain sulphur concentration a further addition of sulphur does not cause a proportional increase in cell resistance. Additionally, even at 240 ppm H_2S the cell structure did not seem to be affected since the cell resistance regained its initial level after removal of the sulphur from the fuel gas. The exposure period was, however, short (24 h) and any potential long-term effects of high sulphur concentrations were therefore not detected here. High sulphur levels may also decrease the SOFC anode's catalytic activity towards reforming of hydrocarbons. Any such effect could not

be detected through these experiments as no hydrocarbons were present in the fuel gas. The present results are therefore only connected to the electrochemical reactions at the anode-electrolyte interface and possibly the electronic conductivity of the anode layer.

Four main conclusion can be drawn from the work presented in this thesis:

1. Biomass gasification producer gases may contain high ppm levels of several potential SOFC performance degrading compounds; H_2S, KOH, K and KCl are the most significant ones.

2. Depending on the amount of potassium present in the producer gas, liquid and solid alkali carbonates may condense if the gas is cooled below the condensation temperature of the gas; SOFC operation below this temperature may cause the carbonates to deposit on the SOFC anode and may thus block the porous anode structure.

3. Biomass gasification gases are suitable as fuel for the SOFC, at least when the gases are free from particulates, tars and trace species. In that case, the SOFC may perform as well as when using reformed natural gas as fuel.

4. The SOFC may be operated using fuel gases containing H_2S at concentrations well above 200 ppm. The performance will, however, be reduced as sulphur is introduced.

Biomass gasification producer gases may thus seem to be an interesting option as fuel for Solid Oxide Fuel Cells. Most important, the cell performance is expected to be satisfactory compared to reformed natural gas. In addition, the high sulphur tolerance reported in this work is a benefit as the requirements for sulphur removal may be limited.

11.2 Recommendations for further work

Considering the main gas composition only, biomass gasification producer gases are suitable as fuel for SOFCs. As a total filtering of the producer gases may both be difficult and significantly add cost to the system, it is important to investigate the influence other species and components in the producer gas may have on the SOFC and its performance. The SOFC may, as reported in this work, be fueled by fuel gases containing high sulphur concentrations and the performance loss was found to be essentially the same at 80 and 240 ppm H_2S. The exposure period was, however, relatively short (24 hours). Any potential long term effects of using fuel gases containing high sulphur concentrations were therefore not detected. An experimental series aiming at investigating such long term effects should be performed. This should include two identical experimental setups with two single cell SOFCs from the same production batch. One setup should use a fuel gas containing no sulphur and the other should be fueled by a similar fuel gas but with a preferably high sulphur concentration. Doing so, any long term sulphur effects are separated from the inherent long term effects of the cell operation itself.

The effect gaseous components of chlorine and alkali metals may possibly have on the SOFC performance should furthermore be experimentally investigated. No experimental data reporting exposure of SOFC materials by such species have been published so far. An experimental setup enabling accurate addition of chlorine and alkali metal compounds into the fuel gas should therefore be constructed. This is by no means straightforward as especially alkali metals in gas phase requires a high temperature and can not be put into

ordinary gas bottles as opposed to e.g. H_2S. When such a setup is constructed, however, an experimental series similar to the one presented in paper III should be carried out. Exposure to liquid and solid alkali carbonates would perhaps be of less interest, as such components will most probably deposit on the anode surface thus blocking the gas transport through the electrode.

Biomass gasification producer gases may, in addition to the above mentioned species, also contain significant levels of particles and tars. Particles should most probably be removed from the fuel gas upstream the SOFC. Otherwise blocking of gas channels may occur, especially of the relatively narrow gas distribution channels in the interconnects of the SOFC stacks. This has not been experimentally verified and could therefore be of some interest to future researchers. Of greater interest, however, is the effect of tars in the fuel gas. Tars are mainly heavy hydrocarbons and could therefore potentially be cracked and reformed to light hydrocarbons and eventually hydrogen and carbon monoxide. This might be possible, either in a separate tar cracker or at least partly over the catalytic SOFC anode itself. Thus the tars may act as fuel for the SOFC and in the end contribute to the electric power production in the SOFC. Again, no published literature supports these considerations.

Summing up, the recommendations or suggestions for future work on SOFC in this field are, in preferred order, as follows:

- Long term sulphur exposure tests.
- Chlorine and alkali metal exposure tests.
- Investigations into tar behaviour and SOFC response.

APPENDIX

A. PAPER IV

Published in the proceedings of the Second World Biomass Conference, Rome, Italy, May 2004.

BIOSOFC - TECHNOLOGY DEVELOPMENT FOR INTEGRATED SOFC, BIOMASS GASIFICATION AND HIGH TEMPERATURE GAS CLEANING

Johan E. Hustad, Øyvind Skreiberg, Torbjørn Slungaard, Arnstein Norheim and Otto K. Sønju
Norwegian University of Science and Technology, Department of Energy and Process Engineering, N-7491 Trondheim, Norway
Hustad: phone: +47-73592513 fax: +47-73598390 e-mail: johan.e.hustad@ntnu.no

Hermann Hofbauer, Reinhard Rauch and Anita Grausam
Vienna University of Technology, Institute of Chemical Engineering, Getreidemarkt 9/166, A-1060 Vienna, Austria
Hofbauer: phone: +43-1-58801-15970 fax: +43-1-58801-15999 e-mail: hhofba@mail.zserv.tuwien.ac.at

Arild Vik and Jan Byrknes
Prototech AS, P.O.Box 6034, Postterminalen, N-5892 Bergen, Norway
Vik: phone: +47-55574121 fax: +47-55574114 e-mail: arild.vik@prototech.no

ABSTRACT: Solid Oxide Fuel Cells (SOFCs) in combination with biomass gasification has a potential for high efficiency electricity production. The biomass gasification technology should yield the highest possible hydrogen content in the producer gas. Hence, steam gasification is an ideal gasification technology in combination with SOFCs. However, trace compounds in the producer gas, such as H_2S, alkali metal compounds, chlorine compounds and tars may be damaging for the SOFCs, depending on their levels. Therefore, there is a need for laboratory studies and testing of the influence of trace compounds on the Solid Oxide Fuel Cell (SOFC) performance, and long term onsite testing of a SOFC stack using producer gas from a steam gasification unit at normal operation. Gas cleaning is a necessity to remove particles from the producer gas before entering the SOFC stack. To optimize system efficiency, high temperature gas cleaning is the optimum option, and is a subject of extensive research worldwide.

The project described herein combines both novel fundamental and applied studies, including onsite testing of a 1 kW SOFC stack. As such, the novelty of this work is quite unique, and will contribute to future high efficiency electricity production from biomass. Onsite testing of the SOFC stack will take place using a slipstream from a steam gasification reactor, and a granular Panel Bed Filter for high temperature gas cleaning. This paper focuses on describing the project, its purpose and goals, challenges and status. Initial results from high temperature gas cleaning and SOFC performance using synthesis gas are presented. Modelling results on the influence of producer gas trace compounds on the SOFC performance, using the FACTSage chemical equilibrium program, are also presented.

This paper is part of an ongoing research project funded by the Research Council of Norway and Norwegian and Austrian industry.

1 INTRODUCTION

The EU strategies for Renewable Energy Sources (RES) involve an increase of the use of these resources from 6% (1997) to 12% (2010) and the Electricity from Renewable Energy Resources (RES-E) is subject to an increase from 14% (1997) to 22% (2010). A major part of this increase is planned to come from biomass. Increased production of heat and electricity will have to come from a large variety of processes, technologies and scales. Both combustion and gasification processes will contribute. The rapid increase in renewable electricity put focus on gasification technologies in particular, circulating and bubbling fluidised bed technologies being most attractive. To increase the electric efficiency in future gasification plants, a shift from gas engines and gas turbines to high temperature fuel cells is needed. Both the Solid Oxide Fuel Cell (SOFC) and the Molten Carbonate Fuel Cell (MCFC) are candidates for medium sized Combined Heat and Power plants (CHP). In this work a 1 kW SOFC stack will be tested by taking a slipstream from the Fast Internally Circulating Fluidised Bed (FICFB) gasifier at Biomasse Kraftwerk Güssing in Güssing, Austria, hereafter called the Güssing plant. The biomass gasification technology should yield as high as possible hydrogen content in the producer gas, and steam gasification is then ideal in combination with Solid Oxide Fuel Cells (SOFCs). Trace compounds in the producer gas, such as H_2S, alkali metal compounds, chlorine compounds and tars may be damaging for SOFCs, depending on their levels. There is a need for laboratory studies of the influence of these trace compounds on the performance of SOFCs, and long term onsite testing of a SOFC stack using producer gas from a steam gasification unit at normal operation. However, it is necessary to remove particles from the producer gas before it enters the SOFC stack. To optimise system efficiency, high temperature gas cleaning is the optimum option, and is a subject of extensive research worldwide.

This paper reports from an ongoing project which combines both novel fundamental and applied studies, including preliminary results from laboratory tests as well as from onsite testing in connection with biomass steam gasification. As such, the novelty of the project is quite unique, and will contribute to future development of high efficiency electricity production from biomass.

2 METHODS

2.1 Steam gasification – The Güssing plant

The Güssing plant has now been in successful operation for a number of years and results thereof have been reported extensively. See the website http://www.ficfb.at/ for a number of publications. The FICBC gasifier is an indirectly fired steam gasification unit where the producer gas is utilized in a gas engine today. The thermal input to the plant is 8 MW using wood chips as fuel, and the electric efficiency is about 20 %. In addition heat is delivered to a district heating system. The dry producer gas has a high content of hydrogen of up to 45 vol%, CO of up to 30 vol%, CO_2 of

about 20 vol% and methane of up to 12 vol%. Small amounts of nitrogen are also found in the producer gas, about 2 vol%. Using wood chips as fuel the H_2O content of the producer gas is about 40 vol%, giving a lower heating value of about 9 MJ/kg.

2.2 High temperature particle cleaning

The fact that high temperature gas cleaning of particles and trace compounds in general still remains to be solved satisfactorily has made producer gas cleaning an objective of extensive research worldwide for many years. In addition to granular filters, attention has mainly been directed towards ceramic and metallic candle filters for particle cleaning. Less focus has been put on high temperature removal of trace compounds that may be damaging for SOFCs, depending on their levels. Thus, very high demands are put on the hot gas cleanup (removal of gaseous and particulate emissions) in the BioSOFC project.

Cooling the producer gas from the Güssing plant gasifier outlet temperature of about 900°C, to below about 550°C, reduces the alkali and chlorine content in the gas to some extent in the filter. This leaves H_2S and tars as the potentially most difficult compounds. Further cooling might introduce operational problems due to tar condensation on the filter, although the critical temperature limit is being highly dependent upon gasifier operation.

Granular bed filters are insensitive to the impinging gas. This combined with the possibility to provide chemical processing of the gas makes the novel Panel Bed Filter (PBF) a promising alternative for high temperature cleaning of gasification producer gas [1, 2]. This cleaning concept utilises the transient behaviour of granular filtration and operates in surface filtration mode.

The PBF used in this project is a heated system, with several louvers supporting the granular material as shown in Figure 1. Temperatures, pressures and filter pressure drop build-up are logged. The inlet size of the current module has a width of 80 mm and a height of 300 mm (240 cm^2). Actual filtration surface is up to twice this area. Pressure pulse cleaning of the filter surface makes this unit suitable for continuous testing of high temperature gas cleaning.

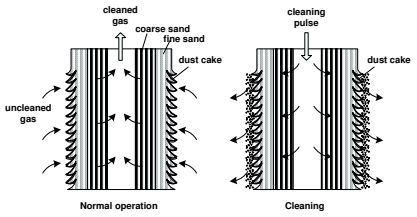

Figure 1: Working principle of the panel bed filter

The PBF has been successfully demonstrated in full-scale operation on biomass combustion flue gases [1]. Furthermore, filter cake formation upon a free horizontal surface of unbound filter media has been successfully demonstrated when filtering producer gas from a laboratory scale, air blown down draft stratified gasifier (fuelled with birch pellets) at elevated temperatures (300-540°C). Tars and heavier hydrocarbons were efficiently converted when applying catalytic bed material in this Horizontal Bed Unit (HBU) at about 540°C, and no deactivation of the catalyst was detected [2].

The HBU is also a heated system with a horizontal fixed granular bed in a circular container. Temperatures, pressures and filter pressure drop build-up are logged. The size of the granular bed is 85 mm in diameter and about 40 mm in height. There is no automatic removal of the filter cake formed on top of the granular material, and the unit is mainly used for studying filter cake build-up.

2.3 High temperature H_2S cleaning

The sulphur content in the producer gas from biomass gasification is much lower than from coal gasification, but still sulphur can pose a major problem for SOFC materials. However, the exact limit of acceptable H_2S concentration in the gas is not yet determined since literature reports different limiting values [3, 4]. This limit is also dependent on the material used in the specific SOFC application. An activity using different sorbent materials at high temperatures is planned using a small fixed bed reactor at well controlled conditions with varying gas compositions. Further, a high temperature H_2S cleaning solution is needed when testing the 1 kW SOFC stack at the Güssing plant.

2.4 SOFC

SOFCs have the potential to become a major technology for electricity generation in the coming decades. They combine very high electrical efficiency (45-60%) with extremely low emissions of major air pollutants (unburned species and NO_x). The high operation temperature of a SOFC lends itself readily to CHP operation, resulting in potential overall energy efficiencies above 80%. SOFCs thus represent one of the most promising technologies for cogeneration and decentralised electricity production. They can potentially be operated on a range of fuels, including pipeline natural gas, gasified biomass and coal, ammonia and reformed liquid hydrocarbons.

SOFCs of today are mainly designed to run on reformed natural gas. Several investigators and commercial companies have done extensive research on this. The most important issues are the formation of a carbon layer on the fuel electrode and sulphur poisoning of the fuel electrode. Producer gas has a different composition compared to natural gas, and can contain several species that may be damaging for SOFCs. As far as we know, there has been done no experimental work on running SOFCs on producer gas from a biomass gasification unit.

A key issue for commercial implementation of fuel cells is to achieve stringent cost targets. EC's short term and long-term targets for stationary generation are €9000/kW and €1000/kW, respectively. The long term target of lifetime is >40,000 hours.

The planar SOFC technology offers higher volumetric power densities than tubular geometries and most development work worldwide is directed towards planar technology.

In order to be able to reduce the operating temperature, a second generation "Anode Supported Cell" using the anode as a supporting member has been developed. In this concept the electrolyte is

approximately 0.01 mm thick. The mostly used material for the electrolyte is yttrium stabilised zirconia (YSZ) whereas the anode and cathode is made of a Ni-YSZ cermet and Sr-doped $LaMnO_3$, respectively. Current densities up to 1.2 W/cm^2 have been obtained on hydrogen with anode supported cells and traditional electrolyte materials and advanced electrodes. There is currently much work devoted to the development of other electrolytes based on gallium, ceria and others. Current densities up to 1.8 W/cm^2 have similarly been obtained at 800°C on hydrogen with these new materials. Current densities at real operating conditions and high fuel utilisation will be significantly lower than the values quoted above, and current densities of 0.7-0.9 W/cm^2 are more realistic. Operating anode supported cells at higher temperatures will increase the power density, an increase from 800°C to 920°C will typically double the power density. For the reason of the possible increase in power density, and for the benefit of combined processes, Prototech is developing stacks with flexible operating temperature in the range 750–950°C.

To estimate the performance of a SOFC fuelled by producer gas compared to natural gas, a single cell SOFC setup was made at the laboratory of Prototech, Norway. The cell used in these experiments is similar to those that will be used in the 1 kW fuel cell stack at the Güssing plant, i.e. a planar, anode supported SOFC. However, in the experiments at Prototech, a geometrically smaller, circular shaped cell with a diameter of 40 mm was used. The experiments were carried out with excess fuel and air flows, i.e. low fuel conversion. Thus, the operating conditions of the single cell are comparable to the inlet conditions for a real-sized cell. The performance differences are therefore larger than for a real-sized cell since the conditions at higher fuel conversion will be more equal independent on the inlet gas composition. Gas flow, temperature in the cell, cell voltage and current drawn from the cell were logged. The experiments were carried out at 975°C which is about the same operation temperature planned used in the onsite tests at the Güssing plant.

SOFC performance is reported to decrease when sulphur in the form of H_2S is included in the fuel gas [3, 4]. At low H_2S levels (<100 ppm) the performance loss is reported to be reversible but as the H_2S level increases significantly above 100 ppm, the performance loss is reported to be irreversible. However, the reason for the performance loss has not been fully understood. Alstrup et al. [5] among others propose H_2S chemisorption on nickel as the main reason at low H_2S levels. At higher H_2S levels the sulphur may also react chemically with nickel to form nickel sulphides/sulphates.

2.5 Modelling

The conversion of a typical producer gas is investigated in the SOFC operating temperature range (750-1000°C) by equilibrium calculations. Of particular interest are changes in gas composition as different parameters such as temperature, fuel conversion and content of sulphur, alkali metals and chlorine change. Different amounts and combinations of amounts of trace elements (S, K, Na and Cl) have been investigated, representing typical values valid for different biomass fuels in producer gas.

Based on the findings in the equilibrium calculations, phase diagrams for nickel in both H_2/H_2O and CO/CO_2 atmospheres are established. From the equilibrium calculations the most important, compounds of S, K, Na, and Cl are identified. In addition, typical maximum levels of the different compounds are estimated. Thus, phase diagrams for nickel under the influence of the different trace compounds can be produced. This may give an indication of which species that should be included in a further experimental investigation aiming on examining whether they have any negative influence on the SOFC performance.

3 RESULTS AND DISCUSSIONS

3.1 Steam gasification – The Güssing plant

The Güssing plant dry producer gas composition during three weeks in 2003 using wood chips as fuel can be seen in Figure 2. The dry producer gas composition can be regarded as rather stable, which is important for stable SOFC operation.

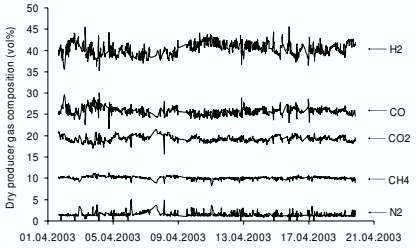

Figure 2: The Güssing plant dry producer gas composition during three weeks in 2003 using wood chips as fuel

In the product gas 100-200 ppm H_2S is present. In addition, a considerable amount of particles (≈ 50 g/Nm³) and tar (1-2 g/Nm³) is present. Today these elements are removed by a low temperature bag filter and a scrubber, but when using SOFCs particles and H_2S should be removed at a higher temperature to optimize the system efficiency.

3.2 High temperature particle cleaning

The HBU is now tested onsite at the Güssing plant. All the HBU tests show successful dust cake build-up, and thereby successful dust cleaning, at about 540°C. These results are important for planning of PBF tests.

The HBU tests completed so far are summarized in Table I. A slipstream was taken out from the gasifier freeboard at close to isokinetic velocity. The slipstream was passed through 15 meter of heated line at about 600°C down to the test site. A cyclone was used for lowering the dust concentration from 40-60 g/Nm^3 in the gasifier down to 2-3 g/Nm^3 in the HBU. The same heated line and cyclone will be used for testing of the PBF and the complete system with a SOFC stack added. After the HBU it was used a total filter, tar condensing box immersed in an ice/water mixture, silica gel container for water removal, valve for flow adjustment, critical nozzle for flow measurement, suction pump and a long tube for cleaned gas venting above the plant roof.

Table I: HBU tests performed at the Güssing plant

#	Bed type	Velocity [cm/s]	Temp. [°C]	Flow [Nm^3/h]	Pressure drop [$Pa/(mg/cm^2)$]
1	565µm sand	20.2	548	1.22	565
2	468µm spheres	20.2	537	1.26	694
3	687µm spheres	20.3	537	1.27	488
4	687µm spheres	10.2	544	0.657	423-549

3.3 SOFC

Figure 3 shows the performance of a single cell SOFC fuelled by pre-reformed (S/C=2.2) pipeline natural gas compared to the Güssing producer gas [6]. Throughout the interval investigated the SOFC performance is essentially the same for the two fuels. As the power drawn from the cell increases, there is however a small increasing difference in the performance. The conclusion from these experiments is that the SOFCs fuelled by the producer gas will perform at a level comparable to the level achieved when fuelled by natural gas.

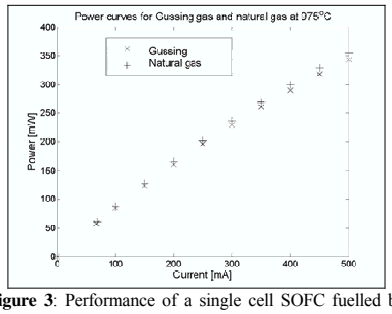

Figure 3: Performance of a single cell SOFC fuelled by natural gas and the Güssing plant producer gas

3.4 Modelling

Figure 4 shows a phase diagram for pure nickel in an atmosphere of H_2 and H_2O and a H_2S concentration of 300 ppm. The typical SOFC operating range is indicated by an arrow in the upper right corner. It is seen that the cell is not operated in the area of stable NiS, but as the fuel conversion increases (i.e. follows the direction of the arrow) one moves toward the NiS area.

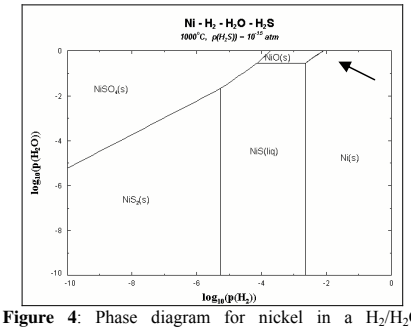

Figure 4: Phase diagram for nickel in a H_2/H_2O atmosphere and 300 ppm H_2S at 1000°C

4 CONCLUSIONS

The BioSOFC project combines steam gasification of biomass, high temperature gas cleaning and electricity production using SOFCs. Each of these subjects are challenging on their own, and put together they represent a highly complex system, but potentially also the most promising future of high efficiency electricity production from biomass.

Several sub-tasks in this project have been carried out, with the final goal of onsite testing of a complete system for high efficiency electricity production from biomass. However, several aspects still need further attention. An efficient, reliable and cost-effective producer gas cleaning, including both particles and H_2S removal at high temperatures, is critical to ensure stable long term operation of SOFCs.

5 ACKNOWLEDGEMENTS

The Research Council of Norway is acknowledged for their financial support to the BioSOFC project, as is the project industry partners; Prototech, Statkraft and Vang Filter Technology. The Technical University of Vienna is acknowledged for their invaluable support to the project. Biomasse Kraftwerk Güssing is acknowledged for giving the BioSOFC project access to the plant for performing experiments, and for their help during mounting of experimental equipment.

6 REFERENCES

[1] H. Risnes & O.K. Sønju, Evaluation of a novel granular bed filtration system for high temperature applications. Progress in Thermochemical Biomass Conversion, Vol. 1 (2001) 730.

[2] H. Risnes, Ph.D. thesis, Norwegian University of Science and Technology, 2002:8.

[3] Y. Matsuzaki & I. Yasuda, The poisoning effect of sulphur-containing impurity gas on a SOFC anode: Part I. Dependence on temperature, time, and impurity concentration, Solid State Ionics, (2000) 263.

[4] D.W. Dees, U. Balachandran, S.E. Dorris, J.J. Heiberger, C.C. McPheeters & J.J. Picciolo, Interfacial effects in monolithic solid oxide fuel cells, Proceedings of the 1st International Symposium on Solid Oxide Fuel Cells (SOFC-I), (1989) 318.

[5] I. Alstrup, J.R. Rostrup-Nielsen & S. Røen, High temperature sulfide chemisorption on nickel catalysts, Applied Catalysis 1, (1981) 303.

[6] A. Norheim, J. Byrknes, J.E. Hustad & A. Vik, Performance data of a solid oxide fuel cell utilised for biomass gasification gases. Paper submitted to STCBC, (2004).

B. PAPER V

To be published in the proceedings of the 14th European Biomass Conference and Exibition, Paris, France, October 2005.

BIOSOFC - TECHNOLOGY DEVELOPMENT FOR INTEGRATED SOFC, BIOMASS GASIFICATION AND HIGH TEMPERATURE GAS CLEANING – ACHIEVEMENTS

Johan E. Hustad, Øyvind Skreiberg, Torbjørn Slungaard, Daniel Stanghelle, Arnstein Norheim and Otto K. Sønju
Norwegian University of Science and Technology, Department of Energy and Process Engineering, NO-7491 Trondheim, Norway

Hermann Hofbauer, Reinhard Rauch and Anita Grausam
Vienna University of Technology, Institute of Chemical Engineering, Getreidemarkt 9/166, A-1060 Vienna, Austria

Arild Vik, Ivar Wærnhus and Jan Byrknes
Prototech AS, P.O.Box 6034, Postterminalen, NO-5892 Bergen, Norway

ABSTRACT: Solid Oxide Fuel Cells (SOFCs) in combination with biomass gasification has a potential for high efficiency electricity production. The biomass gasification technology should yield the highest possible hydrogen content in the producer gas. Hence, steam gasification is an ideal gasification technology in combination with SOFCs. However, trace compounds in the producer gas, such as H_2S, alkali metal compounds, chlorine compounds and tars may be damaging for the SOFCs, depending on their levels. Therefore, there is a need for laboratory studies and testing of the influence of trace compounds on the Solid Oxide Fuel Cell (SOFC) performance, and long term onsite testing of a SOFC stack using producer gas from a steam gasification unit at normal operation. Gas cleaning is a necessity to remove particles from the producer gas before entering the SOFC stack. To optimize system efficiency, high temperature gas cleaning is the optimum option, and is a subject of extensive research worldwide.

The project described herein combines both novel fundamental and applied studies, including onsite testing of a 1 kW SOFC stack. As such, the novelty of this work is quite unique, and will contribute to future high efficiency electricity production from biomass.

Onsite testing of the SOFC stack takes place using a slipstream from a steam gasification reactor (the Fast Internally Circulating Fluidised Bed (FICFB) gasifier at Biomasse Kraftwerk Güssing in Güssing, Austria), a granular Panel Bed Filter for high temperature particle cleaning and a H_2S reactor with metal oxides for high temperature H_2S cleaning. This paper introduces the project; its purpose, goals and challenges, and follows up with a status of recent achievements. Results from high temperature gas cleaning, including both particle and H_2S cleaning, and SOFC experiments are presented.

This paper is part of an ongoing research project funded by the Research Council of Norway and Norwegian and Austrian industry, and the project will continue to the end of 2007.
Keywords: gasification, hot gas cleaning, electricity generation

1 INTRODUCTION

The EU strategies for Renewable Energy Sources (RES) involve an increase of the use of these resources from 6% (1997) to 12% (2010) and the Electricity from Renewable Energy Resources (RES-E) is subject to an increase from 14% (1997) to 22% (2010). A major part of this increase is planned to come from biomass. Increased production of heat and electricity will have to come from a large variety of processes, technologies and scales. The rapid increase in renewable electricity put focus on gasification technologies in particular, circulating and bubbling fluidised bed technologies being most attractive. To increase the electric efficiency in future gasification plants, a shift from gas engines and gas turbines to high temperature fuel cells is needed.

In this work a 1 kW SOFC stack is tested by taking a slipstream from the Fast Internally Circulating Fluidised Bed (FICFB) steam gasifier at Biomasse Kraftwerk Güssing in Güssing, Austria, hereafter called the Güssing plant. The high hydrogen content in the producer gas is ideal in combination with Solid Oxide Fuel Cells (SOFCs). Trace compounds in the producer gas, such as H_2S, alkali metal compounds, chlorine compounds and tars may be damaging for SOFCs, depending on their levels. There is a need for laboratory studies of the influence of these trace compounds on the performance of SOFCs, and long term onsite testing of a SOFC stack using producer gas from a steam gasification unit at normal operation. However, it is necessary to remove particles from the producer gas before it enters the SOFC stack. To optimise system efficiency, high temperature gas cleaning is the optimum option, and is a subject of extensive research worldwide.

This paper reports achievements from a project which combines both novel fundamental and applied studies, including laboratory tests as well as onsite testing at the Güssing plant.

2 METHODS

2.1 Steam gasification – The Güssing plant

The Güssing plant has now been in successful operation for a number of years and results thereof have been reported extensively. See the website http://www.ficfb.at/ for a number of publications. The FICBC gasifier is an indirectly fired steam gasification unit where the producer gas is utilized in a gas engine today. The thermal input to the plant is 8 MW using wood chips as fuel, and the electric efficiency is about 25 %. In addition heat is delivered to a district heating system. The dry producer gas contains up to 45 vol% H_2, 30 vol% CO and 12 vol% CH_4. Using wood chips as fuel the H_2O content of the producer gas is about 40 vol%, giving a lower heating value of about 9 MJ/kg.

2.2 High temperature particle cleaning

High temperature producer gas cleaning of particles is still a considerable challenge and has been an objective of extensive research worldwide for many years. Less focus has been put on high temperature cleaning of trace compounds that may be damaging for SOFCs, depending on their levels. High temperature producer gas cleaning is therefore an essential part of the BioSOFC project.

Cooling the producer gas from the Güssing plant gasifier outlet temperature of about 900°C, to 550°C, reduces the alkali and chlorine content in the gas to some extent in the filter. This leaves H_2S and tars as the potentially most difficult compounds. Further cooling might introduce operational problems due to tar condensation on the filter.

Granular bed filters are insensitive to the impinging gas. This combined with the possibility to provide chemical processing of the gas makes the novel Panel Bed Filter (PBF), invented by A.M. Squires, a promising alternative for high temperature cleaning of gasification producer gas [1, 2]. This cleaning concept utilises the transient behaviour of granular filtration and operates in surface filtration mode.

The PBF used in this project is a heated system, with several louvers supporting the granular material as shown in Figure 1. Temperatures, pressures and filter pressure drop build-up are logged. The inlet size of the current module has a width of 80 mm and a height of 300 mm (240 cm^2). Actual filtration surface is up to twice this area. Pressure pulse cleaning of the filter surface makes this unit suitable for continuous testing of high temperature gas cleaning.

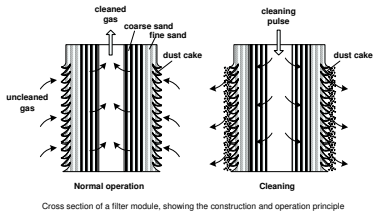

Figure 1: Working principle of the panel bed filter

The PBF has earlier been demonstrated in full-scale operation on biomass combustion flue gases [1]. It has in this study also been verified to satisfactorily clean producer gas from an indirectly fired steam gasification unit (FICBC gasifier) in Güssing. A variety of tests have been performed for several hours at about 550°C, and with varying filtration velocities. The successful Horizontal Bed Unit tests reported earlier [3] are verified on the PBF as discussed in section 3.2.

2.3 High temperature H_2S cleaning

The sulphur content in the producer gas from biomass gasification is much lower than from coal gasification, but still the sulphur (mainly as H_2S) can pose a major problem for SOFC materials. However, the limit of acceptable H_2S concentration in the gas is not yet established in the literature, which reports different limiting values [4, 5]. In reality the limit will depend on the material used in the specific SOFC application.

Experiments using different sorbent materials at high temperatures have been carried out using a small fixed bed reactor at well controlled conditions with varying gas composition. Furthermore, a high temperature H_2S cleaning reactor (fixed bed) needed when testing the 1 kW SOFC stack at the Güssing plant has been designed, and has been tested at the Güssing plant.

2.4 SOFC

SOFCs have the potential to become a major technology for electricity generation in the coming decades. They combine very high electrical efficiency (45-60%) with extremely low emissions of major air pollutants (unburned species and NO_x). The high operation temperature of a SOFC lends itself readily to Combined Heat and Power (CHP) operation, resulting in potential overall energy efficiencies above 80%. SOFCs thus represent one of the most promising technologies for cogeneration and decentralised electricity production. They can potentially be operated on a range of fuels, including pipeline natural gas, gasified biomass and coal, ammonia and reformed liquid hydrocarbons.

SOFCs of today are mainly designed to run on reformed natural gas. The most important issues are the formation of a carbon layer on the fuel electrode and sulphur poisoning of the fuel electrode. Producer gas has a different composition compared to natural gas, and can contain several species that may be damaging for SOFCs.

The planar SOFC technology offers higher volumetric power densities than tubular geometries and most development work worldwide is directed towards planar technology. Planar SOFC technology was therefore selected in this work. See [3] for further info.

To estimate the performance of a SOFC fuelled by producer gas compared to natural gas, a single cell SOFC setup was made at the laboratory of Prototech, Norway. The cell used in these experiments is similar to those that would be used in the 1 kW fuel cell stack at the Güssing plant, i.e. a planar, anode supported SOFC. However, in the experiments at Prototech, a geometrically smaller, circular shaped cell with a diameter of 40 mm was used. The experiments were carried out with excess fuel and air flows, i.e. low fuel conversion. Thus, the operating conditions of the single cell are comparable to the inlet conditions for a real-sized cell. The performance differences are therefore larger than for a real-sized cell since the conditions at higher fuel conversion will be more equal independent on the inlet gas composition. Gas flow, temperature in the cell, cell voltage and current drawn from the cell were logged. The experiments were carried out at 975°C which is about the same operation temperature planned used in the onsite tests at the Güssing plant.

A 100 W SOFC stack was designed and tested in the laboratory, followed by an up-scaling to the 1 kW stack for testing at the Güssing plant.

2.5 Modelling

The conversion of a typical producer gas is investigated in the SOFC operating temperature range (750-1000°C) by equilibrium calculations. Of particular interest are changes in gas composition as different parameters such as temperature, fuel conversion and content of sulphur, alkali metals and chlorine change. Different amounts and combinations of amounts of trace elements (S, K, Na and Cl) have been investigated, representing typical values valid for different biomass fuels in producer gas.

Based on the findings in the equilibrium calculations, phase diagrams for nickel in both H_2/H_2O and CO/CO_2 atmospheres are established. From the equilibrium calculations the most important compounds of S, K, Na, and Cl are identified. In addition, typical maximum levels of the different compounds are estimated. Thus, phase diagrams for nickel under the influence of the different trace compounds can be produced.

3 RESULTS AND DISCUSSIONS

3.1 Steam gasification – The Güssing plant

The Güssing plant has been running stable for long periods at a time, and has allowed the BioSOFC project to carry out a series of well controlled experiments.

3.2 High temperature particle cleaning

The PBF has been tested onsite at the Güssing plant. The tests showed successful dust cake build-up, and thereby successful dust cleaning, at about 550°C.

A slipstream was taken out from the gasifier freeboard at close to isokinetic velocity. The slipstream was passed through 15 meter of heated line at about 600°C down to the test site. A cyclone was used for lowering the dust concentration from 40-60 g/Nm^3 in the gasifier down to 2-3 g/Nm^3 into the PBF. After the PBF it was used a total filter, tar condensing box immersed in an ice/water mixture, silica gel container for water removal, valve for flow adjustment, critical nozzle for flow measurement, suction pump and a long tube for cleaned gas venting above the plant roof. The dust concentration after the filter was much less than 1 mg/Nm^3 and not detectable by weighing the total filter after the tests.

Eleven tests where conducted with the PBF at flow rates between 0.5 and 2.02 Nm^3/h. The flow was close to constant throughout each individual test. All the tests were carried out using alumina-oxide spheres (d_p = 687 μm) as bed material.

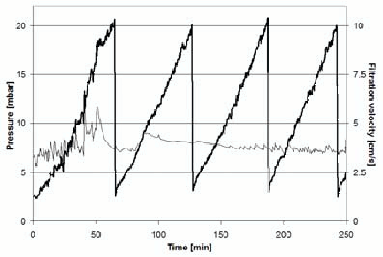

Figure 2: PBF test 13.03.05 Güssing, Austria

Figure 2 and 3 shows the pressure over the bed (dP_{BED}) on the left axis and the filtration flow [cm/s] on the right axis. The low dP_{BED} values in the beginning of the first pressure build-up are a result of initial deep-bed and rooting cake filtration while the surface cake is being established. dP_{BED} increases as the filter-cake grows and drops to approximately the same value after each cleaning cycle and indicates that the cleaning pulse was sufficient.

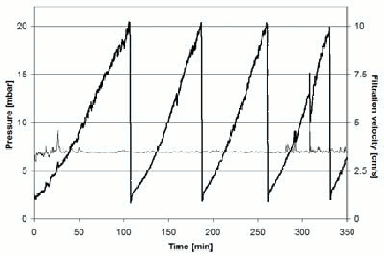

Figure 3: PBF test 15.03.05 Güssing, Austria

PBF test 13.03.05 and PBF test 15.03.05 were performed with an average gas flow of 1 Nm^3/h. The time differences for the pressure build-up are assumed to be a result of the fuel feed into the gasifier. The gradient of the pressure build-up was 26 ± 3 Pa/min for the 13.03.05 test and 29 ± 3 Pa/min for the 15.03.05 test.

3.3 High temperature H_2S cleaning

Laboratory experiments in a small quarts glass fixed bed reactor have been carried out at controlled conditions to investigate the performance of three metal oxide absorbents. Their ability to reduce the H_2S level in gas mixtures similar to the Güssing plant producer gas was investigated at various levels of H_2S and at different temperatures. The performance of the absorbents varied, but they all reduced the H_2S level significantly. However, only one of the absorbents was able to reduce the H_2S level from about 200 ppm to a few ppms at a temperature of above 500°C. This absorbent was selected for use in the Güssing plant H_2S cleaning experiments.

For the **Güssing plant experiments** a fixed bed H_2S cleaning reactor was designed. It was placed right after the PBF, operating at a temperature above 500°C. The reactor operated in batch mode. H_2S measurements were carried out to assess the cleaning efficiency of the H_2S reactor. Most of the H_2S was removed in the reactor, however, the cleaning efficiency was not as good as in the laboratory experiments and the results were more variable. Further work is needed on the H_2S cleaning.

3.4 SOFC

SOFC single cell experiments have been performed in order to investigate the influence sulphur has on the cell performance. At an operating temperature of 800°C, the sulphur concentrations investigated were in the interval ranging from 5 to 240 ppm H_2S. It was found that sulphur in the fuel gas reduces the cell performance significantly even at 5 ppm H_2S. However, above an H_2S concentration of around 10-20 ppm, a further increase in the sulphur concentration only causes marginal additional cell performance degradation. Thus, it was found that the performance degradation was close to equal when 80, 120 and 240 ppm H_2S was added to the fuel gas. As shown in Figure 4, the performance degradation when 120 or 240 ppm H_2S was added to the fuel gas is less than 5%.

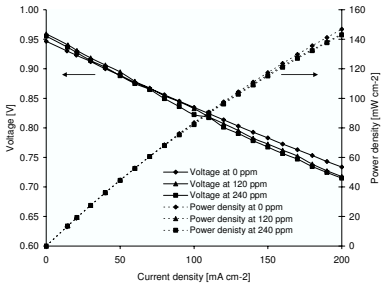

Figure 4: Cell voltage (left axis) and power density (right axis) as a function of current density at 0, 120 and 240 ppm H_2S at 800°C

Another experimental series aiming at investigating the influence alkali metals and chlorine might have on the SOFC performance has been started recently. The initial results indicate that addition of up to 100 ppm KCl or 100 ppm KOH does not seem to have any effect on the SOFC performance.

Results from the **SOFC stacks** tests will be published elsewhere when the final test with the 1 kW stack at the Güssing plant have been completed and the results have been analysed in detail.

3.5 Modelling

Some results from the modelling work were reported in [3], and further results have been published in [7].

The major trace components present in the gas from gasification of biomass have been identified for several levels of sulphur, potassium, chlorine and sodium in the SOFC operating temperature interval.

Sulphur is present mainly as $H_2S(g)$ whereas potassium is mainly present as KOH(g) and to some extent K(g) depending mainly on the temperature. High chlorine content in the fuel favours KCl(g) production. Cl is also found as HCl(g) in some cases, especially if there is limited or no potassium present in the gas. The calculations show very limited molar amounts of liquid and solid species present. However, in the temperature interval between 750 and 900°C there is a small amount of carbonate-rich liquid phase and solid carbonates in equilibrium with the gasifier gas. The temperature at which the potassium salts condense depends on the amount of potassium present in the fuel gas. Thus, if the potassium level is lowered, the temperature at which the salts condense is also in general lowered.

4 CONCLUSIONS

The BioSOFC project combines steam gasification of biomass, high temperature gas cleaning and electricity production using SOFCs. This is potentially the most promising future of high efficiency electricity production from biomass. The final goal of this project has been onsite testing of a complete system, where an efficient and reliable producer gas cleaning at high temperatures of both particles and H_2S is critical to ensure stable long term operation of SOFCs.

Several studies have been successfully carried out in this project, however, several aspects still need further attention. The BioSOFC project has received additional funding from the Research Council of Norway and the industry partners Prototech, Vang Filter Technology, Agder Energi, Hadeland Energi, Trondheim Energiverk and Vardar for the three-year period 2005-2007. This project will focus on additional up-scaling of the units in the system, with the final goal of onsite testing of a 10 kW SOFC stack. In addition further detailed laboratory studies and also system modelling will be carried out.

5 ACKNOWLEDGEMENTS

The Research Council of Norway is acknowledged for their financial support to the BioSOFCup project, as is the project industry partners; Prototech, Statkraft and Vang Filter Technology. The Technical University of Vienna is acknowledged for their invaluable support to the project. Biomasse Kraftwerk Güssing is acknowledged for giving the BioSOFC project access to the plant for performing experiments, and for their help during mounting of experimental equipment.

6 REFERENCES

[1] H. Risnes & O.K. Sønju, Evaluation of a novel granular bed filtration system for high temperature applications. Progress in Thermochemical Biomass Conversion, Vol. 1 (2001) 730.

[2] K.C. Lee, I. Rodon, M.S. Wu, R. Pfeffer & A.M. Squires, The panel bed filter. EPRI AF-560, Final report, May (1977).

[3] J.E. Hustad, Ø. Skreiberg, T. Slungaard, A. Norheim, O.K. Sønju, H. Hofbauer, R. Rauch, A. Grausam, A. Vik & J. Byrknes. BioSOFC - Technology development for integrated SOFC, biomass gasification and high temperature gas cleaning. Biomass Conference, Biomass for Energy, Industry and Climate Protection, Proceedings of the World Conference held in Rome, Italy, 10-14 May 2004, pp. 1094-1097, 2004.

[4] Y. Matsuzaki & I. Yasuda, The poisoning effect of sulphur-containing impurity gas on a SOFC anode: Part I. Dependence on temperature, time, and impurity concentration, Solid State Ionics, (2000) 263.

[5] D.W. Dees, U. Balachandran, S.E. Dorris, J.J. Heiberger, C.C. McPheeters & J.J. Picciolo, Interfacial effects in monolithic solid oxide fuel cells, Proceedings of the 1st International Symposium on Solid Oxide Fuel Cells (SOFC-I), (1989) 318.

[6] I. Alstrup, J.R. Rostrup-Nielsen & S. Røen, High temperature sulfide chemisorption on nickel catalysts, Applied Catalysis 1, (1981) 303.

[7] A. Norheim, D. Lindberg, J.E. Hustad & R. Backman. Equilibrium calculations of the composition of trace compounds from biomass gasification in the Solid Oxide Fuel Cell operating temperature interval. To be published in Fuel.

C. ADDITIONAL SINGLE CELL TESTS

In addition to the results presented in Paper II, other single cell experiments were performed. The experimental setup used was the same as that described in Section 8.3 i.e. an state-of-the-art LSM/YSZ/Ni-YSZ anode supported flat plate SOFC cut in a circular shape and put into a Prototech in-house made setup.

C.1 Water-gas shift reaction test

In this test a SOFC delivered by Forschungszentrum Jülich was applied. These cells have a thick anode (1.5-2.0 mm) giving high mechanical strength and a thin electrolyte (down to 5μm) enabling low operating temperature [63].

The results presented here are from a series in which the sum of the partial pressures of H_2 and CO was kept constant while changing their mutual ratios. At the same time, the sum of partial pressures of CO_2 and H_2O was kept constant in the same manner. The fuel gas mixtures entering the cell, both as mixed at room temperature and the equilibrium composition at 975^{o}C are shown in Table (C.1).

Gas component	H_2		CO		H_2O		CO_2	
Experiment	Input	Equilib.	Input	Equilib.	Input	Equilib.	Input	Equilib.
1	50	50	0	0	50	50	0	0
2	40	38	10	12	40	42	10	8
3	30	27	20	23	30	33	20	17
4	20	17	30	33	20	23	30	27
5	10	8	40	42	10	12	40	38
6	0	0	50	50	0	0	50	50

Tab. C.1: Partial pressure of fuel gas components as mixed at room temperature and at thermodynamic equilibrium at 975^{o}C.

Keeping in mind that the electrochemical oxidation reactions produce CO_2 and H_2O, there was in all these experiments the same total partial pressure of reactants and total partial pressure of reaction products entering the fuel cell. The variation was thus in the ratio of partial pressures of CO and H_2 (p_{CO}/p_{H_2}) and that of CO_2 and H_2O (p_{CO_2}/p_{H_2O}). The ratios between H_2 and H_2O (p_{H_2}/p_{H_2O}) and between CO and CO_2 were constant at room temperature and nearly constant at equilibrium.

The fuel and air volume flows were both kept high (200 ml/min of both at room temperature) compared to that needed for the current production in the single cell. Thus, one may assume that the bulk gas composition was essentially the same entering and leaving the cell compartment.

The IV-curves established from these experiments are shown in Figure (C.1). It is clearly seen, that as more CO and CO_2 is introduced and the partial pressures of H_2 and H_2O are reduced, the cell performance, in terms of operating voltage at a given current

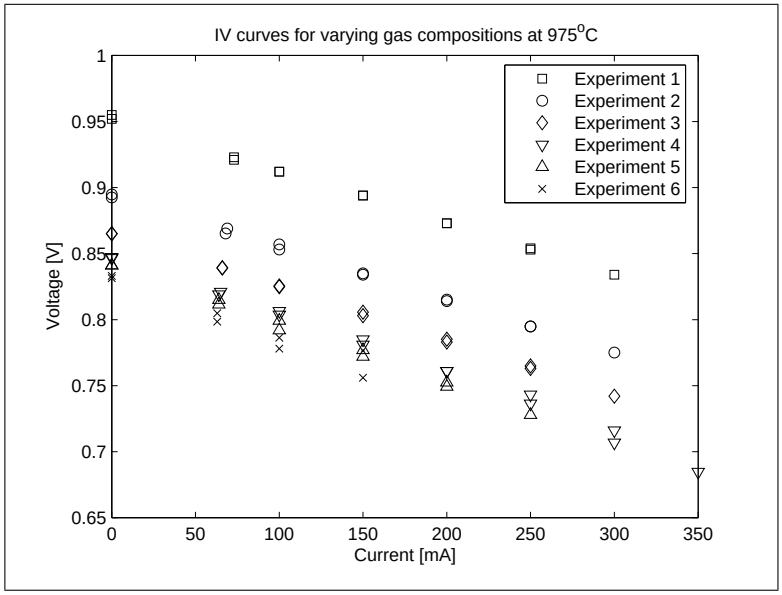

Fig. C.1: Single cell performance at 975°C with varying gas composition; experiment no. refer to Table (C.1).

level, is lowered. This happens even when p_{H_2}/p_{H_2O} is nearly unchanged. This may indicate that the electrochemical oxidation of CO contributes even in the cases when sufficient hydrogen is available and steam is available for the water-gas shift reaction to occur. Another explanation for the reduced performance in this case may be that the reduced H_2 partial pressure causes a reduced H_2 diffusion through the anode. In addition, CO may occupy larger fractions of the TPB as more CO is introduced thus increasing the interfacial resistance between anode and electrolyte.

In Table (C.2) the total cell resistance for all six experiments are shown, calculated as the voltage variation divided by current. There is a clear trend towards higher cell resistance as the level of CO is increased. This is in accordance with the work of Matsuzaki and Yasuda [74]. They found the polarisation resistance at the interface between the Ni-YSZ anode and YSZ electrolyte to increases with increasing CO concentration thus lowering the cell performance.

In addition, the change in Gibbs free energy is lower for CO oxidation than for H_2 oxidation. This may certainly be the reason for the lower operating voltage as more CO is introduced.

	Total cell resistance		
Experiment	At 200 mA [Ω]	At max load [Ω]	Max load [mA]
1	0.40	0.39	300
2	0.39	0.39	300
3	0.40	0.41	300
4	0.43	0.46	350
5	0.44	0.45	250
6	0.51	-	150

Tab. C.2: Total cell resistance for experiment 1 to 6.

C.2 Addition of H_2O versus CO_2

These experiments are divided into two parts. No gas fraction was kept constant in either part, but an attempt was, nevertheless, made to employ a systematic procedure. The first part was performed on a thinner anode supported SOFC made by InDEC while the second part was done with the above mentioned Jülich-plates. That is not ideal for comparing the performance at different fuel gas mixtures. Also on the time scale there should be an as small as possible difference between the different experiments. All experiments should also be performed after an initial stabilisation period of around 3-400 hours of operation. This was clearly seen in Paper III as the cell structure seems to undergo certain initial changes increasing the cell performance significantly.

During the experiments leading up to the results presented here and in Paper II, however, especially the InDEC cells caused significant problems due to their relatively low mechanical strength. This caused fractures probably during mounting of the setup. Additionally, there were problems connected to gas leakages around the cell perimeter. This caused some cells to crack after some time due to thermal stresses induced by the high temperatures from combustion of hydrogen.

However, each part was carried out over a limited period of time reducing the time induced performance variations. Thus, the results from each part may be compared to each other.

C.2.1 Addition of CO_2

In the first five series in this part, p_{H_2} was kept constant and p_{CO_2} was gradually reduced while increasing p_{CO} at an equal amount as shown in Table (C.3). In the next five series p_{CO} was kept constant while varying p_{H_2} and p_{CO_2} in a similar manner.

Gas component	H_2		CO		H_2O		CO_2	
Experiment	Input	Equilib.	Input	Equilib.	Input	Equilib.	Input	Equilib.
1	50	22	0	28	0	28	50	22
2	50	27	10	33	0	23	40	17
3	50	32	20	38	0	18	30	12
4	50	38	30	42	0	12	20	8
5	50	44	40	46	0	6	10	4
6	40	35	50	55	0	5	10	5
7	30	22	50	58	0	8	20	12
8	20	12	50	58	0	8	30	22
9	10	5	50	55	0	5	40	35
10	0	0	50	50	0	0	50	50

Tab. C.3: Partial pressure of fuel gas components as mixed at room temperature and at thermodynamic equilibrium at 975°C.

The results of the first five series and last five series are shown in Figure (C.2) and Figure(C.3), respectively. The total cell resistances for all experiments, calculated as the voltage difference divided by current, are shown in Table (C.4). The differences in the maximum load obtained are based on a desire not to operated the cell below around 0.65 V.

In most of the experimental series, the total cell resistance is seen to be fairly constant, the variations are probably inside the limits of uncertainty of the measurements. The

	Total cell resistance		
Experiment	At 200 mA [Ω]	At max load [Ω]	Max load [mA]
1	0.47	0.45	300
2	0.40	0.42	400
3	0.44	0.43	400
4	0.44	0.44	450
5	0.43	0.43	450
6	0.41	0.42	450
7	0.42	0.42	400
8	0.43	0.43	250
9	0.41	0.42	300
10	0.42	0.42	200

Tab. C.4: Total cell resistance for experiment 1 to 10.

exception is experiment number 1. The reason for the higher cell resistance in this case may be, by comparing the equilibrium gas compositions in Table (C.3), that the ratio p_{H_2}/p_{H_2O} is lowest here.

It is difficult to compare the results obtained in these experiments since there are too many parameters changing at the same time. However, by comparing e.g. the mixture of 50/30/20 $H_2/CO/CO_2$ (Experiment 4) and 30/50/20 $H_2/CO/CO_2$ (Experiment 7), it is clear from Figure (C.2) and Figure (C.3), respectively, that the former, more hydrogen-rich mixture gives a better cell performance in terms of higher operating voltage at all current levels. This is the case for the other experiments as well, even if there are insignificant changes only in the total cell resistances and the sums of p_{H_2} and p_{CO} are the same. There are thus some contradictions between these results and the ones presented in the previous section regarding the influence the CO concentration have on the total cell resistance.

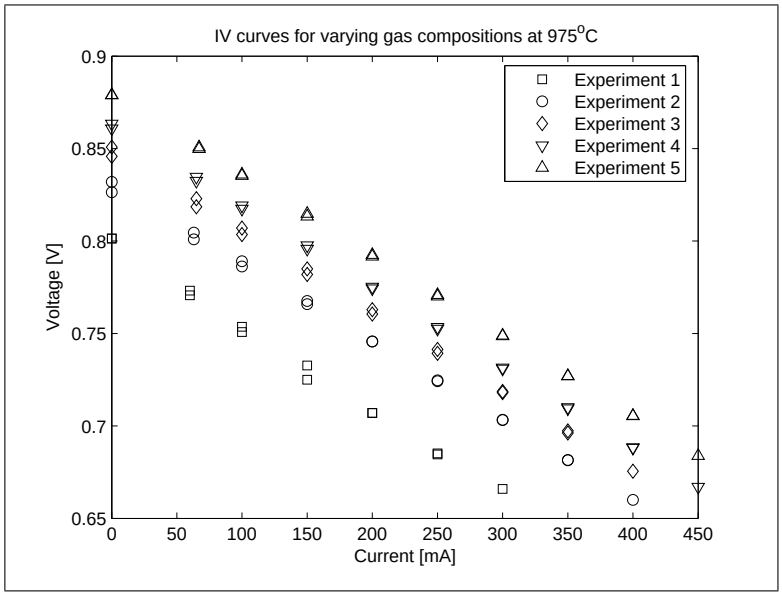

Fig. C.2: Single cell performance at 975°C with varying gas composition; experiment no. refer to Table (C.3).

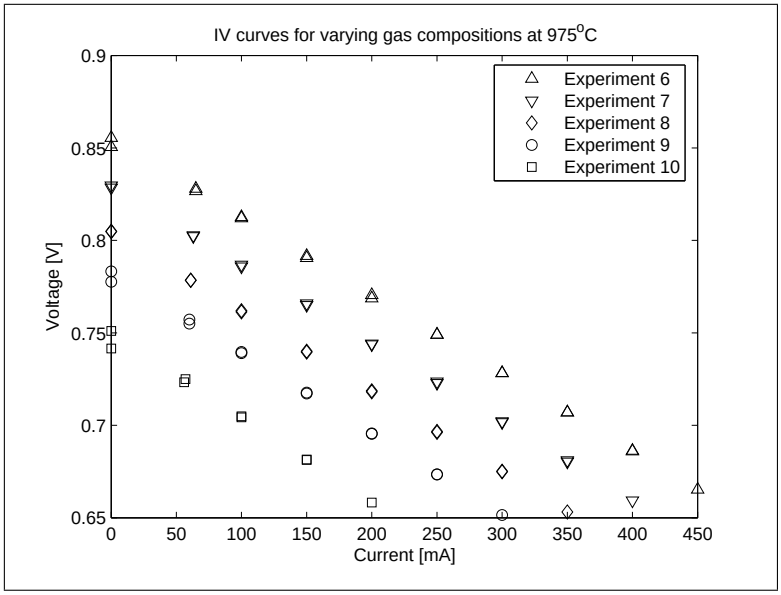

Fig. C.3: Single cell performance at 975°C with varying gas composition; experiment no. refer to Table (C.3).

C.2.2 Addition of H_2O

Similar to the experiments described above, ten different tests were performed. Accordingly, in the first five series, p_{H_2} was kept constant and p_{H_2O} was gradually reduced while increasing p_{CO} at an equal amount. In the next five series p_{CO} was kept constant while varying p_{H_2} and p_{H_2O} in a similar manner. The different fuel gas mixtures as mixed at room temperature and at equilibrium at the operating temperature (975°C) are shown in Table (C.5). These experiments were carried out using a Jülich flat plate single cell as mentioned previously.

Gas component	H_2		CO		H_2O		CO_2	
Experiment	Input	Equilib.	Input	Equilib.	Input	Equilib.	Input	Equilib.
1	50	50	0	0	50	50	0	0
2	50	53	10	7	40	37	0	3
3	50	54	20	16	30	26	0	4
4	50	54	30	26	20	16	0	4
5	50	53	40	37	10	7	0	3
6	40	44	50	46	10	6	0	4
7	30	38	50	42	20	12	0	8
8	20	32	50	38	30	18	0	12
9	10	27	50	33	40	23	0	17
10	0	22	50	28	50	28	0	22

Tab. C.5: Partial pressure of fuel gas components as mixed at room temperature and at thermodynamic equilibrium at 975°C.

The results of the first five series and last five series are shown in Figure (C.4) and Figure(C.5), respectively. The total cell resistance for each experiment, calculated as previously mentioned, are shown in Table (C.6). No significant difference in total cell resistance can be seen in these experiments.

	Total cell resistance		
Experiment	At 200 mA [Ω]	At max load [Ω]	Max load [mA]
1	0.39	0.39	450
2	0.39	0.38	450
3	0.38	0.38	450
4	0.38	0.38	450
5	0.38	0.38	450
6	0.38	0.38	450
7	0.38	0.38	450
8	0.38	0.39	450
9	0.38	0.39	450
10	0.39	0.40	400

Tab. C.6: Total cell resistance for experiment 1 to 10.

There are differences, however, in the cell performance as the gas composition is varied. The one with 50/50 H_2/H_2O (Experiment 1) clearly outperforms the others in terms of a significantly higher voltage at all current levels as shown in Figure (C.4). Considering the equilibrium compositions shown in Table (C.6) this may seem strange as p_{H_2}/p_{H_2O} is lowest in this experiment (50:50) with the exception of Experiment 10 (22:28). The fact that the increasing CO concentration causes a decrease in cell performance may therefore mean that CO also contributes directly in the electrochemical reactions. If not, the cell voltage and consequently the cell performance should be governed by p_{H_2}/p_{H_2O} only, which is clearly not the case here.

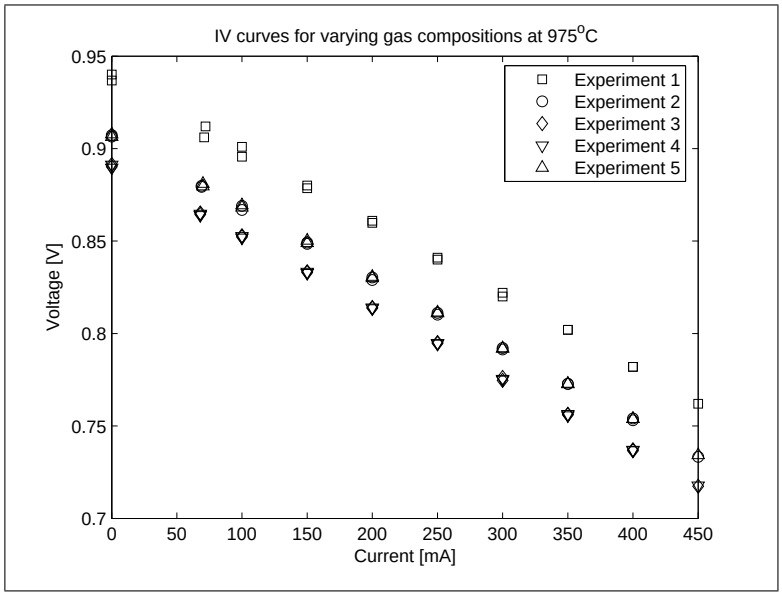

Fig. C.4: Single cell performance at 975°C with varying gas composition; experiment no. refer to Table (C.5).

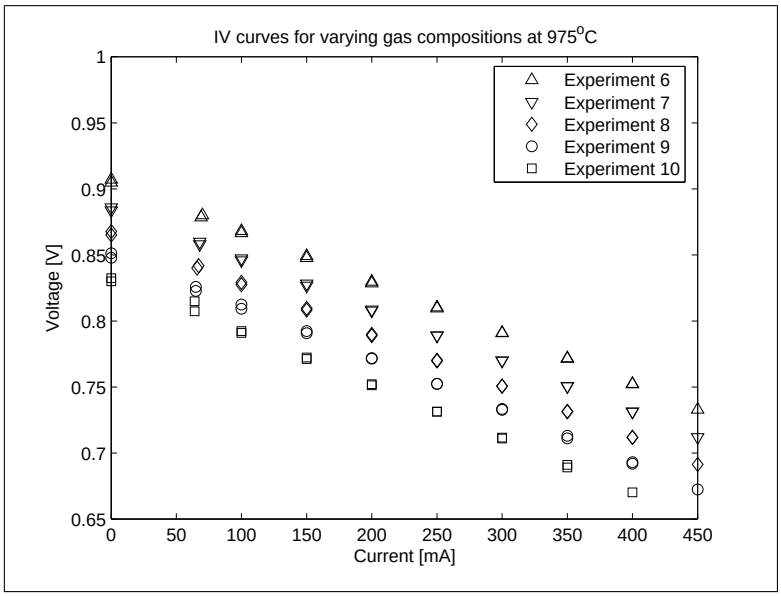

Fig. C.5: Single cell performance at 975°C with varying gas composition; experiment no. refer to Table (C.5).

D. SINGLE CELL STABILITY VERSUS H_2S CONCENTRATION

The results presented in Paper III were acquired by means of an automated data logging system (LabView-based FieldPoint). As the data are continuously recorded, an enormous amount of data can be obtained. However, during all the H_2S-related experiments a sampling time of 5 seconds was chosen. This was based on the fact that on a 24-hour basis not much happens during five seconds. Additionally, five seconds is little enough to obtain a significant amount of data points at each load (current level) during the establishment of the IV-curves. Thus, the IV-curves and consequently the cell resistance calculations presented in Paper III are based on averaged voltage measurements at the presented current or current density levels.

As data were collected every fifth second during over three weeks, a substantial amount of data was gathered. Most of the time during this period, the cell (circular cut Jülich plate), was operated at a constant load of 50 mA cm^{-2}. By putting the measured cell voltage data collected during each hour of operation into a statistical software (Minitab by Minitab Inc.), average cell voltage and standard deviation were rather easily calculated. Thus, the effect of sulphur addition or removal was revealed both in terms of cell performance over time at the constant load and also voltage stability. In addition, the voltage stability i.e. voltage standard deviation during the IV-series was calculated and the stability versus sulphur concentration was thus documented.

D.1 Cell voltage and stability at constant load

As mentioned above, the cell was operated at a constant load of 50 mA cm^{-2} at all times except during the establishment of IV-curves. The cell voltage during these constant load periods was logged every fifth second and averaged over every hour. The cell voltage's standard deviation during each one hour period was then calculated. Average cell voltage and standard deviation for each one hour period during the experimental period are presented in the figures below. On the time scale in each graph, zero is the time when the sulphur concentration was changed to or from the indicated H_2S concentration.

The cell was operated for approximately 24 hours at each sulphur concentration. When switching over to the clean gas with no sulphur, the cell was also operated for around 24 hours before a new sulphur level was introduced. This was found to be sufficient for the cell performance to stabilise after each variation in sulphur concentration.

As can be seen from the following results, it is difficult to draw any solid conclusions regarding the cell performance stability versus sulphur concentration. After the first experiment at 80 ppm H_2S the cell voltage is varying a lot and the voltage stability is rather poor as can be seen in Figure (D.5). Referring to the results presented in Paper III, the area specific cell resistance is decreasing during the first 3-400 hours of the experimental period. It is not established what exactly causes this performance increase, and it does not seem to have any direct connection to the voltage stability as some of the data presented below shows a close to constant and stable cell performance during this period.

The last experiments performed at 800°C and high sulphur concentration show stable operation both with and without sulphur as can be seen in Figures (D.8) to (D.10). The area specific cell resistance at 0 ppm H_2S is close to constant during these experiments. It is therefore not possible to conclude that the addition of even high levels of sulphur concentration changes the stability of the cell performance.

D.1.1 Series 1 - 5 to 80 ppm H_2S at 800°C

The first series contains data for experiments performed at an operating temperature of 800°C and H_2S concentrations ranging from 5 to 80 ppm. The data are shown in Figure (D.1) to Figure (D.5). After the first experiment of 80 ppm H_2S at 800°C the cell was operated for almost 70 hours at 0 ppm H_2S as shown in Figure (D.5). This happened in a weekend during which no experiments were performed.

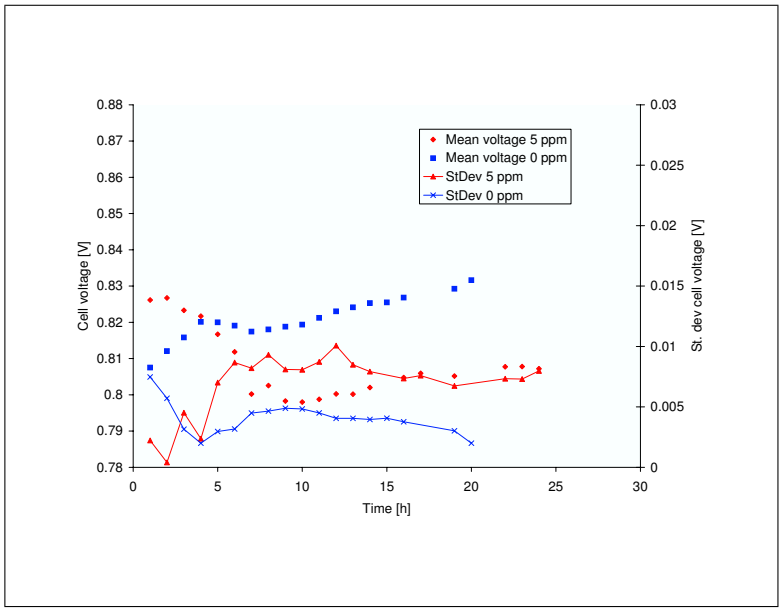

Fig. D.1: Single cell averaged voltage and voltage stability at 800°C and 5 ppm H_2S.

D.1.2 Series 2 - 40 to 80 ppm H_2S at 850°C

After the 80 ppm H_2S test, the cell temperature was increased to 850°C to investigate if the effect of sulphur on SOFC performance is temperature dependent. Two experiments were performed at this temperature; 40 and 80 ppm H_2S tests with 0 ppm tests before and after each test. Again, a stabilisation period of around 24 hours was allowed after each change in sulphur concentration. The results are shown in Figure (D.6) and Figure (D.7) for the 40 and 80 ppm test, respectively.

D.1.3 Series 3 - 80 to 240 ppm H_2S at 800°C

Finally, after reducing the operating temperature to 800°C again, three final experiments were performed at sulphur concentrations of 80, 120 and 240 ppm. As before, before and after each test, which again lasted around 24 hours, the cell was operated around 24 hours at 0 ppm H_2S. The 240 ppm H_2S lasted, however, around 40 hours. This was done to verify that 24 hours is sufficient for the cell performance to stabilise. The

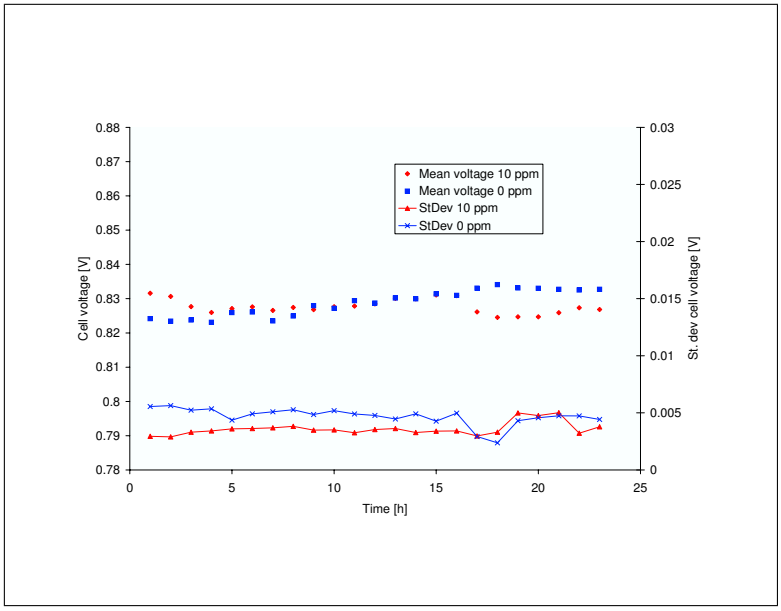

Fig. D.2: Single cell averaged voltage and voltage stability at 800^{o}C and 10 ppm H_2S.

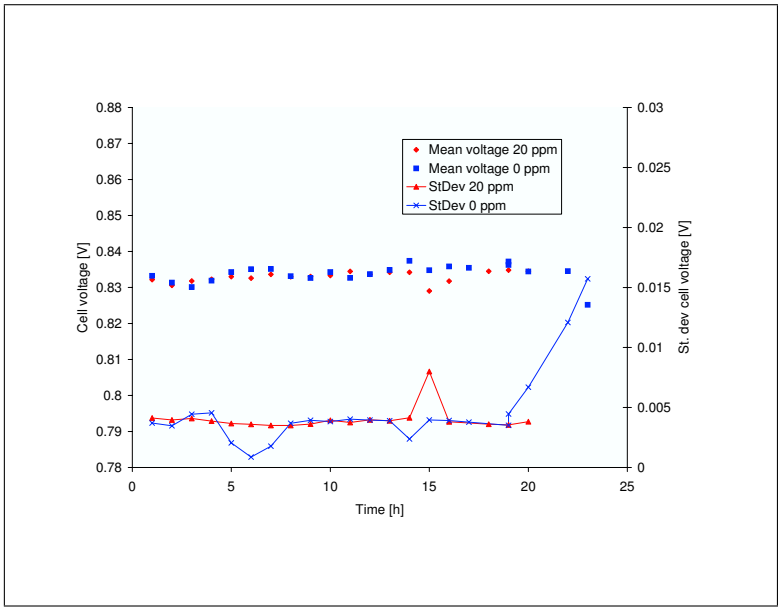

Fig. D.3: Single cell averaged voltage and voltage stability at 800^{o}C and 20 ppm H_2S.

hourly averaged cell voltages and standard deviations for these experiments are shown in Figures (D.8) to (D.10)

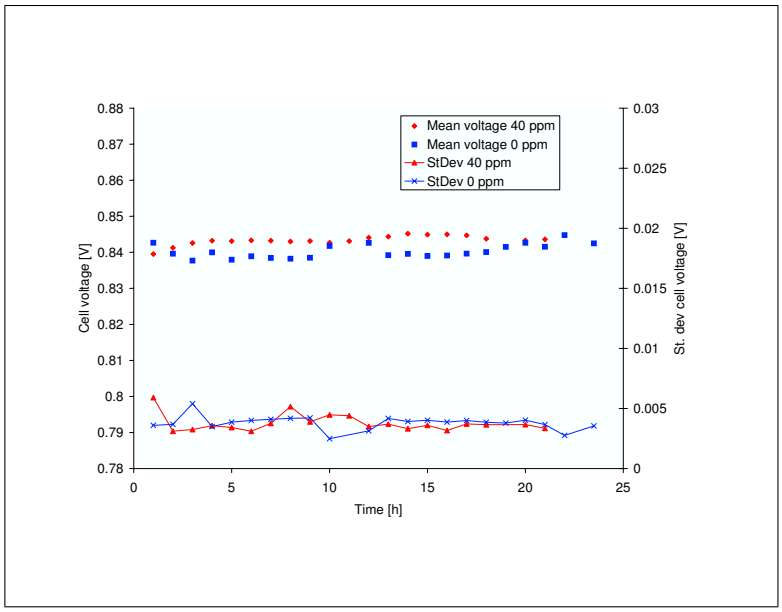

Fig. D.4: Single cell averaged voltage and voltage stability at 800°C and 40 ppm H_2S.

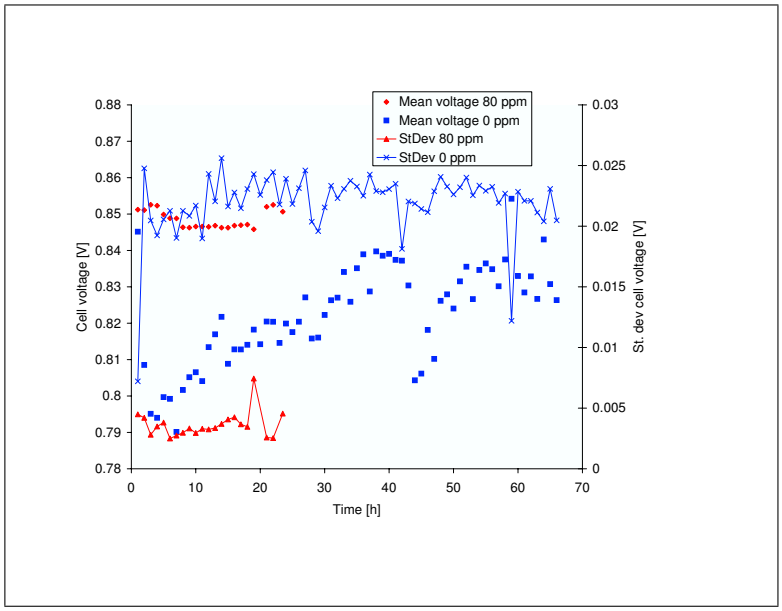

Fig. D.5: Single cell averaged voltage and voltage stability at 800°C and 80 ppm H_2S.

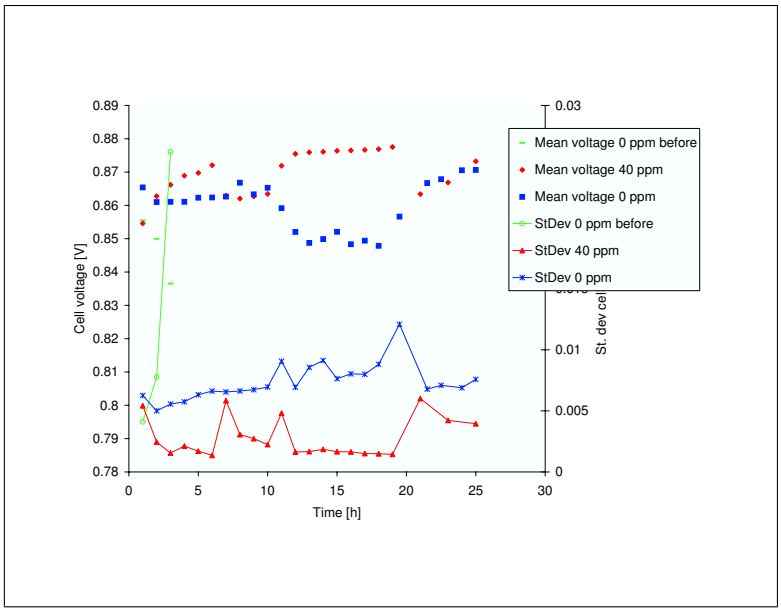

Fig. D.6: Single cell averaged voltage and voltage stability at 850^{o}C and 40 ppm H_2S.

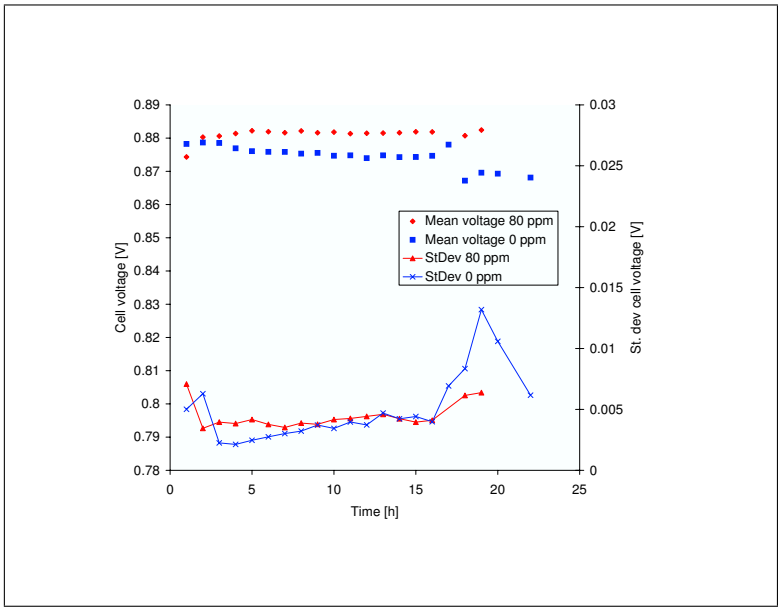

Fig. D.7: Single cell averaged voltage and voltage stability at 850^{o}C and 80 ppm H_2S.

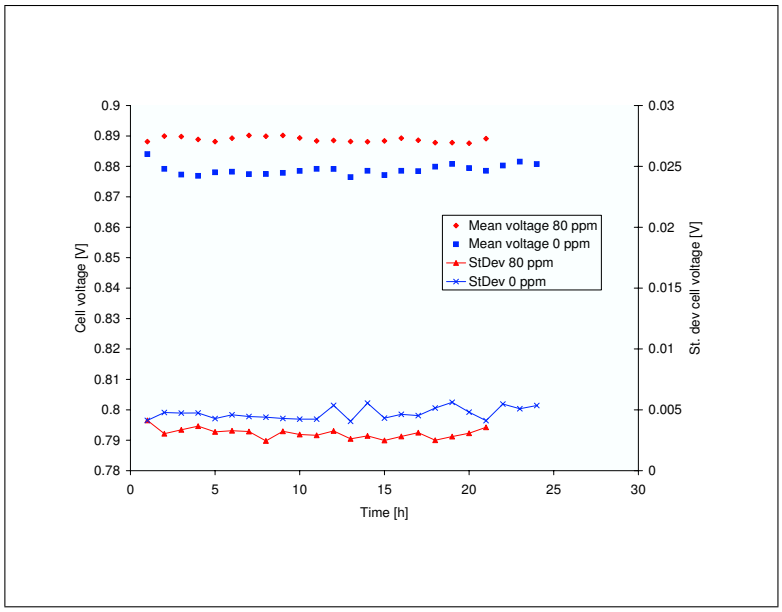

Fig. D.8: Single cell averaged voltage and voltage stability at 800^{o}C and 80 ppm H_2S.

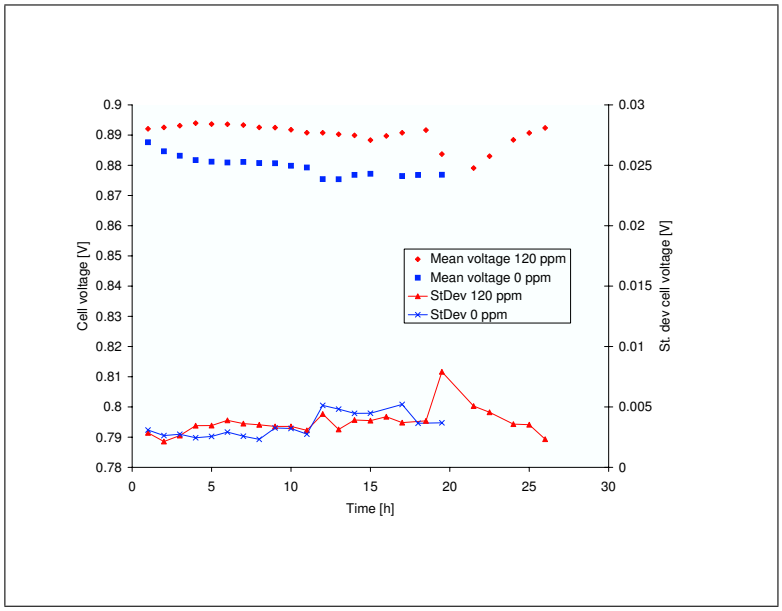

Fig. D.9: Single cell averaged voltage and voltage stability at 800^{o}C and 120 ppm H_2S.

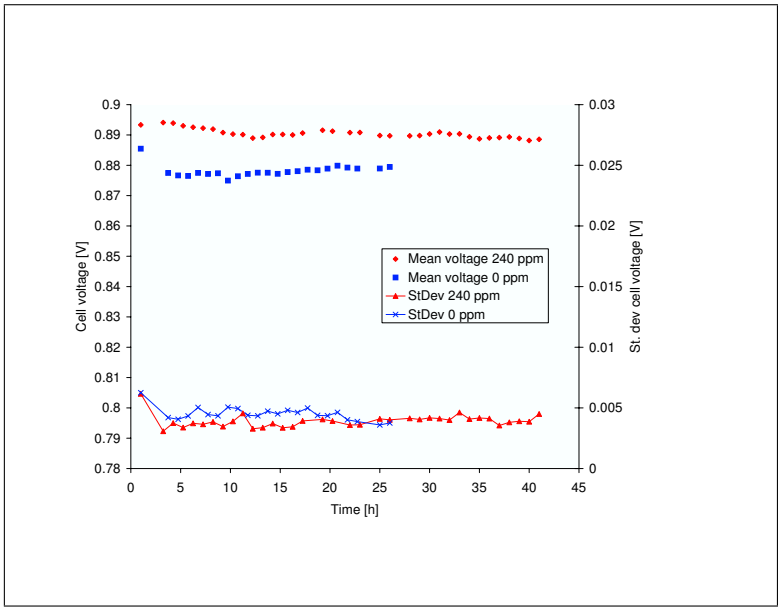

Fig. D.10: Single cell averaged voltage and voltage stability at 800^{o}C and 240 ppm H_2S.

E. SHORT STACK TESTING

A 4-cell planar SOFC stack was built and tested at Prototech. The individual cells had an active cell area of 81 cm^2. Problems connected especially to gas distribution occurred causing several cells to perform rather poorly. One of the middle cells, however, performed relatively well and the results presented here are taken from the data of this single cell. The experiments aimed at investigating the influence on cell performance of addition of ammonia and sulphur.

The main gas composition in these tests were mixed from gas bottles to simulate, in thermodynamic equilibrium, the producer gas from the steam gasifier in Güssing, Austria. Steam was produced by means of a liquid mass flow controller in combination with a steam generator. A significant amount of nitrogen was, however, added in an attempt to reduce leakages and simultaneously increase the total flow through the cells. The resulting main gas composition and flow rates through the stack are shown in the table below:

Gas component	Fraction (vol%)	Fraction without N_2 (vol%)	Flow rate (ml/min)
H_2	51	71	1817
CO_2	17	24	620
H_2O	4	5	140
N_2	28	-	1000

Tab. E.1: Main gas composition and flow rates in 4-cell stack testing.

Four different experimental series were performed; various H_2S experiments at 800 and 900^{o}C and 2600 ppm NH_3 tests at 800 and 900^{o}C.

E.1 Sulphur experiments

E.1.1 Experiments at 900^{o}C

The first sulphur experiments were done at an operating temperature of 900^{o}C. The sulphur concentrations investigated in the first part was 0, 5, 0, 25, 50 and 0 ppm H_2S. Thereafter, a series of 0, 50, 75, 100, 140 and 0 ppm H_2S was carried out. Finally, two relatively short swaps between 0 and 140 ppm H_2S were done.

The data for the first series are shown in Figure (E.1). The series at 50 ppm H_2S deviated significantly from the others. The cell performance was observed to be better at this sulphur concentration compared to the one at the first 0 ppm H_2S series. However, the series at 0, 5 and 25 ppm H_2S showed a reasonable trend of increasing cell resistance, namely 0.028, 0.029 and 0.031 Ω, respectively. That corresponds to a area specific total cell resistance of 2.32, 2.36 and 2.54 Ω cm^{-2} at 0, 5 and 25 ppm H_2S, respectively.

The next experiment in which the sulphur concentration was varied while keeping the current constant at 1 A through the stack, did not reveal much. The data, shown in

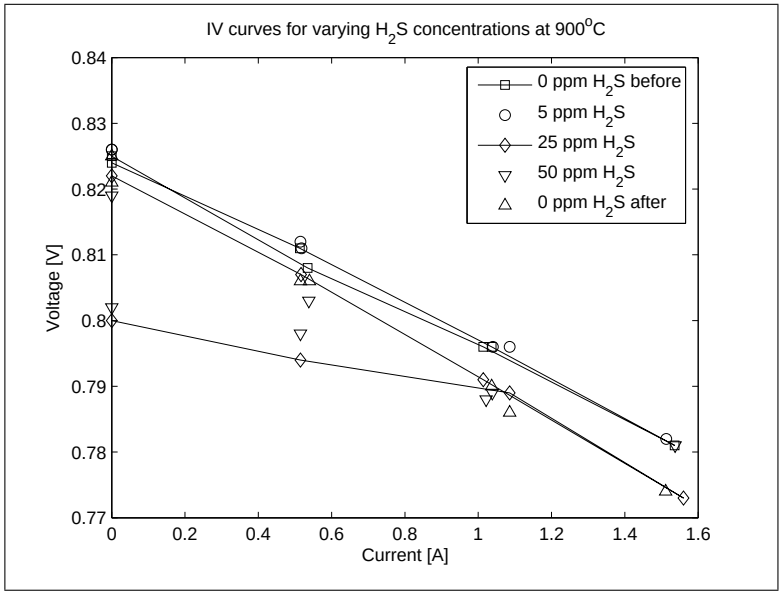

Fig. E.1: Single cell performance at 900^{o}C with varying H_2S concentrations; the cell is mounted in a 4-cell stack.

Figure E.2 did not show any particular trend as the sulphur concentration was increased or decreased.

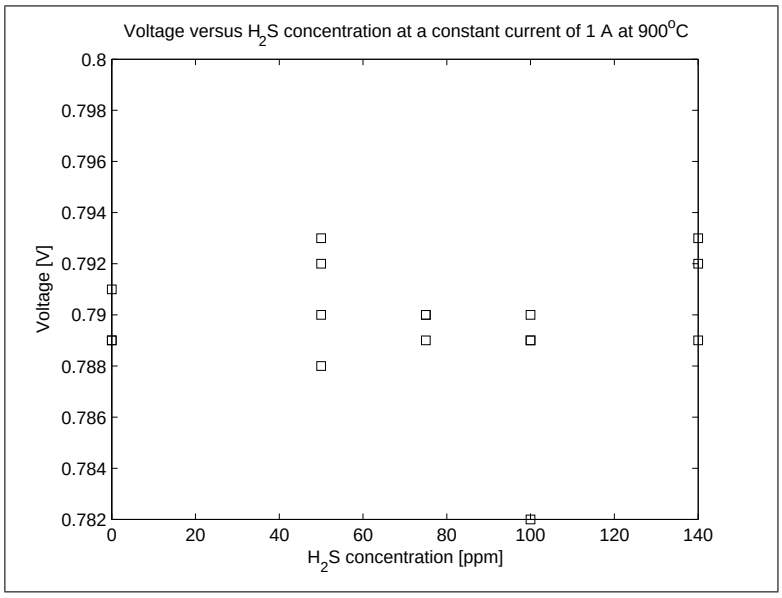

Fig. E.2: Single cell performance at 900^{o}C with varying H_2S concentrations and constant current of 1A; the cell is mounted in a 4-cell stack.

The final sulphur experiment at 900^{o}C involved two short switches between 0 and 140 ppm H_2S while keeping the load constant at 1 A. As shown in Figure E.3, there is a systematic reduction in cell voltage at the constant load of 2-4 mV as 140 ppm H_2S is introduced. This corresponds to a performance loss of around 0.5%.

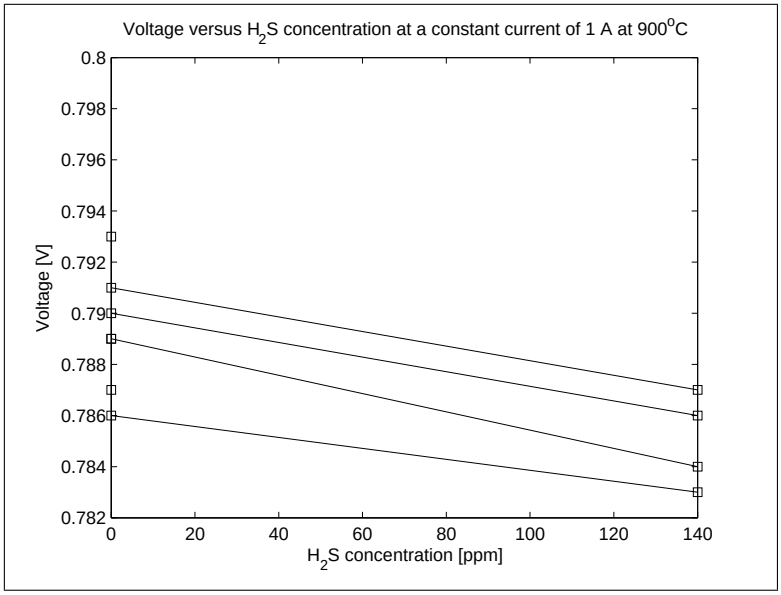

Fig. E.3: Single cell performance at 900^{o}C with varying H_2S concentrations and constant current of 1A; the cell is mounted in a 4-cell stack.

E.1.2 Experiments at 800^{o}C

The sulphur experiments at 800^{o}C were performed after the sulphur and ammonia experiments at 900^{o}C and after the ammonia experiments at 800^{o}C. Here, only tests at a constant current load of 1 A were performed at varying H_2S concentrations. The results are shown in Figure (E.4).

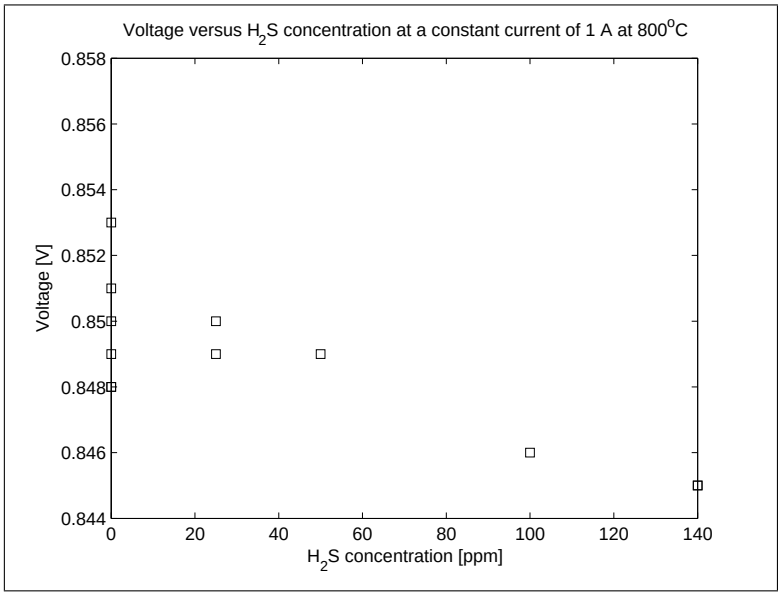

Fig. E.4: Single cell performance at 800^{o}C with varying H_2S concentrations and constant current of 1A; the cell is mounted in a 4-cell stack.

There seem to be a relatively clear trend of a performance reduction of the single cell as more H_2S is introduced. This trend was not so clear at the low ppm experiments at 900^{o}C, and may thus indicate a temperature dependency on the poisoning effect of

sulphur at low sulphur levels. The effect of adding 100 to 140 ppm H_2S, however, seems to be comparable at the two temperatures, i.e. a voltage reduction of around 4 mV at a load of 1 A.

It it is important to bear in mind that in these experiments there were no hydrocarbons present in the fuel gas. Therefore, any effect sulphur may have on the reforming reactions in the SOFC anode was not detected here. There are numerous published articles and other works on sulphur deactivation of steam reforming catalysts, and this effect must therefore be investigated further in the SOFC application.

E.2 Ammonia experiments

The ammonia was introduced to the fuel gas mixture from a premixed bottle containing 5000 ppm NH_3 in hydrogen. A valve was used to switch between the bottle containing pure hydrogen and that of the ammonia mixture while maintaining constant gain on the mass flow controller. Thus, when switching over to the ammonia/hydrogen mixture, there was approximately 5000 ppm less pure hydrogen in the fuel gas. However, since each ammonia molecule contains 1.5 H_2, there was slightly more hydrogen available if the ammonia was cracked to H_2 and N_2 in the SOFC anode.

The ammonia concentration in the mixed fuel gas was, by referring to Table (E.1), around 2600 ppm since the 5000 ppm ammonia/hydrogen mixture was diluted by CO_2, H_2O and N_2.

E.2.1 Experiments at 900^{o}C

The ammonia experiments at 900^{o}C were carried out after the H_2S experiments at that temperature. Two series with around 2600 ppm NH_3 were carried out. Before and after each series the stack was operated without ammonia for a while for reference.

It can be seen in Figure (E.5) that for the three series in the middle, i.e. two with ammonia and one without, there does not seem to be any significant difference in performance of the single cell. The two series with no ammonia before and after the three middle series show a somewhat diverging performance. The reason for this divergence is not clear, but does not necessarily have anything to do with the introduction of ammonia. It is therefore concluded here that the addition of up to around 3000 ppm NH_3 does not cause a significant change on SOFC performance. This is in accordance with the work of Wojcik et al. [106].

E.2.2 Experiments at 800^{o}C

After the ammonia experiments at 900^{o}C, the stack temperature was decreased to 800^{o}C. A similar series as that performed at 900^{o}C was carried out thereafter, i.e. two series with an ammonia concentration of around 2600 ppm with 0 ppm reference tests before and after each series. The IV-curves of the single cell investigated are shown in Figure (E.6).

Also in these tests there are no significant performance variations when switching from 0 to 2600 ppm NH_3. The very first and last series, both at 0 ppm NH_3 are again a bit diverging. Compared to the experiments at 900^{o}C, however, there does not seem to be any systematised trend behind this.

Again, it is concluded that there does not seem to be any effect on the SOFC performance as around 2600 ppm NH_3 is introduced to the fuel gas.

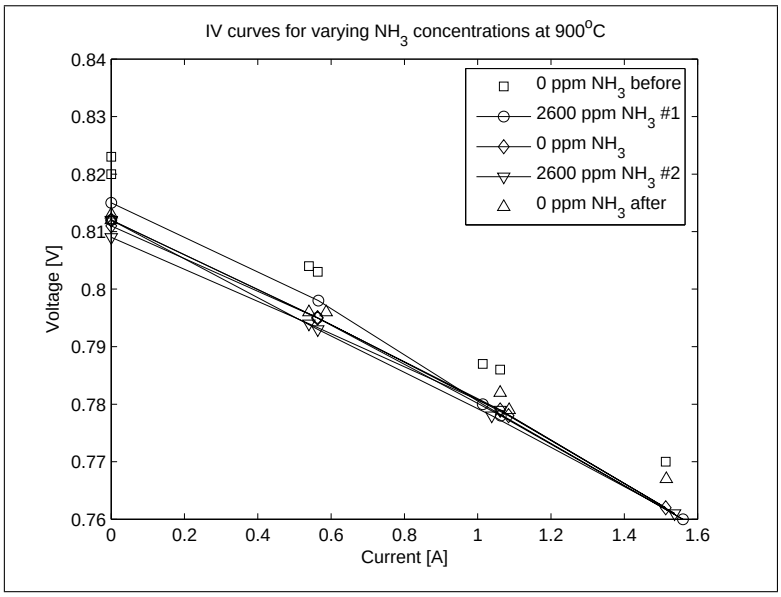

Fig. E.5: Single cell performance at 900^{o}C with varying NH_3 concentrations; the cell is mounted in a 4-cell stack.

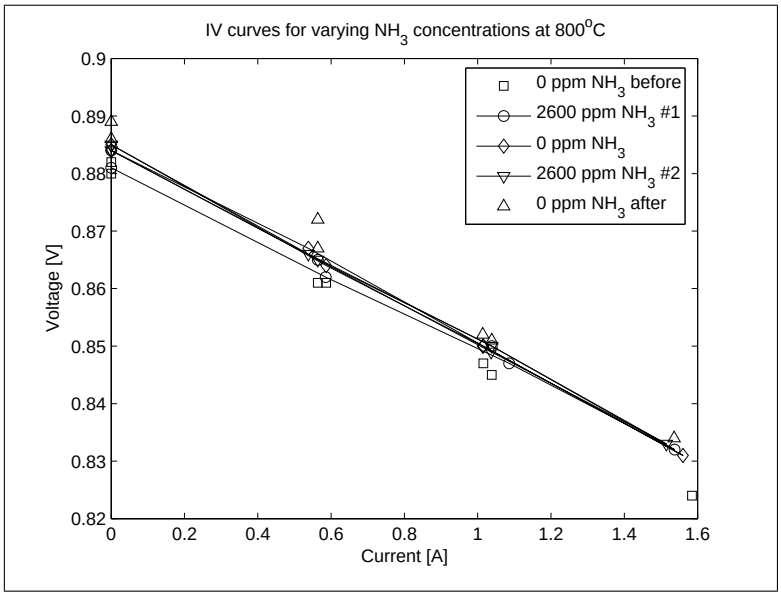

Fig. E.6: Single cell performance at 800^{o}C with varying NH_3 concentrations; the cell is mounted in a 4-cell stack.

BIBLIOGRAPHY

[1] K. Maniatis (2000) *Progress in biomass gasification: an overview*, European Comission, Brussels, Progress in Thermochemical Biomass Conversion, Blackwell Science Ltd., UK

[2] H. Hofbauer, G. Veronik, T. Fleck, R. Rauch, H. Mackinger & E. Fercher (1997) *The FICFB-gasification process*, Developments in Thermochemical Biomass Conversion 2, 1016-1025

[3] H. Risnes (2002) *High temperature filtration in biomass combustion and gasification processes*, Ph.D. thesis, Norwegian University of Science and Technology

[4] M. Grønli (1996) *A theoretical and experimental study of the thermal degradation of biomass*, Ph.D. thesis, Norwegian University of Science and Technology

[5] Ø. Skreiberg (1997) *Theoretical and experimental studies on emissions from wood combustion*, Ph.D. thesis, Norwegian University of Science and Technology

[6] L. Sørum (2000) *Environmental aspects of municipal solid waste combustion*, Ph.D. thesis, Norwegian University of Science and Technology

[7] M. Barrio (2002) *Experimental investigation of small-scale gasification of woody biomass*, Ph.D. thesis, Norwegian University of Science and Technology

[8] M. Fossum (2002) *Biomass gasification - Combustion of gas mixtures*, Ph.D. thesis, Norwegian University of Science and Technology

[9] S. van Loo & J. Koppejan (eds.) (2002) *Handbook of Biomass Combustion and Co-Firing*, International Energy Agency

[10] P. McKendry (2002) *Energy production from biomass (part1): overview of biomass*, Bioresource Technology 83, 37-46

[11] C. Di Blasi (1998) *Multi-phase moisture transfer in the high-temperature drying of wood particles*, Chemical Engineering Science 53 (2), 353-366

[12] C. Di Blasi, C. Branca, S. Sparano & B. La Mantia (2003) *Drying characteristics of wood cylinders for conditions pertinent to fixed-bed countercurrent gasification*, Biomass and Bioenergy 25, 45-58

[13] P.M. Lv, Z.H. Xiong, J. Chang, C.Z. Wu, Y. Chen & J.X. Zhu (2004) *An experimental study on biomass air-steam gasification in a fluidized bed*, Bioresource Technology 95, 95-101

[14] K.W. Ragland, D.J. Aerts & A.J. Baker (1991) *Properties of wood for combustion analysis*, Bioresource Technology 37, 161-168

[15] A. Nordin (1994) *Chemical elemental characteristics of biomass fuels*, Biomass and Bioenergy 6 (5), 339-347

[16] A. van der Drift, J. van Doorn & J.W. Vermeulen (2001) *Ten residual biomass fuels for circulating fluidized-bed gasification*, Biomass and Bioenergy 20, 45-56

[17] X.T. Li, J.R. Grace, C.J. Lim, A.P. Watkinson, H.P. Chen & J.R. Kim (2004) *Biomass gasification in a circulating fluidized bed*, Biomass and Bioenergy 26, 171-193

[18] A. Faaij, R. van Ree, L. Waldheim, E. Olsson, A. Oudhuis, A. van Wijk, C. Daey-Ouwens & W. Turkenburg (1997) *Gasification of biomass wastes and residues for electricity production*, Biomass and Bioenergy 12 (6), 387-407

[19] X.L. Yin, C.Z. Wu, S.P. Zheng & Y. Chen (2002) *Design and operation of a CFB gasification and power generation system for rice husk*, Biomass and Bioenergy 23, 181-187

[20] S. Turn, C. Kinoshita, Z. Zhang, D. Ishimura & J. Zhou (1998) *An experimental investigation of hydrogen production from biomass gasification*, International Journal of Hydrogen Energy 23 (8), 641-648

[21] P. McKendry (2002) *Energy production from biomass (part 2): conversion technologies*, Bioresource Technology 83, 47-54

[22] C. Di Blasi & C. Branca (2001) *Kinetics of primary product formation from wood pyrolysis*, Ind. Eng. Chem. Res 40, 5547-5556

[23] S. Zecevic, E.M. Patton & P. Parhami (2004) *Carbon-air fuel cell without a reforming process*, Carbon 42, 1983-1993

[24] P. McKendry (2002) *Energy production from biomass (part 3): gasification technologies*, Bioresource Technology 83, 55-63

[25] H. Hofbauer, R. Rauch, K. Bosch, R. Koch & C. Aichernig (2003) *Biomass CHP plant Güssing - A success story*, in A.V. Bridgewater (ed.), Pyrolysis and Gasification of Biomass and Waste, CPL PRess, Newbury, UK

[26] M. Barrio, M. Fossum & J.E. Hustad (2001)*A small-scale stratified downdraft gasifier coupled to a gas engine for combined heat anyud power production*, in A.V. Bridgwater (ed.), Progress in Thermochemical Biomass Conversion, Blackwell Science Ltd.

[27] S.C. Bhattacharya, S.S. Hla & H.L. Pham (2001) *A study on a multi-stage hybrid gasifier-engine system*, Biomass and Bioenergy 21, 445-460

[28] A.V. Bridgwater (1995) *The technical and economic feasibility of biomass gasification for power generation*, Fuel 74 (5), 631-653

[29] R.H. Williams & E.D. Larson (1996) *Biomass gasifier gas turbine power generating technology*, Biomass and Bioenergy 10 (2-3), 149-166

[30] P.H. Steinwall (1997) *Integration of biomass gasification and evaporative gas turbine cycles*, Energy Conversion Management 38 (15-17), 1665-1670

[31] T. Kivisaari, P. Björnbom & C. Sylwan (2002) *Studies of biomass fuelled MCFC systems*, Journal of Power Sources 104, 115-124

[32] M. Kübel, R. Berger & K.R.G. Hein (2002) *Biomass gasification: An option for SOFC Fuel?*, Proc. Fifth European Solid Oxide Fuel Cell Forum, vol. 2, 995-1002

[33] T.B. Reed & A. Das (1988) *Handbook of biomass downdraft gasifier engine systems*, The Biomass Energy Foundation Press, Golden, CO

[34] A.A.C.M. Beenackers (1999) *Biomass gasification in moving beds, a review of European technologies*, Renewable Energy 16, 1180-1186

[35] J. Larminie & A. Dicks (2000) *Fuel Cell Systems Explained*, Wiley

[36] N.M. Sammes & R. Boersma (2000) *Small-scale fuel cells for residential applications*, Journal of Power Sources 86, 98-110

[37] G. Cacciola, V. Antonucci & S. Freni (2001) *Technology up date and new strategies on fuel cells*, Journal of Power Sources 100, 67-79

[38] G.F. McLean, T. Niet, S. Prince-Richard & N. Djilali (2002) *An assessment of alkaline fuel cell technology*, International Journal of Hydrogen Energy 27, 507-526

[39] E. Gülzow & M. Schulze (2004) *Long-term operation of AFC electrodes with CO_2 containing gases*, Journal of Power Sources 127, 243-251

[40] K. Kordesh, V. Hacker, J. Gsellmann, M. Cifrain, G. Faleschini, P. Enziger, R. Fankhauser, M. Ortner, M. Muhr & R.R. Aronson (2000) *Alkaline fuel cells applications*, Journal of Power Sources 86, 162-165

[41] R. Song & D.R. Shin (2001) *Influence of CO concentration and reactant gas pressure on cell performance in PAFC*, International Journal of Hydrogen Energy 26, 1259-1262

[42] K. Matsumoto K & K. Kasahara (1998) *Long-term commitment of Japanese gas utilities to PAFCs and SOFCs*, Journal of Power Sources 71, 51-57

[43] J.P.P Huijsmans, G.J. Kraaij, R.C. Makkus, G. Rietveld, E.F. Sitters, H.Th.J. Reijers (2000) *An analysis of endurance issues for MCFC*, Journal of Power Sources 86, 117-121

[44] S. Terada, K. Higaki, I. Nagashima & Y. Ito (1999) *Stability and solubility of electrolyte matrix support material for molten carbonate fuel cells*, Journal of Power Sources 83, 227-230

[45] K. Joon (1996) *Critical issues and future prospects for molten carbonate fuel cells*, Journal of Power Sources 61, 129-133

[46] C.W. Bale, P. Chartrand, S.A. Degterov, G. Eriksson, K. Hack, R. Ben Mahfoud, J. Melançon, A.D. Pelton & S. Petersen (2002) *FactSage thermochemical software and databases*, Calphad 26 (2), 189-228

[47] M. Mogensen & T. Lindegaard (1993) *The kinetics of hydrogen oxidation on a Ni-YSZ SOFC electrode at 1000°C*, Proc. 3rd Int. Symp on Solid Oxide Fuel Cells, The Electrochemical Society Proc. (93-4), 484-493

[48] F.P.F. van Berkel, F.H. van Heuveln & J.P.P. Huijsmans (1994) *Characterization of solid oxide fuel cell electrodes by impedance spectroscopy and I-V characteristics*, Solid State Ionics 72, 240-247

[49] J. Mizusaki, H. Tagawa, T. Saito, T. Yamamura, K. Kamitani, K. Hirano, S. Ehara, T. Takagi, T. Hikita, M. Ippommatsu, S. Nakagawa & K. Hashimoto (1994) *Kinetic studies of the reaction at the nickel pattern electrode on YSZ in H_2-H_2O atmospheres*, Solid State Ionics 70/71, 52-58

[50] M. Mogensen & S. Skaarup (1996) *Kinetic and geometric aspects of solid oxide fuel cell electrodes*, Solid State Ionics, 86-88, 1151-1160

[51] A.V. Virkar, J. Chen, C. W. Tanner, Jai-Woh Kim (2000) *The role of electrode microstructure on activation and concentration polarizations in solid oxide fuel cells*, Solid State Ionics 131, 189-198

[52] D.W Dees, T.D. Claar, T.E. Easler, D.C. Fee & F.C. Mrazek (1987) *Conductivity of porous Ni/ZrO_2-Y_2O_3 cermets*, Journal of the Electrochemical Society 134 (9), 2141-2146

[53] T. Kawada, N. Sakai, H. Yokokawa, M. Dokiya, M. Mori & T. Iwata (1990) *Characteristics of slurry-coated nickel zirconia cermet anodes for Solid Oxied Fuel Cells*, Journal of the Electrochemical Society 137 (10), 3042-3047

[54] W.Z. Zhu & S.C. Deevi (2003) *A review on the status of anode materials for solid oxide fuel cells*, Materials Science & Engineering A362, 228-239

[55] H. Koide, Y. Someya, T. Yoshida & T. Maruyama (2000) *Properties of Ni/YSZ cermet as anode for SOFC*, Solid State Ionics 132, 253-260

[56] T. Kawada, N. Sakai, H. Yokokawa, M. Dokiya, M. Mori & T. Iwata (1990) *Structure and polarization characteristics of solid oxide fuel cell anodes*, Solid State Ionics 40/41, 402-406

[57] M. Brown, S. Primdahl & M. Mogensen (2000) *Structure/performance relations for Ni/yttria-stabilized zirconia anodes for solid oxide fuel cells*, Journal of The Electrochemical Society 147 (2), 475-485

[58] S. Primdahl & M. Mogensen (1997) *Oxidation of hydrogen on Ni/yttria-stabilized zirconia cermet anodes*, Journal of the Electrochemical Society, 144 (10), 3409-3419

[59] D.W. Dees, U. Balachandran, S.E. Dorris, J.J. Heiberger, C.C. McPheeters & J.J. Picciolo (1989) *Interfacial effects in monolithich solid oxide fuel cells*, Proc. 1st Int. Symp. Solid Oxide Fuel Cells, The Electrochemical Society Proc. (89-11), 317-321

[60] H. Tu & U. Stimming (2005) *Advances, aging mechanisms and lifetime in solid-oxide fuel cells*, Journal of Power Sources 127, 284-293

[61] K. Vels Jensen (2002) *The Nickel-YSZ interface - Structure, composition and electrochemical properties at 1000°C*, PhD thesis, Risø National Laboratory, Roskilde, Denmark

[62] S.C. Singhal & K. Kendall (2003) *High Temperature Solid Oxide Fuel Cells - Fundamentals, design and applications*, Elsevier, UK

[63] R.N Basu, G. Blaß, H.P. Buchkremer, D. Stöver, F. Tietz, E. Wessel & I.C. Vinke (2001) *Fabrication of simplified anode supported planar SOFCs - A recent attempt*, Proc. 7th Int. Symp. Solid Oxide Fuel Cells, The Electrochemical Society Proc. (2001-16), 995-1001

[64] S.P.S. Badwal (1992) *Zirconia-based electrolytes: microstructure, stability and ionic conductivity*, Solid State Ionics 52, 23-32

[65] R.M Dell & A. Hopper in P. Hagenmuller & W. van Gool (eds.) (1978) *Solid electrolytes - General principles, characterization, materials, application*, Academic Press, New York, USA

[66] I.R. Gibson, G.P. Dransfield & J.T.S. Irvine (1998) *Influence of yttia concentration upon electrical properties and susceptibility to ageing of yttria-stabilised zirconias*, Journal of the European Ceramic Society 18, 661-667

[67] S. Ikeda, O. Sakurai, K. Uematsu, N. Mizutani & M. Kato (1985) *Electrical conductivity of yttia-stabilized zirconia single crystals*, Journal of Materials Science 20, 4593-4600

[68] C. Haering, A. Roosen & H. Schichl (2005) *Degradation of the electrical conductivity in stabilised zirconia systems Part I: yttria-stabilised zirconia*, Solid State Ionics 176, 253-259

[69] C.C. Appel, N. Bonanos, A. Horsewell & S. Linderoth (2001) *Ageing behaviour of zirconia stabilised by yttria and manganese oxide*, Journal of Materials Science 36, 4493-4501

[70] C. Clausen, C. Bagger, J.B. Bilde-Sørensen & A. Horsewell (1994) *Microstrucutral and microchemical characterization of the interface between* $La_{0.85}Sr_{0.15}MnO_3$ *and* Y_2O_3*-stabilized* ZrO_2, Solid State Ionics 70/71, 59-64

[71] S.P. Jiang & S.H. Chan (2004) *A review of anode materials development in solid oxide fuel cells*, Journal of Materials Science 39, 4405-4439

[72] C.W. Tanner, K. Fung & A.V. Virkar (1997) *The effect of porous composite electrode structure on solid oxide fuel cell performance - I. Theoretical analysis*, Journal of The Electrochemical Society 144 (1), 21-30

[73] T. Norby, O.J. Velle, H. Leth-Olsen & R. Tunold (1993) *Reaction resistance in relation to three phase boundary length of Ni/YSZ electrodes*, Proc. 3rd Int. Symp. Solid Oxide Fuel Cells, The Electrochemical Society Proc. (93-4), 473-478

[74] Y. Matsuzaki & I. Yasuda (2000) *Electrochemical oxidation of* H_2 *and CO in a* H_2-H_2O-CO-CO_2 *system at the interface of a Ni-YSZ cermet electrode and YSZ electrolyte*, Journal of the Electrochemical Society 147 (5), 1630-1635

[75] J. Mizusaki, H. Tagawa, T. Saito, K. Kamitani, T. Yamamura, K. Hirano, S. Ehara, T. Takagi, T. Hikita, M. Ippommatsu, S. Nakagawa & K. Hashimoto (1993) *Preparation of nickel pattern electrodes on YSZ and their electrochemcial properties in* H_2-H_2O *atmosphere*, Proc. 3rd Int. Symp. Solid Oxide Fuel Cells, The Electrochemical Society Proc. (93-4), 533-541

[76] S.P.S. Badwal & K. Foger (1997) *Materials for solid oxide fuel cells*, Materials Forum 21, 187-244

[77] Y.C. Hsiao & J.R. Selman (1997) *The degradation of SOFC electrodes*, Solid State Ionics 98, 33-38

[78] S. Primdahl & M. Mogensen (2000) *Durability and thermal cycling of Ni/YSZ cermet anodes for solid oxide fuel cells*, Journal of Applied Electrochemistry 30, 247-257

[79] A. Gubner, H. Landes, J. Metzger, H. Seeg & R. Stübner (1997) *Investigations into the degradation of the cermet anode of a solid oxide fuel cell*, Proc. 5th Int. Symp. Solid Oxide Fuel Cells, The Electrochemical Society Proc. (97-40), 844-850

[80] T. Iwata (1996) *Characterization of Ni-YSZ anode degradation for substrate-type solid oxide fuel cells*, Journal of the Electrochemical Society 143 (5), 1521-1525

[81] S.C. Singhal (1997) *Recent progress in tubular solid oxide fuel cell technology*, Proc. 5th Int. Symp. Solid Oxide Fuel Cells, The Electrochemical Society Proc. (97-40), 37-50

[82] M. Pastula, R. Boersma, D. Prediger, M. Perry, A. Horvath, J. Devitt & D. Gosh (2000) *Development of low temperature SOFC systems for remote power applications*, Proc. 4th European Solid Oxide Fuel Cell Forum 1, 123-132

[83] D. Stolten, R. Späh & R. Schamm (1997) *Status of SOFC development at Daimler-Benz/Dornier*, Proc. 5th Int. Symp. Solid Oxide Fuel Cells, The Electrochemical Society Proc. (97-40), 88-93

[84] C.C. Chen, M.M. Nasrallah & H.U. Anderson (1993) *Cathode/electrolyte interactions and their expected impact on SOFC performance*, Proc. 3rd Int. Symp. Solid Oxide Fuel Cells, The Electrochemical Society Proc. (93-4), 598-612

[85] I. Alstrup, J.R. Rostrup-Nielsen & S. Røen (1981) *High temperature hydrogen sulfide chemisorption on nickel catalysts*, Applied Catalysis 1, 303-314

[86] Y. Matsuzaki & I. Yasuda (2000) *The posioning effect of sulfur-containing impurity gas on SOFC anode: Part I. Dependence on temperature, time and impurity concentration*, Solid State Ionics 132, 261-269

[87] Y. Matsuzaki & I. Yasuda (2001) *Effect of a sulfur-containing impurity on electrochemical properties of a Ni-YSZ cermet electrode*, Proc. 7th Int. Symp. Solid Oxide Fuel Cells, The Electrochemical Society Proc. (2001-16), 769-782

[88] J. Geyer, H. Kohlmüller, H. Landes & R. Stübner (1998) *Investigations into the kinetics of the Ni-YSZ-cermet-anode of a solid oxide fuel cell*, Proc. 5th Int. Symp. Solid Oxide Fuel Cells, The Electrochemical Society Proc. (97-40), 585-594

[89] S. Primdahl & M. Mogensen (1999) *Limitations in the hydrogen oxidation rate on Ni/YSZ anodes*, Proc. 6th Int. Symp. Solid Oxide Fuel Cells, The Electrochemical Society Proc. (99-19), 530-540

[90] S.C. Singhal (2000) *Advances in solid oxide fuel cell technology*, Solid State Ionics 135, 305-313

[91] M.A. Petrik, C.E. Milliken, R.C. Ruhl % B.P. Lee (1998) *Status of TMI solid oxide fuel cell technology*, 1998 Fuel Cell Seminar, California, 124-127

[92] M. Mogensen, K. Vels Jensen, M. Juhl Jørgensen and S. Primdahl (2002) *Progress in understanding SOFC electrodes*, Solid State Ionics 150, 123-129

[93] S. Onuma, A. Kaimai, K. Kawamura, Y. Nigara, T. Kawada, J. Mizusaki, H. Tagawa (2000) *Influence of the coexisting gases on the electrochemical reaction rates between 873 and 1173 K in a CH_4-H_2O/Pt/YSZ system*, Solid State Ionics 132, 309-331

[94] O. Costa-Nunes, R.J. Gorte & J.M. Vohs (2005) *Comparison of the performance of Cu-CeO_2-YSZ and Ni-YSZ composite anodes with H_2, CO, and syngas*, Journal of Power Sources 141, 241-249

[95] A. Schuler, T. Zähringer, B. Doggwiler & A. Rüegge (2000) *Sulzer Hexis SOFC running on home heating oil*, Proceedings of the Fourth European Solid Oxide Fuel Cell Forum 1, 107-114

[96] G.A. Tompsett, C. Finnerty, K. Kendall, T. Alston & N.M. Sammes (2000) *Novel applications for micro-SOFCs*, Journal of Power Sources 86, 376-382

[97] N.M. Sammes, R.J. Boersma & G.A. Tompsett (2000) *Micro-SOFC system using butane fuel*, Solid State Ionics 135, 487-491

[98] Z. Zhan, J. Liu & S.A. Barnett (2004) *Operation of anode-supported solid oxide fuel cells on propane-air mixtures*, Applied Catalysis A: General 262, 255-259

[99] J. Liu & S.A. Barnett (2003) *Operation of anode-supported solid oxide fuel cells on methane and natural gas*, Solid State Ionics 158, 11-16

[100] K. Ahmed, J. Gamman & K. Föger (2002) *Demonstration of LPG-fueled solid oxide fuel cell systems*, Solid State Ionics 152-153, 485-492

[101] G.J. Saunders & K. Kendall (2002) *Reactions of hydrocarbons in small tubular SOFCs*, Journal of Power Sources 106, 258-263

[102] G.J. Saunders, J. Preece & K. Kendall (2004) *Formulating liquid hydrocarbon fuels for SOFCs*, Journal of Power Sources 131, 23-26

[103] S. Assabumrungrat, V. Pavarajarn, S. Charojrochkul & N. Laosiripojana (2004) *Thermodynamic analysis for a solid oxide fuel cell with direct internal reforming fueled by ethanol*, Chemical Engineering Science 59, 6015-6020

[104] J. Stainforth & K. Kendall (1998) *Biogas powering a small tubular solid oxide fuel cell*, Journal of Power Sources 71, 275-277

[105] J. Stainforth & K. Kendall (2000) *Cannock landfill gas powering a small tubular solid oxide fuel cell - a case study*, Journal of Power Sources 86, 401-403

[106] A. Wojcik, H. Middleton, I. Damopoulos % J. Van herle (2003) *Ammonia as a fuel in solid oxide fuel cells*, Journal of Power Sources 118, 342-348

[107] G. Eriksson % K. Hack (1990) *ChemSage - A computer program for the calculation of complex chemical equilibria*, Metallurgical Transactions B 21 B, 1013-1023

[108] K. Sasaki, Y. Hori, R. Kikuchi, E. Eguchi, A. Ueno, H. Takeuchi, M. Aizawa, K. Tsuijumoto, H. Tajiri, H. Nishikawa & Y. Uchida (2002) *Current-voltage characteristics and impedance analysis of solid oxide fuel cells for mixed H_2 and CO gases*, Journal of The Electrochemical Society 149 (3), A227-A233